

Abstract of “Scattering amplitudes in  $N=4$  SYM and  $N=8$  SUGRA” by Congkao Wen, Ph.D., Brown University, May 2012.

The main subject of this thesis is scattering amplitudes in  $\mathcal{N} = 4$  super-Yang-Mills theory (SYM) and  $\mathcal{N} = 8$  super-gravity theory (SUGRA). We study several aspects of the scattering amplitudes of Yang-Mills theories as well as gravity theories using modern techniques. After the introductory chapter, we apply these methods to study the scattering amplitudes both in  $\mathcal{N} = 4$  SYM and  $\mathcal{N} = 8$  SUGRA. We first study two dual formulations of  $\mathcal{N} = 4$  SYM, namely the Arkani-Hamed et al Grassmannian formulation and Witten’s twistor string theory. We present a new, explicit formula for all tree-level amplitudes in  $\mathcal{N} = 4$  SYM. The formula is written as a certain contour integral of the connected prescription of Witten’s twistor string, expressed in link variables. A very simple deformation of the integrand gives directly the Grassmannian integrand proposed together with the explicit contour of integration. Then we calculate for the first time the five-point three-loop amplitudes of  $\mathcal{N} = 4$  SYM using the leading singularity method. Using the method of obstructions we numerically evaluate two previously unfixed coefficients which appear in the three-loop BDS ansatz. After the study of  $\mathcal{N} = 4$  SYM, we turn our journey to  $\mathcal{N} = 8$  SUGRA by first presenting and proving a new formula for MHV amplitude in SUGRA. Some of interesting features of the formula set it apart as being significantly different from many more familiar formulas. We then present an algorithm for writing down explicit formulas for all tree amplitudes in  $\mathcal{N} = 8$  SUGRA, obtained from solving the supersymmetric on-shell recursion relations. The formula is patterned after one recently obtained for all tree amplitudes in  $\mathcal{N} = 4$  SYM which involves nested sums of dual superconformal invariants. We find that all graviton amplitudes can be written in terms of exactly the same structure of nested sums with two modifications: the dual superconformal invariants are promoted from  $\mathcal{N} = 4$  to  $\mathcal{N} = 8$  superspace in the simplest manner possible—by squaring them—and certain additional non-dual conformal gravity dressing factors (independent of the superspace coordinates) are inserted into the nested sums. To illustrate the procedure we give explicit closed-form formulas for all NMHV, NNMHV and NNNMV gravity superamplitudes. The obtained results are further simplified by applying bonus relations between gravity amplitudes, which arise from the soft behaviour of tree-level gravity amplitude.



Scattering amplitudes in N=4 SYM and N=8 SUGRA

by  
Congkao Wen  
B. Sc., Zhejiang University, 2002

Submitted in partial fulfillment of the requirements  
for the Degree of Doctor of Philosophy in the  
Department of Physics at Brown University

Providence, Rhode Island  
May 2012

© Copyright 2011 by Congkao Wen

This dissertation by Congkao Wen is accepted in its present form by  
the Department of Physics as satisfying the dissertation requirement  
for the degree of Doctor of Philosophy.

Date \_\_\_\_\_  
Anastasia Volovich, Director

Recommended to the Graduate Council

Date \_\_\_\_\_  
Antal Jevicki, Reader

Date \_\_\_\_\_  
Marcus Spradlin, Reader

Date \_\_\_\_\_  
Chung-I Tan, Reader

Approved by the Graduate Council

Date \_\_\_\_\_

---

Peter M. Weber  
Dean of the Graduate School

# Curriculum Vitæ

## Author

Congkao Wen

## Education

Zhejiang University, Hangzhou, Zhejiang, China, B.S. in Physics (2002)  
Brown University, Providence, RI, U.S. Ph.D. in Physics (2011)

## Publications

1. Note on Bonus Relations for  $\mathcal{N} = 8$  Supergravity Tree Amplitudes.  
with S. He, D. Nandan,  
*JHEP* **1102**, 005 (2011)  
arXiv:1011.4287 [hep-th].
2. The Grassmannian and the Twistor String:  
Connecting All Trees in  $N=4$  SYM.  
with J. L. Bourjaily, J. Trnka, and A. Volovich  
*JHEP* **1101**, 038 (2011)  
arXiv:1006.1899 [hep-th].
3. A Grassmannian Etude in NMHV Minors.  
with D. Nandan and A. Volovich,  
*JHEP* **1007**, 061 (2010)  
arXiv:0912.3705 [hep-th].
4. The Tree Formula for MHV Graviton Amplitudes.  
with D. Nguyen, M. Spradlin and A. Volovich,  
*JHEP* **1007**, 045 (2010)  
arXiv:0907.2276 [hep-th].

5. Correlation Functions in Non-Relativistic Holography.  
 with A. Volovich,  
*JHEP* **0905**, 087 (2009)  
 arXiv:0903.2455 [hep-th].
6. Tree-Level Amplitudes in N=8 Supergravity.  
 with J.M.Drummond, M. Spradlin and A. Volovich,  
*Phys. Rev. D* **79**, 105018 (2009)  
 arXiv:0901.2363 [hep-th].
7. Three Applications of a Bonus Relation for Gravity Amplitudes.  
 with M. Spradlin and A. Volovich,  
*Phys. Lett. B* **674**, 69 (2009)  
 arXiv:0812.4767 [hep-th].
8. Three-Loop Leading Singularities and BDS Ansatz for Five particles.  
 with M. Spradlin and A. Volovich,  
*Phys. Rev. D* **78**, 085025 (2008)  
 arXiv:0808.1054 [hep-th].
9. Glueball masses from AdS(6) gravity theory.  
 with B. Cai and H. Yang,  
 Prepared for International Conference on Nonperturbative Quantum Field Theory: Lattice and Beyond, Guangzhou, Canton, China, 18-20 Dec 2004.  
 Published in *Mod.Phys.Lett.* A22:719-725,2007.
10. Loops in super Yang-Mills theories.  
 with G. Chen and M. Luo,  
 Prepared for International Conference on Nonperturbative Quantum Field Theory: Lattice and Beyond, Guangzhou, Canton, China, 18-20 Dec 2004.  
 Published in *Mod.Phys.Lett.* A22:675-681,2007.
11. Compact formulas for all tree amplitudes of six partons.  
 with M. Luo,  
*Phys. Rev. D* **71**, 091501 (2005) [arXiv:hep-th/0502009].
12. Recursion relations for tree amplitudes in super gauge theories.  
 with M. Luo,  
*JHEP* **0503**, 004 (2005) [arXiv:hep-th/0501121].
13. An Alternative Dp-brane solution of type IIB supergravity.  
 with B. Cai and H. Yang,  
 [arXiv:hep-th/0411082].

14. Systematics of one-loop scattering amplitudes in  $N=4$  super Yang-Mills theories.  
with M. Luo,  
Phys. Lett. B **609**, 86 (2005) [arXiv:hep-th/0410118].
15. One-loop maximal helicity violating amplitudes in  $N=4$  super Yang-Mills theories.  
with M. Luo,  
JHEP **0411**, 004 (2004) [arXiv:hep-th/0410045].
16. QCD(4) glueball masses from AdS(6) black hole description.  
with H. Yang,  
Mod. Phys. Lett. A **20**, 997 (2005) [arXiv:hep-th/0404152].

# Acknowledgments

Many people have helped me during the years working on my PhD. I would like to sincerely thank all of them.

First and foremost, my advisor Anastasia Volovich for her tireless guidance, patience, teaching me many things about physics and how to build a deep understanding of nature, answering my many questions, and too many other things she has helped me with throughout the years, for which this space is too small to list them all.

I would like to thank my collaborators, Jacob Bourjaily, Jaroslav Trnka, James Drummond, Song He, Dhritiman Nandan, Dung Nguyen and Marcus Spradlin, both for collaborating on papers with me, and for also teaching me a lot of things, and for helping me out both in physics related and non-physics related matters.

I would like to thank the readers, Professor Antal Jevicki and Professor Chung-I Tan, for taking the time to read my thesis, and all the other professors of the High Energy Theory group together with Antal and Chung-I for many fruitful and interesting physics discussions.

I would like to thank Kewang Jin, Marko Djuric, Ari Pakman, Shubho Roy and Cristian Vergu for many useful physics discussions.

All my colleagues from room 540, throughout the years, for creating a great atmosphere and providing with their knowledge and thinking a great place to do physics, also deserve a big thanks.

Mary Ann Rotondo and Barbara Dailey have been a great help throughout my time at Brown in providing a lot of administrative help and advice, and I thank them.

I would like to thank the US Department of Energy, Brown, and everyone else who has provided financial support for my work.

Last but not least, I am very grateful to my family and all my friends for their invaluable support!

*This thesis is dedicated to my parents and sister.*

# Contents

<b>List of Tables</b>	<b>xv</b>	
<b>List of Figures</b>	<b>xvi</b>	
<b>1</b>	<b>Introduction</b>	<b>1</b>
<b>2</b>	<b>Twistor string theory and Grassmannian: NMHV amplitude</b>	<b>6</b>
2.1	Introduction . . . . .	6
2.2	Review of the Developments . . . . .	8
2.2.1	Review of Dual S-Matrix Formulation . . . . .	8
2.2.2	NMHV tree amplitude from ACCK . . . . .	9
2.2.3	Review of the Linked-Connected Prescription . . . . .	10
2.2.4	NMHV tree amplitude from the connected prescription . . . . .	11
2.3	From the Connected to ACCK Using GRT . . . . .	14

2.3.1	$n=6$ and $n=7$	14
2.3.2	All $n$ proof	16
<b>3</b>	<b>Twistor string theory and Grassmannian: All tree-level amplitude</b>	<b>25</b>
3.1	Introduction	25
3.2	All Tree Amplitudes in $\mathcal{N} = 4$ Super Yang-Mills	27
3.3	Building the General Contour, one Particle at a Time	31
3.3.1	NMHV amplitudes	33
3.3.2	$N^2$ MHV Amplitudes	34
3.3.3	$N^3$ MHV Amplitudes and Beyond	38
3.3.4	General Properties of the Result	41
3.4	Transformation to the Twistor String in Link Variables	44
3.4.1	Transforming the $\delta(F_\ell^j)$ 's	45
3.4.2	Collecting Prefactors	49
<b>4</b>	<b>Five point three-loop amplitude in <math>\mathcal{N} = 4</math> SYM</b>	<b>50</b>
4.1	Introduction	50
4.2	Outline of the Calculation	51
4.2.1	Review of the Leading Singularity Method	52

4.2.2	Integration Strategy: Collapse and Expand . . . . .	53
4.2.3	Choosing a Sufficient Set of Contours . . . . .	57
4.3	The 3-loop 5-particle Amplitude . . . . .	63
4.4	The Three-Loop BDS Ansatz . . . . .	65
4.5	Summary . . . . .	70
<b>5</b>	<b>Tree formula for MHV gravity amplitude</b>	<b>72</b>
5.1	Introduction . . . . .	72
5.2	The MHV Tree Formula . . . . .	75
5.2.1	Statement of the Tree Formula . . . . .	75
5.2.2	Examples . . . . .	76
5.2.3	Soft Limit of the Tree Formula . . . . .	77
5.3	The MHV Tree Formula in Twistor Space . . . . .	78
5.4	Proof of the MHV Tree Formula . . . . .	81
5.5	Discussion and Open Questions . . . . .	84
<b>6</b>	<b>All tree-level amplitudes in <math>\mathcal{N} = 8</math> SUGRA</b>	<b>85</b>
6.1	Introduction . . . . .	85
6.2	Setting up the Calculation . . . . .	87

6.2.1	Supersymmetric Recursion	87
6.2.2	Gravity Subamplitudes	88
6.2.3	From $\mathcal{N} = 4$ to $\mathcal{N} = 8$ Superspace	91
6.2.4	Review of SYM Amplitudes	92
6.3	Examples of Gravity Amplitudes	96
6.3.1	MHV Amplitudes	96
6.3.2	NMHV Amplitudes	98
6.3.3	NNMHV Amplitudes	104
6.4	Discussion of General Tree-Level Amplitudes	108
<b>7</b>	<b>Bonus relations in gravity amplitudes</b>	<b>113</b>
7.1	Review of tree amplitudes in SUGRA and bonus relations	113
7.1.1	Applying Bonus Relations to MHV Amplitudes	114
7.2	Applying Bonus Relations to Non-MHV Gravity Tree Amplitudes	115
7.2.1	General Strategy	115
7.2.2	NMHV Amplitudes	118
7.2.3	$N^2$ MHV amplitudes	124
7.3	Generalization to all gravity tree amplitudes	130

7.4	Conclusion and outlook	135
<b>8</b>	<b>Conclusions</b>	<b>137</b>
.1	The Nine-Point $N^2$ MHV Tree Amplitude	140

# List of Tables

# List of Figures

4.1	The planar 3-loop 5-particle topologies associated to leading singularities. Each figure represents a sum over that subset of Feynman diagrams in which all of the indicated propagators are present. We label the external momenta clockwise with $k_1$ at the leg indicated with the arrow. . . . .	56
4.2	The 17 independent integrals appearing in the ansatz. Other integrals can be obtained by rotations or reflections. As in Fig. 4.1 we label the external momenta clockwise with $k_1$ at the position indicated by the arrow. . . . .	63
5.1	All factorizations contributing to the on-shell recursion relation for the $n$ -point MHV amplitude. Only the first diagram contributes to the residue at $z = \langle 1 3 \rangle / \langle 2 3 \rangle$ . . . . .	82

6.1 A diagrammatic representation of the relation (6.2.6) between a physical gravity amplitude $\mathcal{M}_n$ and the sum over its ordered subamplitudes $M(1, \dots, n)$ . We draw an arrow indicating the cyclic order of the indices between the special legs $n$ and 1. . . . .	89
6.2 The recursion for MHV amplitudes. . . . .	97
6.3 The two kinds of diagrams contributing to the recursion of NMHV amplitudes. . . . .	98
7.1 All factorizations contributing to (7.1.2) for the MHV amplitude. . . . .	114
7.2 Different types of diagrams for a general $N^k$ MHV amplitude, where $k = p + q + 1$ . We use a dashed line $---$ connecting three legs to denote a bonus-simplified lower-point amplitude, in which these three legs are kept fixed. For lower-point amplitudes without dashed lines, we use the usual $(n - 2)!$ form. . . . .	117
7.3 Diagrams for NMHV amplitudes. . . . .	119
7.4 Diagrams for 5-point NMHV amplitude and the boundary term of 6-point NMHV amplitude. Fig. 6(a) and Fig. 6(b) are used to calculate the bonus-simplified 5-point right-hand-side amplitude of Fig. 6(c). . . . .	122
7.5 Diagrams for $N^2$ MHV amplitudes. . . . .	127
7.6 Diagrams for 6-point $N^2$ MHV amplitude. . . . .	130



# Chapter 1

## Introduction

The main subject of this thesis is scattering amplitudes in  $\mathcal{N} = 4$  super-Yang-Mills theory (SYM) and  $\mathcal{N} = 8$  super-gravity theory (SUGRA). In weakly coupled field theories, the natural object to study is the perturbative  $S$ -matrix. The perturbative expansion of the  $S$ -matrix is conventionally computed using Feynman rules. It was observed long time ago that scattering amplitudes show simplicity that is not apparent from the Feynman rules and usual local formulations. For example, the maximally helicity violating (MHV) amplitudes of Yang-Mills theory can be expressed as very simple holomorphic functions.

Recently there have been enormous progresses on unraveling the structure of scattering amplitudes both in gauge theory and gravity, such as generalized unitary-cut method at loop level [1], and Britto-Cachazo-Feng-Witten (BCFW) recursion relations at tree level, for Yang-Mills theory [2, 3] and for gravity[4, 5], and BCFW-type recursion relations for loop-level amplitudes have also been discovered very recently[6].

A particularly important example is the structure of amplitudes in  $\mathcal{N} = 4$  super Yang-Mills theory(SYM), which has remarkable simplicities obscured by the usual local formulation and Feynman-diagram calculations. For instance, dual conformal symmetry (even Yangian symmetry) of  $\mathcal{N} = 4$  SYM appears very naturally in the BCFW solutions of the theory [7, 6]. And two beautiful dual formalisms for the  $S$ -matrix in  $\mathcal{N} = 4$  SYM, twistor string theory and the Grassmannian formulation, have been constructed.

Another reason to be interested in supersymmetric  $\mathcal{N} = 4$  Yang-Mills is that it provides the simplest incarnation of the celebrated AdS/CFT correspondence. It is believed that the supersymmetric  $\mathcal{N} = 4$  Yang-Mills in four dimensions is *equivalent* to Type IIB string theory on a  $AdS_5 \times \mathbb{S}^5$  background. There is by now a fairly detailed dictionary between observables on both sides of the correspondence but computations of dual quantities can usually only be performed in non-overlapping regions of the parameter space. Integrability techniques yield exact solutions and have afforded non-trivial tests of the AdS/CFT correspondence. It is important to note here that perturbative computations at weak and strong coupling played a decisive role in finding solutions for the integrable models which appeared in studying the dilatation operator for the supersymmetric  $\mathcal{N} = 4$  theory.

Indeed duality is one of most important ideas of modern high energy theoretical physics. In this thesis, we also study the perturbative dual formalisms of  $\mathcal{N} = 4$  SYM. In particular, the dual formalisms concerning to us are Witten's twistor string theory and Grassmannian formulation, which both perturbatively compute the  $S$ -matrix of  $\mathcal{N} = 4$  SYM. Specially the focus will be on the tree-level contours for the Grassmannian formulation and the relation between the Grassmannian formulation

and the twistor string theory.

Arkani-Hamed, Cachazo, Cheung and Kaplan [8] proposed a duality between the leading singularities of planar  $N^{(k-2)}\text{MHV}$  scattering amplitudes in  $\mathcal{N} = 4$  super Yang-Mills and certain contour integrals denoted  $\mathcal{L}_{n,k}$  over the Grassmannian manifold  $G(k, n)$  of  $k$ -planes in  $n$ -dimensions.

One of important open questions of the Grassmannian formulation is to determine the appropriate contours in the Grassmannian for computing any general tree amplitude in  $\mathcal{N} = 4$  super Yang-Mills. It turns out that the twistor string connected prescription is able to provide a preferred choice of integration contour and that its integrand may be smoothly deformed to the integrand  $\mathcal{L}_{n,k}$ .

We prove the equivalence between the connected prescription for the twistor string and  $\mathcal{L}_{n,k}$  for all NMHV amplitudes in [9, 10]. These proofs rely on repeated use of the global residue theorem, and show that the combination of residues contributing to any NMHV amplitude computed via the twistor string can be re-expressed as a direct sum of residues of  $\mathcal{L}_{n,k}$ . Moreover, an amazing and much stronger property is observed: the two integrands were in fact related by a *smooth deformation*, which interpolates between the connected prescription of twistor string theory and the Grassmannian integrand  $\mathcal{L}_{n,k}$ . The deformation connecting the two descriptions moves the locations of each pole, and changes the value of each residue; but the sum of residues which define the tree amplitude is itself found to be invariant. All those properties are actually very general, and we propose a new, explicit formula for all  $N^{(k-2)}\text{MHV}$  tree amplitudes in  $\mathcal{N} = 4$ .

Then we turn to study the loop-level amplitudes in  $\mathcal{N} = 4$  SYM using leading

singularity methods. Much of the recent interest in multi-loop scattering amplitudes has been stimulated by the ABDK/BDS ansatz [11, 12] which suggested that multi-loop MHV amplitudes satisfy a powerful iteration relation implying a simple exponential form for the full all-loop amplitude. Although the ABDK/BDS ansatz was successfully tested for four particles at two [11] and three [12] loops, as well as for five particles at two loops [13, 14], some doubts raised in [15, 16, 17] necessitated an explicit calculation of the two-loop six-particle amplitude [18] which conclusively demonstrated the incompleteness of the BDS ansatz. Indeed six particles is the earliest that the hypothesized dual conformal symmetry of amplitudes could have allowed BDS ansatz to break down; for  $n = 4, 5$  the symmetry fixes the form of the amplitude up to a few numerical constants [15, 19].

It was conjectured that leading singularity is enough to determine the whole amplitudes in a maximally supersymmetric theory, including  $\mathcal{N} = 4$  SYM. Our calculation on five-point three-loop amplitudes confirms this conjecture, indeed we determine the amplitudes purely by knowing the leading singularities. Using the method of obstructions we also numerically evaluate two previously unfixed coefficients which appear in the three-loop BDS ansatz.

Meanwhile it has been pointed out [20] that there are reasons to suspect  $\mathcal{N} = 8$  SUGRA to have even richer structure and to be ultimately even simpler than SYM. It motivates us to study various aspects of  $\mathcal{N} = 8$  SUGRA tree-level amplitudes. First we present and prove a new formula for MHV amplitude in SUGRA, which has many nice properties as a gravity amplitudes. Some of interesting features of the formula set it apart as being significantly different from many more familiar formulas. Further more, it has a simple “link representation”, which may be helpful

to understand the dual formulation of the S-matrix of gravity amplitudes. Then by solving supersymmetric on-shell recursion relations explicitly, we present an algorithm for writing down an arbitrary tree-level SUGRA amplitude based on the idea of color-ordered subamplitudes in SUGRA amplitudes, and a KLT-like structure between Gravity amplitudes and Yang-Mills amplitudes are obtained. The formula is patterned after one recently obtained for all tree amplitudes in  $\mathcal{N} = 4$  SYM which involves nested sums of dual superconformal invariants. We find that all graviton amplitudes can be written in terms of exactly the same structure of nested sums with two modifications: the dual superconformal invariants are promoted from  $\mathcal{N} = 4$  to  $\mathcal{N} = 8$  superspace in the simplest manner possible—by squaring them—and certain additional non-dual conformal gravity dressing factors (independent of the superspace coordinates) are inserted into the nested sums. To illustrate the procedure we give explicit closed-form formulas for all NMHV, NNMHV and NNNMV gravity superamplitudes. The result can be written as a summation over  $(n - 2)!$  “ordered gravity subamplitudes” with different permutations of particles  $2, \dots, n - 1$ . While in contrast to SYM color-ordered amplitudes, the SUGRA amplitudes actually have a faster,  $1/z^2$ , falloff and the contour integral  $\oint dz M(z)$  gives the bonus relations. we will see that these relations can be used to further simplify the explicit all tree-level formulae for the amplitudes in  $\mathcal{N} = 8$  SUGRA by reducing the  $(n - 2)!$ -permutation sum to a new  $(n - 3)!$ -permutation one.

Finally, we will present some closing comments, and directions for future research.

# Chapter 2

## Twistor string theory and Grassmannian: NMHV amplitude

### 2.1 Introduction

The twistor string theory formulation of Yang-Mills scattering amplitudes has been a great step forward in unearthing a host of properties of scattering amplitudes, hitherto unseen via the standard methods of quantum field theory. A connected prescription formula for computing all tree level superamplitudes in twistor string theory has been written down in [21], based on Witten’s proposal that the  $N^{k-2}\text{MHV}$  superamplitude should be given by the integral of an open string current algebra correlator over the space of degree  $k-1$  curves in supertwistor space  $\mathbb{P}^{3|4}$ . Furthermore, a “linked” version of the formula had been written in [22] and [23] by reformulating the original connected prescription amplitude in terms of the link variables introduced in [24]. A

remarkable new contour integral over a Grassmannian of these link variables, which apparently encapsulates information about leading singularities of  $\mathcal{N} = 4$  Yang-Mills loop amplitudes in addition to tree-level information, has been written down by Arkani-Hamed, Cachazo, Cheung and Kaplan (ACCK) in [8].

In this chapter we make the connection between the linked-connected prescription formula from twistor string theory and the ACCK proposal more transparent by offering a simple analytic proof between the two formulas for all tree-level NMHV superamplitudes. Also we note that a simple deformation of the connected prescription integrand by non-zero parameters gives directly the Grassmannian integrand in the limit when the deformation parameters equal zero. Specifically, the ACCK Grassmannian integrand arises from the linked-connected formula in a simple limit when the second terms in all sextic polynomials are zero (see formula (2.2.18)).

In section II we review some of the recent developments and write down a general formula (2.2.15) for  $n$ -point NMHV amplitudes in terms of minors in a convenient way. In section III we show how to get the BCFW contours from the linked-connected prescription for the six and seven point NMHV amplitudes in a simple way, followed by the general proof for all  $n$ -point NMHV amplitude by using the global residue theorem (GRT). In the appendix we present the ten-point case as a concrete example.

## 2.2 Review of the Developments

### 2.2.1 Review of Dual S-Matrix Formulation

Recently Arkani-Hamed, Cachazo, Cheung and Kaplan [8] have conjectured a formula for a dual formulation for the S-Matrix of  $\mathcal{N} = 4$  SYM. According to their proposal the planar, color stripped,  $n$  particle,  $N^{k-2}$ MHV amplitudes are associated with contour integrals over a Grassmannian

$$\mathcal{L}_{n;k}(\mathcal{W}_a) = \frac{1}{\text{Vol}(GL(k))} \int \frac{d^{k \times n} C_{\alpha a}}{(12 \cdots k) (23 \cdots (k+1)) \cdots (n1 \cdots (k-1))} \prod_{\alpha=1}^k \delta^{4|4}(C_{\alpha a} \mathcal{W}_a) \quad (2.1)$$

where the  $\mathcal{W}_a$  are twistor variables obtained by Fourier transforming with respect to the  $\lambda_a : \mathcal{W} = (W|\tilde{\eta}) = (\tilde{\mu}, \tilde{\lambda}|\tilde{\eta})$ , and

$$(m_1 \cdots m_k) \equiv \epsilon^{\alpha_1 \cdots \alpha_k} C_{\alpha_1 m_1} \cdots C_{\alpha_k m_k}. \quad (2.2.2)$$

Here,  $C_{\alpha a}$  is a  $k \times n$  matrix and its ‘minor’,  $(m_1 \cdots m_k)$  is the determinant of the  $k \times k$  submatrix made by only keeping the  $k$  columns  $m_1, \dots, m_k$ . The integrand of this formula has a  $GL(k)$  symmetry under which  $C_{\alpha a} \rightarrow L_\alpha^\beta C_{\beta a}$  for any  $k \times k$  matrix  $L$ , and so one has to gauge fix by dividing by  $\text{Vol}(GL(k))$ . This formula has manifest cyclic, parity, superconformal and also dual superconformal symmetry [25].

The outstanding feature of this formula is that, interpreting the integral as a multi-dimensional contour integral in momentum space, the residues of the integrand give a basis for obtaining tree level amplitudes as well as all loop leading singularities, which was heavily studied in last chapter.

### 2.2.2 NMHV tree amplitude from ACCK

A general formula for determining which residues correspond to tree amplitudes for the  $n$  particle NMHV case has been given in [8] which we will now review. Following their notation we denote a residue when  $n - 5$  minors  $(i_1 \ i_1 + 1 \ i_1 + 2), \dots, (i_{n-5} \ i_{n-5} + 1 \ i_{n-5} + 2) \rightarrow 0$  as  $\{i_1, i_2, \dots, i_{n-5}\}$ , and it is antisymmetric, for instance,  $\{i_1, i_2, i_3\} = -\{i_2, i_1, i_3\}$ . Then NMHV tree amplitude is given by the sum of residues

$$A_{n, \text{BCFW}}^{\text{NMHV}} = (-1)^{n-5} \underbrace{\mathcal{O} \star \mathcal{E} \star \mathcal{O} \star \mathcal{E} \dots}_{(n-5) \text{ factors}} \quad (2.2.3)$$

where  $\mathcal{O}$  is the set of odd numbered particles and  $\mathcal{E}$  is the set of even numbered particles

$$\mathcal{O} = \sum_{k \text{ odd}} \{k\}, \quad \mathcal{E} = \sum_{k \text{ even}} \{k\} \quad (2.2.4)$$

and

$$\{i_1\} \star \{i_2\} = \begin{cases} \{i_1, i_2\} & \text{if } i_1 < i_2 \\ 0 & \text{otherwise} \end{cases} \quad (2.2.5)$$

The above proposal can also be motivated from the geometric picture presented in the recent papers [27] and [26].

To get  $P(\text{BCFW})$  (parity-conjugated BCFW terms) from BCFW, one can simply apply the GRT. For example, the BCFW terms of the seven-point NMHV amplitude can be written as

$$A_7 = \{1, 2\} + \{1, 4\} + \{1, 6\} + \{3, 4\} + \{3, 6\} + \{5, 6\}. \quad (2.2.6)$$

### 2.2.3 Review of the Linked-Connected Prescription

Let us begin by reviewing some details of the connected prescription formula [?]. The  $4|4$  component homogeneous coordinates for the  $i$ -th particle in  $\mathbb{P}^{3|4}$  are  $\mathcal{Z}_i = (\lambda_i^\alpha, \mu_i^{\dot{\alpha}}, \eta_i^A)$  with  $\alpha, \dot{\alpha} = 1, 2$  and  $A = 1, 2, 3, 4$ . The connected formula can be written explicitly in the following form:

$$\mathcal{A}(\mathcal{Z}) = \int \frac{d^{4k|4k} \mathcal{A} d^n \sigma d^n \xi}{\text{vol } GL(2)} \prod_{i=1}^n \frac{\delta^{4|4}(\mathcal{Z}_i - \xi_i \mathcal{P}(\sigma_i))}{\xi_i(\sigma_i - \sigma_{i+1})}, \quad (2.2.7)$$

where  $\mathcal{P}$  is the degree  $k - 1$  polynomial given in terms of its  $k$   $\mathbb{C}^{4|4}$ -valued supercoefficients  $\mathcal{A}_d$  by

$$\mathcal{P}(\sigma) = \sum_{d=0}^{k-1} \mathcal{A}_d \sigma^d. \quad (2.2.8)$$

As emphasized in [21] (see also [28]) the integral (2.2.7) must be interpreted as a contour integral in a multidimensional complex space. The delta functions specify the contour of integration (specifically they indicate which poles to include in the sum over residues). There is also a  $GL(2)$  invariance, of the integrand and the measure, which needs to be gauged. Taking the above connected prescription as a starting point and motivated by [24] one can express the connected prescription (2.2.7) into the form of so-called link representation [22], [23].

One can obtain the physical space amplitude from the link representation

$$\mathcal{A}(\lambda, \tilde{\lambda}) = J \delta(\sum p_i) \oint d\tau U(c_{Ji}(\tau_\gamma)), \quad (2.2.9)$$

where the Jacobian  $J$  generally depends on the parameterization of  $c_{Ji}(\tau_\gamma)$ . A general form of  $U(c_{Ji})$  has been explicitly evaluated by Dolan and Goddard in [23]. For an

amplitude with helicities  $(\epsilon_1, \dots, \epsilon_n)$  comprising  $p$  strings with  $\epsilon_\alpha = +$  and  $p$  strings with  $\epsilon_\beta = -$ , their explicit form is

$$U(c) = F(c) \prod_{k,t} \frac{1}{S_{kt}}, \quad (2.2.10)$$

where  $S_{kt}$  is the sextic  $S_{IJk:RSt} = c_{IS}c_{kt}c_{Jk:RS}c_{IJ:tR} - c_{It}c_{kS}c_{Jk:tR}c_{IJ:RS}$  with  $c_{ij:rs} = c_{ir}c_{js} - c_{jr}c_{is}$ , and

$$F(c) = (c_{IJ:RS})^{N_R-p+2} c_{IR}^{p-3} c_{IS}^{p-3} c_{JR}^{p-3} c_{JS}^{p-3} \prod_{t \in \mathcal{P}'} c_{It}^{l-3} c_{Jt}^{l-3} \prod_{k \in \mathcal{N}'} c_{kR}^{m-3} c_{kS}^{m-3} \prod_{k \in \mathcal{N}} \frac{1}{c_{kt}} \prod_{\alpha=1}^n d_{\alpha,\alpha+1}, \quad (2.2.11)$$

where

$$d_{ir} = c_{ir}, \quad d_{ri} = c_{ir}, \quad d_{ij} = \frac{c_{iR}c_{js}c_{jr}c_{is}}{c_{iR}c_{js} - c_{jr}c_{is}}, \quad d_{rs} = \frac{c_{Ir}c_{js}c_{Is}c_{Jr}}{c_{Ir}c_{js} - c_{Is}c_{Jr}}, \quad i, j \in \mathcal{N}, r, s \in \mathcal{P}.$$

We denote  $\mathcal{P}$  as the set of positive helicity particles and  $\mathcal{N}$  as the set of negative helicity particles, and  $N_R$  is the number of independent sextics,  $l$  is the number of the negative helicity particles,  $m$  the number of the positive helicity particles and  $n = m + p$  is the total number of particles.<sup>1</sup>

## 2.2.4 NMHV tree amplitude from the connected prescription

In order to make the connection between the linked-connected and ACCK formulas more transparent, in this section we will express the linked-connected formula in

---

<sup>1</sup>Here we exchange the helicities  $+$   $\leftrightarrow$   $-$ , at the same time  $c_{ij} \rightarrow c_{ji}$  with respect to [23].

terms of minors as in the ACCK approach.<sup>2</sup>

Let us start with helicity  $(- + - + - + + \cdots + +)$ , and take  $I = 1, J = 3, R = 2, S = 4$ , then formula (2.2.10) becomes

$$U(c) = (c_{52}c_{54}c_{13:24})^{n-6}(c_{12}c_{32}c_{34}c_{54}c_{56}c_{1n}) \prod_{\alpha=6}^{n-1} \frac{c_{1\alpha}c_{1,\alpha+1}c_{3\alpha}c_{3,\alpha+1}}{c_{13:\alpha,\alpha+1}} \prod_{k \in \mathcal{P}, t \in \mathcal{N}} \frac{1}{c_{kt}} \prod_{i=6}^n \frac{1}{S_{135:24i}}. \quad (2.2.12)$$

Using the identity

$$\delta(S_{ijk:rst})\delta(S_{ijk:rst'}) = \delta(S_{ijk:rst})\delta(S_{ijk:rt't}) \frac{c_{it}c_{jk:rt}}{c_{is}c_{jk:rs}}, \quad (2.2.13)$$

we can transform the sextics  $S_{135:24i}$  in (2.2.12) to  $S_{135:246}, S_{135:2,n-1,n}$ , and  $S_{135:i-1,i,i+1}$  to arrive at

$$U'(c) = \frac{c_{35:26}c_{12}c_{13:n-1,n}c_{5,n-1} \prod_{\alpha=8}^n c_{5\alpha} \prod_{\beta=7}^{n-1} c_{3\beta} \prod_{\gamma=6}^{n-2} c_{1\gamma}}{c_{52}c_{14}c_{13:67}c_{35:n-1,n}} \frac{1}{S_1S_2 \dots S_{n-5}}. \quad (2.2.14)$$

We then translate it into minors, the result is<sup>3</sup>

$$A_n = \frac{\mathcal{N}}{(123)(345)(567)(n-1 \ n \ 1)} \frac{1}{S_1S_2 \dots S_{n-5}}, \quad (2.2.15)$$

where the numerator is given as

$$\mathcal{N} = (135)(612)(235)(5 \ n - 1 \ n)(13 \ n - 1) \prod_{\alpha=8}^n (13\alpha) \prod_{\beta=7}^{n-1} (15\beta) \prod_{\gamma=6}^{n-2} (35\gamma). \quad (2.2.16)$$

---

<sup>2</sup> We are grateful to Freddy Cachazo for encouraging us to rewrite everything in terms of minors. There are many different ways to write the formulas, but we will pick the one which makes the proof simpler and has many other nice properties as we will discuss later.

<sup>3</sup>When  $n = 6$  or  $n = 7$  the minor  $(567)$  does not appear in the denominator. And we put the minor  $(135)$  in the numerator by hand to make the scale right, since  $(135) = 1$  for the helicity we started.

The sextics can be written as

$$\begin{aligned}
 S_1 &= (234)(456)(612)(135) - (123)(345)(561)(246), \\
 S_2 &= (n12)(13 \ n - 1)(235)(5 \ n - 1 \ n) - (123)(35 \ n - 1)(5n2)(n - 1 \ n - 1), \\
 S_{i-3} &= (i \ i + 1 \ i + 2)(13 \ i + 2)(15 \ i + 1)(35i) - (135)(3i \ i + 2)(5i \ i + 1)(i + 1 \ i + 2 \ 1),
 \end{aligned} \tag{2.2.17}$$

where  $6 \leq i \leq n - 2$ .

Several comments about this formula are in order.

Firstly, one can deform the sextics by any non-zero parameters  $a_j$ , namely

$$S_j \rightarrow S'_j = (klm)(mnp)(pqr)(qln) - a_j(qkl)(lmn)(npq)(kmp). \tag{2.2.18}$$

As we will prove in next section, interestingly, the final amplitude does not depend on  $a_j$  at all. Taking the limit  $a_j \rightarrow 0$  one gets ACCK formula directly. This appears to be a general fact, not specific to just NMHV amplitudes: the ACCK Grassmannian integrand arises from the linked-connected formula in a simple limit when the second terms in all sextic polynomials are zero.

Secondly, the formula has  $GL(3)$  symmetry for the Grassmannian, even though we had started with the link representation for a particular helicity configuration. We should point out that for some particular gauge fixings, we do not always get the form of each sextic as a polynomial of degree 6 in the  $c'_{Ji}$ s. But, nevertheless, one can numerically check that we do indeed get the tree amplitudes for the connected prescription, namely, the residues at the locus where all the sextics simultaneously vanish.

Thirdly, writing sextics in terms of minors has a simple geometrical interpretation<sup>4</sup>. The minor  $(i \ j \ k) = 0$  in twistor space means the points  $i, j, k$  lie on a line. For NMHV, the sextics  $S_{ijk:lmn} = 0$  means that these six points  $i, j, k, l, m, n$  lie a conic curve [29], which is consistent with the origin of the connected prescription–integrating out degree two curves in twistor space as in formula (2.2.7).

## 2.3 From the Connected to ACCK Using GRT

In this section we will use the multidimensional Global Residue Theorem (GRT) to analytically derive the BCFW contour of ACCK as in (2.2.3) from the connected prescription formula (2.2.15).

### 2.3.1 n=6 and n=7

We begin with  $n = 6$  and  $n = 7$  cases, which were previously done in [22], [23].

- For the six-point amplitude, the connected formula gives

$$A_6 = \frac{(135)}{(123)(345)(561)} \frac{1}{S}, \quad (2.3.1)$$

where

$$S = (234)(456)(612)(135) - (123)(345)(561)(246). \quad (2.3.2)$$

---

<sup>4</sup>This was emphasised to us by Freddy Cachazo.

Cauchy's theorem states that the sum of residues in this expression is zero, so

$$\{S\} = -\{1\} - \{3\} - \{5\}, \quad (2.3.3)$$

which is ACCK formula (2.2.3) for  $n = 6$ .

- For the seven-point amplitude,

$$A_7 = \frac{(135)(235)(612)(136)}{(123)(345)(671)} \frac{1}{S_1 S_2}, \quad (2.3.4)$$

where

$$\begin{aligned} S_1 &= (234)(456)(612)(135) - (123)(345)(561)(246), \\ S_2 &= (567)(712)(235)(136) - (123)(356)(572)(671). \end{aligned} \quad (2.3.5)$$

By applying GRT, we get

$$\{S_1, S_2\} = \{1, S_1\} + \{3, S_1\} + \{6, S_1\}. \quad (2.3.6)$$

On the poles  $(123) = 0$  and  $(345) = 0$ , the second term of  $S_1$  vanishes and we get

$$\{1, S_1\} = \{1, 2\} + \{1, 4\}, \quad \{3, S_1\} = \{3, 2\} + \{3, 4\}. \quad (2.3.7)$$

Note that the terms with non-adjacent minors do not contribute because they would be cancelled by the numerator of  $A_7$ . Moreover, the condition of the residue  $\{3, 2\}$  implies that the points 2, 3, 4, 5 lie on a line and hence  $(235) = 0$ , which is a term in

the numerator of  $A_7$ . To simplify the residue  $\{6, S_1\}$  we use GRT again

$$\{6, S_1\} = -(\{6, S_2\} + \{6, 1\} + \{6, 3\}) \quad (2.3.8)$$

$$= -(\{6, 5\} + \cancel{\{6, 7\}} + \{6, 1\} + \{6, 3\}). \quad (2.3.9)$$

Again,  $(671) = 0$  makes the second term of  $S_2$  vanish, hence  $\{6, S_2\} = \{6, 5\} + \{6, 7\}$ . But the condition of  $\{6, 7\}$  implies that  $(612) = 0$ , which is a term in the numerator of  $A_7$ . So finally, collecting all the residues we get

$$\{S_1, S_2\} = \{1, 2\} + \{1, 4\} + \{1, 6\} + \{3, 4\} + \{3, 6\} + \{5, 6\}. \quad (2.3.10)$$

These are exactly the BCFW contours of the ACCK formula (2.2.3).

Let us conclude this section by saying that there are two useful properties which play an important role in making the above proof simple. First, the second terms of the sextics vanish for some particular contours. Second, the residue vanishes if one of the non-adjacent minors in the first term of the sextic vanishes. We will use these two simple facts in the general proof, which follows in the next section.

### 2.3.2 All $n$ proof

Let us first note that one can easily check that the second terms of the sextics vanish for any BCFW contours. It means that whenever we get a BCFW contour (2.2.3) by applying GRT, we are sure that our NMHV formula for the amplitude is exactly of the same form as in ACCK amplitude, namely all the non-adjacent minors cancel out.

We can further check that there are no ‘spurious’ solutions, having non-vanishing contribution, from the connected contour. Spurious solutions are those where the sextics vanish because individual minors in the expressions for the sextics vanish (non-spurious solutions are those where the two terms in every sextic are separately non-zero). We should exclude these solutions simply because the vanishing of any individual minor of the sextics means that the conic curve is not smooth anymore<sup>5</sup>.

The way to get BCFW contours from connected prescription is simply to get rid of all the sextics in the connected contour by applying GRT repeatedly. Let us remind you that the poles in formula (2.2.15) are

$$(123)(345)(567)(n-1\ n\ 1)S_1S_2\dots S_{n-5}. \quad (2.3.11)$$

Use GRT we have

$$\begin{aligned} \{S_2S_1\dots S_{n-5}\} &= -(\{1S_1S_3\dots S_{n-5}\} + \{3S_1S_3\dots S_{n-5}\} \\ &\quad + \underbrace{\{5S_1S_3\dots S_{n-5}\}}_{\{5S_1678\dots(n-2)\}} + \{(n-1)S_1S_3\dots S_{n-5}\}) \\ &= -(\{12S_3\dots S_{n-5}\} + \{14S_3\dots S_{n-5}\} + \{34S_3\dots S_{n-5}\} \\ &\quad + \underbrace{\{32S_3\dots S_{n-5}\}}_{\{32S_3678\dots(n-2)\}} + \{(n-1)S_16\dots(n-2)\}), \end{aligned} \quad (2.3.12)$$

where  $\{1S_1S_3\dots S_{n-5}\}$  is the residue of  $(123) = S_1 = S_3 = \dots = S_{n-5} = 0$ , and etc.

In order to explain why  $\{5S_1S_3\dots S_{n-5}\} = 0$  first notice that  $\{5S_1S_3S_4\dots S_{n-5}\} = \{5S_1678\dots(n-2)\}$ . This is true because on  $(567) = 0$  the second term of  $S_3$  vanishes and hence  $\{5S_1S_3\dots S_{n-5}\} = \{5S_16S_4\dots S_{n-5}\}$ . Now in addition to  $(567) = 0$ , we also have  $(678) = 0$  which implies that the points 5, 6, 7, 8 lie on a line and hence

---

<sup>5</sup>The same reasoning holds for the validity of identity (3.4.1).

$(578) = 0$ , resulting in the second term of  $S_4$  vanishing. So, we get  $\{5S_16S_4 \dots S_{n-5}\} = \{5S_167S_5 \dots S_{n-5}\}$ . We can again apply similar arguments on  $S_4$  and reduce it to  $(789)$ , and this goes on until the last sextic of the residue, which is  $S_{n-5}$ . Now,  $\{5S_1678 \dots (n-2)\}$  means that the points  $5, 6, \dots, n$  lie on a straight line, so  $(5 \ n-1 \ n)$  in the numerator vanishes, and hence  $\{5S_1S_3 \dots S_{n-5}\} = 0$ .

The equality  $\{(n-1)S_1S_3 \dots S_{n-5}\} = \{(n-1)S_16 \dots (n-2)\}$  in (2.3.12) can also be explained along the same lines, but starting from the fact that, due to  $(n-1 \ n1) = 0$ ,  $S_{n-5}$  is replaced by  $(n-2 \ n-1 \ n)$ . Finally  $\{32S_3 \dots S_{n-5}\} = 0$  simply because  $(345) = (234) = 0$  implies  $(235) = 0$ , which is a term in the numerator.

In the following, we will study each term from (2.3.12) individually. In the process, we will ignore all the vanishing terms without explanation, since the reasons are very similar.

### $\{(n-1)S_16 \dots (n-2)\}$ term

By applying GRT again, with the poles

$$(123)(345)(567)(n-1 \ n1)S_1(n12)(678)(789) \dots (n-2 \ n-1 \ n),$$

we get the following non-vanishing residues

$$\begin{aligned} -\{(n-1)S_16 \dots (n-2)\} &= \{(n-1)16 \dots (n-2)\} + \{(n-1)36 \dots (n-2)\} \\ &\quad + \{(n-1)56 \dots (n-2)\}. \end{aligned} \tag{2.3.13}$$

Actually these three terms are all the contours of the form  $\{i6\dots\}$  and  $i$  can be 1, 3 or 5, and they have the correct signs.

### $\{34S_3\dots S_{n-5}\}$ term

Now, in this case the poles are

$$(123)(345)(567)(n-1\ n1)(234)(456)(n12)S_3S_4\dots S_{n-5}.$$

Again using GRT we get

$$-\{34S_3\dots S_{n-5}\} = \underbrace{\{345S_4\dots S_{n-5}\}}_{A_1} + \{34(n-1)7\dots(n-2)\}. \quad (2.3.14)$$

The second term in the previous equation is a BCFW term and we use GRT again on the term  $A_1$  to generate another BCFW term in the next step

$$\{345S_4\dots S_{n-5}\} = -\left(\underbrace{\{3456S_5\dots S_{n-5}\}}_{A_2} + \{345(n-1)8\dots(n-2)\}\right). \quad (2.3.15)$$

Similarly, we can keep on using GRT repeatedly on one of the two terms, generated at each step by using GRT in the previous step. In the final step of this iteration, by applying GRT we get two terms,  $\{34567\dots(n-4)(n-1)\}$  and  $\{34567\dots(n-3)\}$ . So in this way, we generate  $\{347\dots(n-1)\} + \{3458\dots(n-1)\} + \{34569\dots(n-1)\} + \dots + \{34567\dots(n-3)\}$ , which are all the BCFW contours of the form  $\{34\dots\}$ .

$\{14S_3 \dots S_{n-5}\}$  term

Now, let us consider the contours of the form  $\{14 \dots\}$ . Here the poles are given as

$$(123)(345)(567)(n-1 \ n1)(234)(456)(n12)S_3S_4 \dots S_{n-5}. \quad (2.3.16)$$

Using GRT we get the following

$$-\{14S_3 \dots S_{n-5}\} = \{14(n-1)7 \dots (n-2)\} + \underbrace{\{142S_4 \dots S_{n-5}\}}_{X_1} + \underbrace{\{145S_4 \dots S_{n-5}\}}_{B_1} \quad (2.3.17)$$

Apart from the BCFW term  $\{147 \dots (n-1)\}$  we also have other non-BCFW terms.

Out of these, we will see that the terms like  $X_1$  generated at each step will cancel out later from the same terms generated by  $\{12S_3 \dots S_{n-5}\}$  in the next subsection. We can again apply GRT on  $B_1$ . Now, we can see the pattern of BCFW terms generated from the  $B_i$  terms, and here we will not write the non-BCFW terms explicitly at each step

$$\begin{aligned} \{14S_3 \dots S_{n-5}\} &\Rightarrow \{147 \dots (n-1)\}, \\ \{145S_4 \dots S_{n-5}\} &\Rightarrow \{1458 \dots (n-1)\}, \\ \{1456S_5 \dots S_{n-5}\} &\Rightarrow \{14569 \dots (n-1)\}, \\ &\dots \end{aligned} \quad (2.3.18)$$

In the final step of this series, by applying GRT, we have two terms,  $\{14567 \dots (n-4)(n-1)\}$  and  $\{145678 \dots (n-3)\}$ . So by using GRT repeatedly, we get all the BCFW contours of the type  $\{14 \dots\}$ , namely  $\{147 \dots (n-1)\} + \{1458 \dots (n-1)\} + \{14569 \dots (n-1)\} + \dots + \{145678 \dots (n-3)\}$ .

$\{12S_3 \dots S_{n-5}\}$  term

Finally, we look at the remaining contours  $\{12S_3 \dots S_{n-5}\}$  in equation (2.3.12).

Let us apply GRT and we get

$$\begin{aligned} -\{12S_3 \dots S_{n-5}\} = & \{126 \dots (n-3)3\} + \{126 \dots (n-3)5\} \\ & + \underbrace{\{12S_3 \dots S_{n-6}(n-1)\}}_{C_1} + \underbrace{\{12S_3 \dots S_{n-6}4\}}_{D_1}. \end{aligned} \quad (2.3.19)$$

We can apply GRT on the term  $C_1$  in (2.3.19) again, and we will deal with the term  $D_1$  later. From  $C_1$  we get

$$\begin{aligned} \{12S_3 \dots S_{n-6}(n-1)\} = & -(\{126 \dots (n-4)3(n-1)\} + \{126 \dots (n-4)5(n-1)\}) \\ & + \underbrace{\{12S_3 \dots S_{n-7}(n-2)(n-1)\}}_{C_2} + \underbrace{\{12S_3 \dots S_{n-7}4(n-1)\}}_{E_1}. \end{aligned} \quad (2.3.20)$$

We notice that one of the non-BCFW terms,  $C_2$ , is a similar kind of term to  $C_1$ . Terms which are similar to  $E_1$  and generated at each step, will combine with other terms generated from the subsequent steps of applying GRT. The general trend of BCFW contours generated from the  $C_i$  terms are

$$\begin{aligned} \{12S_3 \dots S_{n-5}\} \Rightarrow & \{1236 \dots (n-3)\} + \{1256 \dots (n-3)\}, \\ \{12S_3 \dots S_{n-6}(n-1)\} \Rightarrow & \{1236 \dots (n-4)(n-1)\} + \{1256 \dots (n-4)(n-1)\}, \\ \{12S_3 \dots S_{n-7}(n-2)(n-1)\} \Rightarrow & \{1236 \dots (n-5)(n-2)(n-1)\} \\ & + \{1256 \dots (n-5)(n-2)(n-1)\}, \\ & \dots \dots \end{aligned} \quad (2.3.21)$$

Note that at each step of the iteration we also generate some non-BCFW terms (not explicitly written down in the above pattern) which need to be dealt with as before. The final step in the above series generates the BCFW terms  $\{1238\dots(n-1)\}$ ,  $\{1258\dots(n-1)\}$  and  $\{1278\dots(n-1)\}$ .

By similar methods we can generate the other BCFW contours of the form  $\{12\dots\}$  by using non-BCFW terms generated in previous steps. Since all the steps are similar, here we only give some examples of generating BCFW terms, without showing the details

$$\begin{aligned}
 \{12S_3\dots S_{n-6}4\} &\Rightarrow \{12347\dots(n-3)\}, \\
 \{125S_4\dots S_{n-6}4\} &\Rightarrow \{123458\dots(n-3)\}, \\
 \{1256S_5\dots S_{n-6}4\} &\Rightarrow \{1234569\dots(n-3)\}, \\
 &\dots
 \end{aligned} \tag{2.3.22}$$

Again the last step of this iterative process is special, the BCFW term generated is  $\{1234\dots(n-5)\}$ . We will give a few examples of how non-BCFW terms combine to generate BCFW terms and we choose these particular examples as they give residues related to the ones in (2.3.22). Firstly

$$\begin{aligned}
 \{12(n-1)S_4\dots S_{n-6}4\} + \{12S_3\dots S_{n-7}4(n-1)\} &\Rightarrow \{12347\dots(n-4)(n-1)\}, \\
 \{12(n-1)S_4\dots S_{n-7}(n-2)4\} + \{12S_3\dots S_{n-8}4(n-2)(n-1)\} \\
 &\Rightarrow \{12347\dots(n-5)(n-2)(n-1)\}, \\
 &\dots
 \end{aligned} \tag{2.3.23}$$

The BCFW term generated from the last step of the above series is  $\{12349\dots(n-1)\}$ .

Next example is

$$\begin{aligned}
 & \{125(n-1)S_5 \dots S_{n-6}4\} + \{12(n-1)S_4 \dots S_{n-7}54\} \Rightarrow \{123458 \dots (n-4)(n-1)\}, \\
 & \{125(n-1)S_5 \dots S_{n-7}(n-2)4\} + \{12(n-1)S_4 \dots S_{n-8}5(n-2)4\} \\
 & \Rightarrow \{123458 \dots (n-5)(n-2)(n-1)\}, \\
 & \dots\dots
 \end{aligned} \tag{2.3.24}$$

The last step generates BCFW term  $\{1234510 \dots (n-1)\}$ . And one more example will be

$$\begin{aligned}
 & \{125(n-1)S_5 \dots S_{n-7}64\} + \{1256(n-1)S_6 \dots S_{n-6}4\} \Rightarrow \{1234569 \dots (n-4)(n-1)\}, \\
 & \{125(n-1)S_5 \dots S_{n-8}6(n-2)4\} + \{1256(n-1)S_6 \dots S_{n-7}(n-2)4\} \\
 & \Rightarrow \{1234569 \dots (n-5)(n-2)(n-1)\}, \\
 & \dots\dots
 \end{aligned} \tag{2.3.25}$$

The BCFW term generated in the last step is  $\{12345611 \dots (n-1)\}$ .

From the above mentioned examples, we can see the general pattern: the first term in (2.3.22),  $\{12347 \dots (n-3)\}$ , combining with all the terms from (2.3.23) generates all the contours of the form  $\{12347 \dots \}$ ; similarly, the second term in (2.3.22),  $\{123458 \dots (n-3)\}$ , and all the terms in (2.3.24) give us all the contours of the form  $\{123458 \dots \}$ ; the third term in (2.3.22),  $\{1234569 \dots (n-3)\}$ , together with all the terms of (2.3.25) give us all the contours of the form  $\{1234569 \dots \}$ . It is not hard to see that all the other BCFW terms of the form  $\{1234 \dots \}$  can be generated in a similar way. So we have generated all the contours of the form  $\{12 \dots \}$  and we notice that they can be grouped into contours of the form,  $\{1236 \dots \}$ ,  $\{1256 \dots \}$ ,

$\{1238\dots\}$ ,  $\{1258\dots\}$ ,  $\{1278\dots\}$  and  $\{1234\dots\}$ .

As we had seen so far, each GRT step also generates terms which have no contribution to BCFW contours. These terms, typically, look like  $\{124\dots i, S_i, \dots, S_{n-5}\}$ , but they just cancel out in pairs at each step. At each of the final steps, we also generate terms like  $\{124\dots i, i+4, \dots, (n-1)\}$  and  $\{124\dots (n-4)\}$ , and they also cancel out.

Let us conclude with our main result

$$\oint_C \frac{\mathcal{N}}{(123)(345)(567)(n-1\ n\ 1)} \frac{1}{S_1 S_2 \dots S_{n-5}} = \oint_B \frac{1}{(123)(234)\dots(n12)}, \quad (2.3.26)$$

where contour  $C$  is the connected contour, and  $B$  is the BCFW contour. One can apply GRT again and show that the same equality is true for the P(BCFW) contour.

Since for any BCFW contour the second terms of sextics vanish, so as a byproduct, we also proved the statement we made before that deforming sextics by some non-zero parameters still gives us the correct tree amplitude.

# Chapter 3

## Twistor string theory and Grassmannian: All tree-level amplitude

### 3.1 Introduction

In this chapter, we present a new, explicit formula for all  $N^{(k-2)}\text{MHV}$  tree amplitudes in  $\mathcal{N} = 4$ , generalizing the NMHV results of last chapter. And this compact formula lacks any recursive-explosion of indices such as was required in the ‘explicit’ formula derived from BCFW in [7]. In section 2 we will present our main formula, equation (3.2.1), and discuss its smooth deformation to a contour in  $\mathcal{L}_{n,k}$ . In section 3 we will describe how this formula can be obtained by iteratively ‘adding particles’ in a natural way to the first non-trivial tree amplitude, the 6-point NMHV amplitude,

while making sure that soft limits and parity are manifest at every stage. In section 4 we will make a series of transformations to map our formula to that of [23], thereby deriving it from twistor string connected prescription.

## 3.2 All Tree Amplitudes in $\mathcal{N} = 4$ Super Yang-Mills

We propose that the general, tree-level, planar, color-stripped,  $n$ -point  $\mathcal{N}^{(k-2)}\text{MHV}$  amplitude is given by

$$\mathcal{A}_n^{(k)} = \frac{1}{\text{vol}[\text{GL}(k)]} \oint_{\mathcal{F}_n^{(k)} = \vec{0}} \frac{dC_{\alpha a} \mathcal{H}_n^{(k)}}{(n-1)(1)(3) \mathcal{F}_n^{(k)}} \prod_{\alpha=1}^k \delta^{4|4} (C_{\alpha a} \mathcal{W}_a), \quad (3.2.1)$$

where the contour  $\mathcal{F}_n^{(k)} = \vec{0}$  is the zero-locus of  $\mathcal{F}_n^{(k)} : \mathbb{C}^{(n-k-2)(k-2)} \rightarrow \mathbb{C}^{(n-k-2)(k-2)}$ , defined in terms of the  $(n-k-2)(k-2)$  Veronese maps  $F_\ell^j$ ,

$$\mathcal{F}_n^{(k)} \equiv \prod_{\ell=k+3}^n \left( \prod_{j=1}^{k-2} F_\ell^j \right), \quad (3.2.2)$$

where each  $F_\ell^j$  can be written in terms of the minors of  $C_{\alpha a}$  according to

$$F_\ell^j \equiv \begin{aligned} & \left( \sigma_\ell^j \ \ell-2 \ \ell-1 \ \ell \right) \left( \sigma_\ell^j \ \ell \ j \ j+1 \right) \left( \sigma_\ell^j \ j+1 \ j+2 \ \ell-2 \right) \left( \sigma_\ell^j \ \ell-1 \ j \ j+2 \right) \\ & - \left( \sigma_\ell^j \ j \ j+1 \ j+2 \right) \left( \sigma_\ell^j \ j+2 \ \ell-2 \ \ell-1 \right) \left( \sigma_\ell^j \ \ell-1 \ \ell \ j \right) \left( \sigma_\ell^j \ j+1 \ \ell-2 \ \ell \right), \end{aligned} \quad (3.2.3)$$

with  $\sigma_\ell^j$  representing collectively the columns  $[1, \dots, j-1] \cup [j+\ell-k, \dots, \ell-3]$  of  $C_{\alpha a}$ , and where  $\mathcal{H}_n^{(k)}$  is the product of all the *non-consecutive* minors in the *first line* of equation (3.2.3); explicitly,

$$\begin{aligned} \mathcal{H}_n^{(k)} &= \mathcal{H}_{n-1}^{(k)} \times (\sigma_{n-1}^{k-2} \ n-1 \ k-2 \ k-1) \\ &\times \prod_{j=1}^{k-3} \left[ (\sigma_n^j \ n \ j \ j+1) (\sigma_{n-1}^{j+1} \ n-3 \ n-2 \ n-1) \right] \prod_{j=1}^{k-2} \left[ (\sigma_n^j \ n-1 \ j \ j+2) (\sigma_n^j \ j+1 \ j+2 \ n-2) \right]. \end{aligned}$$

Noticing that all the minors appearing in a given map  $F_\ell^j$  involve the same set of columns  $\sigma_\ell^j$ , and that the rest are organized according to a ‘ $3 \times 3$ ’ Veronese operator, we may encode the structure of equation (3.2.3) by writing<sup>1</sup>

$$\begin{aligned} F_\ell^j &\equiv \sigma_\ell^j \bowtie S_{\ell-2 \ \ell-1 \ \ell \ j \ j+1 \ j+2}, \\ &\equiv \left( [1, \dots, j-1] \bigcup [j+\ell-k, \dots, \ell-3] \right) \bowtie S_{\ell-2 \ \ell-1 \ \ell \ j \ j+1 \ j+2}, \end{aligned} \quad (3.2.4)$$

where  $S_{a b c d e f}$  represents the primitive Veronese operator which, when acting on  $\mathbb{P}^2$ , tests if the six points  $a, \dots, e$  lie on a conic,

$$S_{a b c d e f} \equiv (a b c)(c d e)(e f a)(b d f) - (b c d)(d e f)(f a b)(c e a). \quad (3.2.5)$$

As will be described below, the structure of the numerators  $\mathcal{H}_n^{(k)}$  is dictated entirely by the proposed duality between equation (3.2.1) and a related expression in  $\mathcal{L}_{n,k}$ . Following the theme of [9, 10], let us introduce a deformation parameter  $t_\ell^j$  for each map  $F_\ell^j$ ,

$$\begin{aligned} F_\ell^j(t_\ell^j) &\equiv \left( \sigma_\ell^j \ \ell-2 \ \ell-1 \ \ell \right) \left( \sigma_\ell^j \ \ell \ j \ j+1 \right) \left( \sigma_\ell^j \ j+1 \ j+2 \ \ell-2 \right) \left( \sigma_\ell^j \ \ell-1 \ j \ j+2 \right) \\ &\quad - t_\ell^j \left( \sigma_\ell^j \ j \ j+1 \ j+2 \right) \left( \sigma_\ell^j \ j+2 \ \ell-2 \ \ell-1 \right) \left( \sigma_\ell^j \ \ell-1 \ \ell \ j \right) \left( \sigma_\ell^j \ j+1 \ \ell-2 \ \ell \right). \end{aligned} \quad (3.2.6)$$

Then the integral  $\mathcal{A}_n^{(k)}(t_\ell^j)$ , with all  $F_\ell^j$  in (3.2.1) replaced by  $F_\ell^j(t_\ell^j)$ , will map precisely to the one appearing for  $\mathcal{L}_{n,k}$  in limit of  $t_\ell^j \rightarrow 0$  for all  $\ell, j$ . This is because, together with the three minors manifest in equation (3.2.1) (namely, (n-1), (1), and (3)) the factors which constitute  $\mathcal{F}_n^{(k)}(t_\ell^j)$  when  $t_\ell^j \rightarrow 0$  will contribute exactly one copy

---

<sup>1</sup>This simplified notation can be justified by observing that only 6 of the  $k+3$  columns which are relevant to a given Veronese operator  $F_\ell^j$  change from one term to another.

of each of the consecutive minors present in the measure of the integral  $\mathcal{L}_{n,k}$ :

$$\mathcal{F}_n^{(k)} = \underbrace{\left( F_{k+3}^1 \cdots F_{k+3}^{k-2} \right)}_{\cup (2),(4)} \underbrace{\left( F_{k+4}^1 \cdots F_{k+4}^{k-2} \right)}_{\cup (5)} \underbrace{\left( F_{k+5}^1 \cdots F_{k+5}^{k-2} \right)}_{\cup (6)} \cdots \underbrace{\left( F_{n-1}^1 \cdots F_{n-1}^{k-2} \right)}_{\cup (n-k)} \underbrace{\left( F_n^1 \cdots F_n^{k-2} \right)}_{\cup (n-k+1), \dots, (n-2), (n)} .$$

And since  $\mathcal{H}_n^{(k)}$  is composed of all the *non-consecutive* minors present in the *first* factors of each  $F_\ell^j$ , we have that

$$\lim_{t_\ell^j \rightarrow 0} \left( \frac{\mathcal{H}_n^{(k)}}{(n-1)(1)(3) \mathcal{F}_n^{(k)}} \right) = \frac{1}{(n-1)(1)(3)} \frac{1}{(2)(4)(5) \cdots (n-3)(n-2)(n)}, \quad (3.2.7)$$

making the connection between the twistor string and  $\mathcal{L}_{n,k}$  manifest.

We strongly suspect that formula (3.2.1) is unchanged by any of the deformations introduced by the parameters  $t_\ell^j$  in (3.2.6). For NMHV amplitudes,  $t_\ell^j$ -independence has been rigorously proven by a direct application of the global residue theorem, [10, 9], and we suspect that similar arguments can be used to prove  $t_\ell^j$ -independence more generally. We have checked this numerically for several nontrivial  $N^2$ MHV amplitudes, including the alternating-helicity amplitude for eight gluons, but we leave the question of proving complete  $t_\ell^j$ -independence to future researches.

Let us end this section by presenting explicitly the  $t_\ell^j \rightarrow 0$  limit of the deformed twistor-string contour (3.2.1), illustrating some of the key differences between the two formulations. When  $t_\ell^j \rightarrow 0$ , each Veronese operator factorizes into the product of the four minors listed in the first line of (3.2.6). In general, all but  $n-3$  of these factors will be non-consecutive, and therefore are included among the factors of the numerator  $\mathcal{H}_n^{(k)}$ . Although it is generally ill-advised to ‘cancel terms’ between the contour-defining maps defining  $\mathcal{F}_n^{(k)}$  and the numerator, there is a good physical

reason for suspecting that the ‘fourth’ minors of each of the  $F_\ell^j(t_\ell^j \rightarrow 0)$ —which are never consecutive—contribute no non-vanishing residues to the contour.<sup>2</sup> As described in [30, 10], CSW operators, when translated into the Grassmannian, are constructed from products of three minors. Although beyond the scope of the present discussion, ensuring that each pole of the integrand is composed of three-minor operators helps one to connect the CSW, or ‘disconnected’, support of tree amplitudes to the ‘connected’ support of the twistor string through a series of global residue theorems. At any rate, there is now enough direct evidence that general tree-contours are entirely supported on the vanishing first three factors of each  $F_\ell^j$  when  $t_\ell^j \rightarrow 0$  to justify the simplification to a ‘3-minor’ form of each map in the contour.

Taking each  $t_\ell^j \rightarrow 0$ , the twistor-string contour  $\mathcal{A}_n^{(k)}(t_\ell^j)$  becomes,

$$\mathcal{A}_n^{(k)}(t_\ell^j) \xrightarrow[t_\ell^j \rightarrow 0]{} \mathcal{A}_n^{(k)} = \frac{1}{\text{vol}[\text{GL}(k)]} \oint_{\mathcal{F}_n^{(k)} = \vec{0}} \frac{dC_{\alpha a} \ \mathcal{H}_n^{(k)}}{(n-1)(1)(3) \ \mathcal{F}_n^{(k)}} \prod_{\alpha=1}^k \delta^{4|4} (C_{\alpha a} \mathcal{W}_a), \quad (3.2.8)$$

where

$$\mathcal{F}_n^{(k)} \equiv \prod_{\ell=k+3}^n \left( \prod_{j=1}^{k-2} f_\ell^j \right) \quad \text{with} \quad f_\ell^j \equiv \sigma_\ell^j \bowtie (\ell-2 \ \ell-1 \ \ell) (\ell \ j \ j+1) (j+1 \ j+2 \ \ell-2), \quad (3.2.9)$$

with  $\sigma_\ell^j$  as before, and where

$$\mathcal{H}_n^{(k)} = \frac{\mathcal{H}_n^{(k)}}{\prod_{\ell=k+3}^n \prod_{j=1}^{k-2} (\sigma_\ell^j \ \ell-1 \ j \ j+2)}, \quad (3.2.10)$$

---

<sup>2</sup>The reason why naïve cancellation of factors between  $\mathcal{H}_n^{(k)}$  and those in  $\mathcal{F}_n^{(k)}(t_\ell^j \rightarrow 0)$  can be misleading is described with several examples in [10]; for example, even the poles supported by purely non-consecutive minors of the  $F_\ell^j$ ’s can have the interpretation of being supported by consecutive minors, and thereby contributing a residue to the contour.

which, as before, represents the product of all non-consecutive minors among the maps  $f_\ell^j$ .

Alternatively, we could have started with formula (3.2.8) for  $\mathcal{A}_n^{(k)}$  and obtained formula (3.2.1) for  $\mathcal{A}_n^{(k)}$  by “adding a missing minor” to each map of  $f$  according to

$$\begin{aligned} f &= \sigma \bowtie (a b c)(c d e)(e f a) \\ \Rightarrow F &= \sigma \bowtie [(a b c)(c d e)(e f a)(b d f) - (b c d)(d e f)(f a b)(c e a)], \end{aligned} \tag{3.2.11}$$

in order to supply a simple geometric meaning to the contour—the maps  $F$ ’s having the natural interpretation of testing the localization of points in  $\mathbb{P}^{(k-1)}$ .

Both formulae give all tree-level amplitudes in  $\mathcal{N} = 4$  super Yang-Mills in terms of a specific contour integral. The first one, equation (3.2.1), naturally arises from twistor string theory, and its contour  $\mathcal{F}_n^{(k)} = \bar{0}$  has a nice geometric meaning: it is the constraint for  $n$  points to lie on a degree- $(k-1)$  curve in twistor space. On the other hand, the formula (3.2.8) provides the integration contour for Grassmannian  $\mathcal{L}_{n,k}$ , and thereby ensures that each contribution is itself manifestly Yangian invariant.

### 3.3 Building the General Contour, one Particle at a Time

In this section we describe how the general contour for any tree amplitude (3.2.1) can be obtained by sequentially extending the contour of the first non-trivial amplitude, the 6-point NMHV amplitude, by adding one particle at a time. Before doing so, however, it will be useful to briefly discuss some of the generally-desirable features

that any such contour-prescription should have.

Let us consider what would be necessary to extend a formula valid for  $\mathcal{L}_{n-1,k}$  to one valid for  $\mathcal{L}_{n,k}$  while keeping  $k$  fixed. Recall that the integral  $\mathcal{L}_{n,k}$ 's measure is given by the product of the  $n$  consecutive  $k \times k$  minors of  $C_{\alpha a}$ . The  $n^{\text{th}}$  particle, being represented by the  $n^{\text{th}}$  column of  $C_{\alpha a}$  participates in  $k$  of these consecutive minors; and these  $k$  minors, taken together, span a range of  $\min(n, 2k - 1)$  columns of  $C_{\alpha a}$ . This suggests that, fixing  $k$ , only for  $n \geq 2k - 1$  will a tree contour be sufficiently general to have a natural extension to all  $n$ . Conveniently however, the  $n = (2k - 1)$ -point  $N^{k-2}$ MHV amplitude,  $\mathcal{A}_{n=2k-1}^{(k)}$ , is nothing but the parity-conjugate of the  $n$ -point  $N^{k-3}$ MHV amplitude,  $\mathcal{A}_{n=2k-1}^{(k-1)}$ , allowing it to be uniquely related to a contour with strictly lower- $k$ . And so we should not be too surprised that it is possible to ‘bootstrap’ a formula valid for any fixed  $k$  to one valid for all  $k$ , using parity when  $n = 2k - 1$  as the bridge which connects each  $k$  to  $k + 1$ .

Just as there are several equally-valid formulae for the general NMHV tree contour (see, e.g. [10, 23, 9, 22]), there are several ways of writing the general  $N^{(k-2)}$ MHV tree contour. The one that we derive here is obtained by starting with the particular NMHV tree contour given in [10] and extending it in such a way that the general contour prescription is invariant under parity for all  $n, k$ . As we will see, these criteria lead uniquely to the contour given here which defines our general result given in equation (3.2.1).<sup>3</sup>

---

<sup>3</sup>We have also found other parity-symmetric contour prescriptions by starting from each of the different forms of the NMHV tree amplitude. We have checked that each of these extensions to all  $n, k$  is unique and that each leads to correct formulae for general tree amplitudes. In addition, there are further possibilities if one foregoes the connection between  $\mathcal{L}_{n,k}$  and the twistor string, but these will not be considered here.

### 3.3.1 NMHV amplitudes

Let us begin with the simplest amplitude which requires a non-trivial contour to be specified. The 6-point NMHV amplitude's contour is essentially unique up to a global residue theorem, and can be written [10, 23, 8, 9, 22],

$$\mathcal{A}_6^{(3)} = \frac{1}{\text{vol}[\text{GL}(3)]} \oint_{\mathcal{F}_6^{(3)} = \vec{0}} dC_{\alpha a} \frac{\mathcal{H}_6^{(3)}}{(5)(1)(3)} \frac{1}{\mathcal{F}_6^{(3)}} \prod_{\alpha=1}^3 \delta^{4|4}(C_{\alpha a} \mathcal{W}_a), \quad (3.3.1)$$

where

$$\mathcal{F}_6^{(3)} = \left[ \cancel{(4)} \cancel{(6)} \cancel{(2)} (135) - (561)(123)(345)(624) \right] = S_{456123} \quad (3.3.2)$$

$$\text{and} \quad \mathcal{H}_6^{(3)} = (135).$$

(Here, we have chosen to de-emphasize the minors which do not appear in the analogous expressions for  $\mathcal{L}_{n,k}$  by colouring them grey, and we have chosen to highlight each of the *consecutive* minors which participate in the contour by colouring them red. This highlighting will be useful when we consider amplitudes involving more particles and with  $k > 3$ .)

As demonstrated in [10], this contour can be extended to all NMHV amplitudes in the following way,

$$\mathcal{A}_n^{(3)} = \frac{1}{\text{vol}[\text{GL}(3)]} \oint_{\mathcal{F}_n^{(3)} = \vec{0}} dC_{\alpha a} \frac{\prod_{\ell=6}^{n-1} [(12\ell)(23\ell-1)]}{(n-1)(1)(3)} \frac{\prod_{\ell=6}^n [(13\ell-1)]}{\mathcal{F}_n^{(3)}} \prod_{\alpha=1}^3 \delta^{4|4}(C_{\alpha a} \mathcal{W}_a), \quad (3.3.3)$$

where

$$\mathcal{F}_n^{(k)} = \prod_{\ell=6}^n \left[ \cancel{(\ell-2 \ \ell-1 \ \ell)} (\ell 1 2)(2 3 \ell-2)(\ell-1 1 3) - (\ell-1 \ \ell 1)(1 2 3)(3 \ell-2 \ell-1)(\ell 2 \ \ell-1) \right] = \prod_{\ell=6}^n S_{\ell-2 \ \ell-1 \ \ell 1 2 3}.$$

Notice that the only operator that involves particle  $n$  is the last,  $F_{\ell=n}^{j=1}$ , and this operator includes in general all but one of the consecutive minors which involve column  $n$ —namely, all but minor  $(n-1)$ . Indeed, each  $F_\ell^1$  can be seen as an operator which adds particle  $\ell$  to the  $(\ell-1)$ -point contour.

Consider for example the contour for  $n=7$ ,

$$\mathcal{F}_7^{(3)} = \left\{ \begin{array}{l} F_6^1 = (4) (612) (2) (513) - (561)(123)(345)(624) = S_{456123} \\ F_7^1 = (5) (7) (235)(613) - (671)(123)(356)(725) = S_{567123} \end{array} \right\}. \quad (3.3.4)$$

By recognizing that  $\mathcal{A}_7^{(3)}$  is nothing but the parity-conjugate of  $\mathcal{A}_7^{(4)}$ , we may use this contour to directly obtain the contour of the first non-trivial  $N^2$ MHV tree-amplitude.

### 3.3.2 $N^2$ MHV Amplitudes

As mentioned above, because the parity-conjugate<sup>4</sup> of the 7-point NMHV amplitude is the 7-point  $N^2$ MHV amplitude, we may use the general NMHV contour to obtain our first non-trivial contour for  $k=4$ ,

$$\mathcal{F}_7^{(4)} = \widetilde{\mathcal{F}_7^{(3)}} = \left\{ \begin{array}{l} F_7^1 = (4) (4712) (2) (4613) - (4123)(4356)(4671)(4268) = [4] \bowtie S_{567123} \\ F_7^2 = (5) (7) (1345)(1624) - (1234)(1456)(1672)(1357) = [1] \bowtie S_{567234} \end{array} \right.$$

From here, there are several ways in which the above contour can be extended to

---

<sup>4</sup>Here, we should point out that we are using a definition of ‘parity’ that both exchanges the column-labels of each minor with their complements, and maps each column  $j \mapsto (n+1) - j$ . This appears to be the most natural definition of parity in the Grassmannian.

one for all  $n$ . For example, one could make the identification made in [10], that

$$F_7^{1,2} = \left\{ \begin{array}{l} [4] \bowtie S_{567123} \\ [1] \bowtie S_{567234} \end{array} \right\} \implies F_\ell^{1,2} \Leftrightarrow \left\{ \begin{array}{l} [\ell-3] \bowtie S_{\ell-2 \ell-1 \ell 1 2 3} \\ [1] \bowtie S_{\ell-2 \ell-1 \ell 2 3 \ell-3} \end{array} \right\}. \quad (3.3.5)$$

However, this extension of the 7-point  $N^2$ MHV amplitude leads to a form of the 8-point  $N^2$ MHV contour which is not manifestly self-conjugate under parity, and which therefore unnecessarily obfuscates the extension to all  $N^{(k-2)}$ MHV amplitudes.<sup>5</sup>

We suggest that the following extension is more natural,

$$F_7^{1,2} = \left\{ \begin{array}{l} [4] \bowtie S_{567123} \\ [1] \bowtie S_{567234} \end{array} \right\} \implies F_\ell^{1,2} \Leftrightarrow \left\{ \begin{array}{l} [\ell-3] \bowtie S_{\ell-2 \ell-1 \ell 1 2 3} \\ [1] \bowtie S_{\ell-2 \ell-1 \ell 2 3 4} \end{array} \right\}. \quad (3.3.6)$$

Notice that the only difference between the contour prescriptions in (3.3.5) and (3.3.6) is that the former associates  $S_{567234}$  with  $S_{\ell-2 \ell-1 \ell 2 3 \ell-3}$  while the latter associates  $S_{567234}$  with  $S_{\ell-2 \ell-1 \ell 2 3 4}$ .

Using this prescription, we find that the 8-point  $N^2$ MHV may be written,

$$\mathcal{A}_8^{(4)} = \frac{1}{\text{vol}[\text{GL}(4)]} \oint_{\mathcal{F}_8^{(4)} = 0} \frac{dC_{\alpha a}}{(7)(1)(3)} \frac{\mathcal{H}_8^{(4)}}{\mathcal{F}_8^{(4)}} \prod_{\alpha=1}^4 \delta^{4|4} (C_{\alpha a} \mathcal{W}_a), \quad (3.3.7)$$

---

<sup>5</sup>That being said, we have every reason to suspect the formula given in [10] is in fact just as correct as the one we present here.

where  $\mathcal{F}_8^{(4)} = F_7^1 F_7^2 \cdot F_8^1 F_8^2$  with the  $F_\ell^j$  given explicitly by<sup>6</sup>

$$\mathcal{F}_8^{(4)} = \left\{ \begin{array}{l} F_7^1 = (4) (4712) (2) (4613) - (4123)(4356)(4671)(4268) = [4] \bowtie S_{567123} \\ F_7^2 = (1567)(1237)(1345)(1624) - (1234)(1456)(1672)(1357) = [1] \bowtie S_{567234} \\ F_8^1 = (5) (5812)(5623)(5713) - (5123)(5367)(5781)(5268) = [5] \bowtie S_{678123} \\ F_8^2 = (6) (8) (1346)(1724) - (1234)(1467)(1782)(1368) = [1] \bowtie S_{678234} \end{array} \right\} \quad (3.3.8)$$

and  $\mathcal{H}_8^{(4)}$  is the product of all *non-consecutive* minors of the first factors of the  $F_\ell^j$ 's,

$$\begin{aligned} \mathcal{H}_8^{(4)} = & (4712)(1567)(1237)(1345)(5812)(5623)(1346) \\ & \times (4613)(1624)(5713)(1724). \end{aligned} \quad (3.3.9)$$

It is not hard to see that this contour is manifestly parity self-conjugate. (We should point out that this contour differs from the one given in [10] by only single minor appearing in  $F_8^2$ ; however, this minor difference turns out to leave essentially all the geometry problems described in [10] unchanged, and so the contour (3.3.8) leads to precisely the same sum of twenty residues described in [10], and therefore reproduces the correct 8-point N<sup>2</sup>MHV tree amplitude for all helicity configurations.)

As a further test of the validity of our contour prescription, let us briefly mention the tree-amplitude obtained for the 9-point N<sup>2</sup>MHV amplitude. As above, we may write,

$$\mathcal{A}_9^{(4)} = \frac{1}{\text{vol}[\text{GL}(4)]} \oint_{\mathcal{F}_9^{(4)} = 0} \frac{dC_{\alpha a}}{(8)(1)(3)} \frac{\mathcal{H}_9^{(4)}}{\mathcal{F}_9^{(4)}} \prod_{\alpha=1}^4 \delta^{4|4} (C_{\alpha a} \mathcal{W}_a), \quad (3.3.10)$$

---

<sup>6</sup>Here, we have highlighted each of the primary ‘consecutive subparts’ of each of the minors in the contour by colouring them blue. These tend to be the most important minors when computing a tree amplitude as a series of ‘geometry problems’ as described in [10].

where  $\mathcal{F}_9^{(4)} = F_7^1 F_7^2 \cdot F_8^1 F_8^2 \cdot F_9^1 F_9^2$  with each  $F_\ell^j$  given explicitly by,

$$\mathcal{F}_9^{(4)} = \left\{ \begin{array}{l} F_7^1 = (4)(4712)(2)(4613) - (4671)(4123)(4356)(4725) = [4] \bowtie S_{567123} \\ F_7^2 = (1567)(1237)(1345)(1246) - (1672)(1234)(1456)(1735) = [1] \bowtie S_{567234} \\ F_8^1 = (5)(5812)(5623)(5713) - (5781)(5123)(5367)(5826) = [5] \bowtie S_{678123} \\ F_8^2 = (1678)(1238)(1346)(1247) - (1782)(1234)(1467)(1836) = [1] \bowtie S_{678234} \\ F_9^1 = (6)(6912)(6723)(6813) - (6891)(6123)(6378)(6927) = [6] \bowtie S_{789123} \\ F_9^2 = (7)(9)(1347)(1824) - (1892)(1234)(1478)(1937) = [1] \bowtie S_{789234} \end{array} \right\}, \quad (3.3.11)$$

Deforming this contour from the twistor string to  $\mathcal{L}_{9,4}$  by sending each  $t_\ell^j \rightarrow 0$ —removing all the contributions shown in coloured grey in (3.3.11)—the problem of computing the tree-amplitude reduces to a series of ‘geometry problems’—finding the localization in the Grassmannian induced by requiring that each of the six maps  $f_\ell^j$  vanish, and determining which of these configurations are supported entirely by the vanishing of consecutive minors.<sup>7</sup> The six maps  $f_\ell^j$  are given explicitly by,

$$\mathcal{F}_9^{(4)} = \left\{ \begin{array}{l} f_7^1 = (4)(4712)(2) \\ f_7^2 = (1567)(1237)(1345) \end{array} \right\} \cup \left\{ \begin{array}{l} f_8^1 = (5)(5812)(5623) \\ f_8^2 = (1678)(1238)(1346) \end{array} \right\} \cup \left\{ \begin{array}{l} f_9^1 = (6)(6912)(6813) \\ f_9^2 = (7)(9)(1347)(1824) \end{array} \right\} \quad (3.3.12)$$

We have found that there are precisely 50 non-vanishing, consecutively-supported residues along the contour (3.3.11) and that these residues perfectly reproduce the fully-supersymmetric 9-point  $N^2$ MHV tree amplitude.

These 50 residues, together with the ‘geometry problems’ giving rise to each, are collected in appendix .1, where we have followed the conventions of [10] for the naming of each residue according to its localization in  $C_{\alpha a}$ .

---

<sup>7</sup>Any configuration along the contour not entirely supported by consecutive minors will have vanishing residue because of the non-consecutive minors which constitute  $\mathcal{H}_9^{(4)}$ .

### 3.3.3 $N^3$ MHV Amplitudes and Beyond

As was the case for the 7-point amplitude, the parity conjugate of the 9-point  $N^2$ NHV amplitude represents the first sufficiently-general  $N^3$ MHV amplitude from which we may ‘bootstrap’ the general  $N^3$ MHV result. We will see that by requiring the 9-point  $N^3$ MHV amplitude to be iteratively-related to the 8-point  $N^3$ MHV amplitude—itself obtained as the parity-conjugate of the 8-point NMHV amplitude—will uniquely fix the structure of the ansatz for all further amplitudes in  $\mathcal{N} = 4$  super Yang-Mills.

Taking the parity-conjugate of the 9-point  $k = 4$  contour (3.3.11), we find,

$$\mathcal{F}_9^{(5)} = \widetilde{\mathcal{F}_9^{(4)}} = \left\{ \begin{array}{l} F_8^1 = [4\ 5] \bowtie S_{6\ 7\ 8\ 1\ 2\ 3} \\ F_8^2 = [1\ 5] \bowtie S_{6\ 7\ 8\ 2\ 3\ 4} \\ F_8^3 = [1\ 2] \bowtie S_{6\ 7\ 8\ 3\ 4\ 5} \end{array} \right\} \cup \left\{ \begin{array}{l} F_9^1 = [5\ 6] \bowtie S_{7\ 8\ 9\ 1\ 2\ 3} \\ F_9^2 = [1\ 6] \bowtie S_{7\ 8\ 9\ 2\ 3\ 4} \\ F_9^3 = [1\ 2] \bowtie S_{7\ 8\ 9\ 3\ 4\ 5} \end{array} \right\}. \quad (3.3.13)$$

Notice that only the last three  $F_\ell^j$ ’s—those of the second set above—involve column 9. Moreover, all of the  $F_\ell^j$ ’s for  $\ell = 8$  involve column 8. Therefore, the requirement that the 9-point  $N^3$ MHV contour is the extension of the 8-point  $N^3$ MHV contour, uniquely fixes the  $\ell$ -dependence of the maps  $F_\ell^j$ . With this, it is not hard to see that the general solution for all  $N^3$ MHV amplitudes must be given by

$$\mathcal{F}_n^{(5)} = \prod_{\ell=8}^n \left( F_\ell^1 \cdot F_\ell^2 \cdot F_\ell^3 \right), \quad \text{with} \quad \left\{ \begin{array}{l} F_\ell^1 = [\ell-4\ \ell-3] \bowtie S_{\ell-2\ \ell-1\ \ell\ 1\ 2\ 3} \\ F_\ell^2 = [1\ \ell-3] \bowtie S_{\ell-2\ \ell-1\ \ell\ 2\ 3\ 4} \\ F_\ell^3 = [1\ 2] \bowtie S_{\ell-2\ \ell-1\ \ell\ 3\ 4\ 5} \end{array} \right\}. \quad (3.3.14)$$

As one further, concrete illustration of this prescription for the tree-amplitude contour, let us briefly consider the 10-point  $N^3$ MHV amplitude,

$$\mathcal{A}_{10}^{(5)} = \frac{1}{\text{vol}[\text{GL}(5)]} \oint_{\mathcal{F}_{10}^{(5)} = \vec{0}} \frac{dC_{\alpha a}}{(9)(1)(3)} \frac{\mathcal{H}_{10}^{(5)}}{\mathcal{F}_{10}^{(5)}} \prod_{\alpha=1}^5 \delta^{4|4} (C_{\alpha a} \mathcal{W}_a), \quad (3.3.15)$$

where  $\mathcal{F}_{10}^{(5)} = F_8^1 F_8^2 F_8^3 \cdot F_9^1 F_9^2 F_9^3 \cdot F_{10}^1 F_{10}^2 F_{10}^3$ , and with each  $F_\ell^j$  given by

$$\mathcal{F}_{10}^{(5)} = \left\{ \begin{array}{llllll} F_8^1 = & (4) & (45812) & (2) & (45713) & - & (45123)(45367)(45781)(45268) \\ F_8^2 = & (15678)(12358)(13456)(15724) & - & (15234)(15467)(15782)(15368) \\ F_8^3 = & (12678)(12348)(12456)(12735) & - & (12345)(12567)(12783)(12468) \\ F_9^1 = & (5) & (56912)(23567)(56813) & - & (56123)(56378)(56891)(56279) \\ F_9^2 = & (16789)(12369)(13467)(16824) & - & (16234)(16478)(16892)(16379) \\ F_9^3 = & (12789)(12349)(12457)(12835) & - & (12345)(12578)(12893)(12479) \\ F_{10}^1 = & (6) & (671012)(23678)(67913) & - & (67123)(67389)(679101)(672810) \\ F_{10}^2 = & (7) & (710123)(13478)(17924) & - & (17234)(17489)(179102)(173810) \\ F_{10}^3 = & (8) & (10) & (12458)(12935) & - & (12345)(12589)(129103)(124810) \end{array} \right\}$$

where again  $\mathcal{H}_{10}^{(5)}$  can be simply read-off from  $F_\ell^j$ 's:

$$\begin{aligned} \mathcal{H}_{10}^{(5)} = & (45812)(15678)(15823)(15346)(12678)(12834)(12456) \\ & \times (56912)(56237)(16789)(16923)(16347)(12789)(12934) \\ & \times (12457)(671012)(67238)(171023)(17348)(12458) \\ & \times (45713)(15724)(12735)(56813)(16824)(12835)(67913)(17924)(12935). \end{aligned}$$

Finally  $F$ 's can be written in a compact way,

$$F_8^1 = [45] \bowtie S_{678123}, F_8^2 = [15] \bowtie S_{678234}, F_8^3 = [12] \bowtie S_{678345} \quad (3.3.16)$$

$$F_9^1 = [56] \bowtie S_{789123}, F_9^2 = [16] \bowtie S_{789234}, F_9^3 = [12] \bowtie S_{789345} \quad (3.3.17)$$

$$F_{10}^1 = [67] \bowtie S_{8910123}, F_{10}^2 = [17] \bowtie S_{8910234}, F_{10}^3 = [12] \bowtie S_{8910345} \quad (3.3.18)$$

Although it would require more space than warranted by an appendix, we have explicitly verified that the contour above includes 175 non-vanishing residues which precisely matches the general, 10-point  $N^3$ MHV amplitude.

Continuing in this manner, we arrive at the general formula (3.2.1),

$$\mathcal{A}_n^{(k)} = \frac{1}{\text{vol}[\text{GL}(k)]} \oint_{\mathcal{F}_n^{(k)} = \vec{0}} \frac{dC_{\alpha a}}{(n-1)(1)(3)} \frac{\mathcal{H}_n^{(k)}}{\mathcal{F}_n^{(k)}} \prod_{\alpha=1}^k \delta^{4|4} (C_{\alpha a} \mathcal{W}_a),$$

where  $\mathcal{F}_n^{(k)} = (F_{k+3}^1 \cdots F_{k+3}^{k-2}) \cdot (F_{k+4}^1 \cdots F_{k+4}^{k-2}) \cdots (F_n^1 \cdots F_n^{k-2})$  with each  $F_\ell^j$  given by

$$F_\ell^j \equiv \sigma_\ell^j \bowtie S_{\ell-2 \ \ell-1 \ \ell \ j \ j+1 \ j+2}. \quad (3.3.19)$$

### 3.3.4 General Properties of the Result

#### Parity

One of the important features of the general contour obtained in the previous subsections is that it is manifestly parity-symmetric. By this, we mean that the parity-conjugate of a given amplitude's contour is the contour for the parity-conjugate amplitude. For example, for all  $n = 2k$ , the contour given by  $\mathcal{F}_{n=2k}^{(k)}$  is manifestly parity self-conjugate.

To see how this works more generally, consider the role played by each of the  $n$  columns of the Grassmannian  $C_{\alpha a}$  in the definition of the Veronese map  $F_\ell^j \equiv \sigma_\ell^j \bowtie S_{\ell-2\ell-1\ell j j+1 j+2}$ . In general, the  $n$  columns break into six contiguous groups,

$$[1 \ 2 \ \cdots \ j-1] \underbrace{[j \ j+1 \ j+2]}_{\in \sigma_\ell^j} [j+3 \ \cdots \ j+(k-\ell)-1] \underbrace{[j+(k-\ell) \ \cdots \ \ell-3]}_{\in \sigma_\ell^j} \underbrace{[\ell-2 \ \ell-1 \ \ell]}_{\in S} [\ell+1 \ \cdots \ n],$$

where the columns of  $C_{\alpha a}$  which do not participate at all in  $F_\ell^j$  have been coloured grey to emphasize the ‘gaps’ in the roles played by various columns. Importantly, parity does not change the ‘contiguity’ of these six groups, or the roles they play by the six columns of the primitive Veronese map  $S_{\ell-2\ell-1\ell j j+1 j+2}$  (coloured red above); parity merely changes the labels we assign each column, and exchanges the  $k - 6$  columns involved in *all* the minors of  $F_\ell^j$ —those of  $\sigma_\ell^j$ , coloured blue above—with the  $n - k - 6$  columns involved in *none* of the minors of  $F_\ell^j$ —those

coloured grey above. That is,

$$\left\{ \begin{array}{l} [1 \ \cdots \ j-1] \\ [j \ j+1 \ j+2] \\ [j+3 \ \cdots \ j+(k-\ell)-1] \\ [j+(k-\ell) \ \cdots \ \ell-3] \\ [\ell-2 \ \ell-1 \ \ell] \\ [\ell+1 \ \cdots \ n] \end{array} \right\} \xrightarrow{\text{parity}} \left\{ \begin{array}{l} [n-j+2 \ \cdots \ n] \\ [n-j-1 \ n-j \ n-j+1] \\ [n+\ell-j-k \ \cdots \ n-j-2] \\ [n-\ell+4 \ \cdots \ n+\ell-j-k-1] \\ [n-\ell+1 \ n-\ell+2 \ n-\ell+3] \\ [1 \ \cdots \ n-\ell] \end{array} \right\}. \quad (3.3.20)$$

This shows that,

$$F_\ell^j \xrightarrow[k \mapsto (n-k)]{i \mapsto (n+1)-i} \widetilde{F}_\ell^j = F_{(n-j+1)}^{(n-\ell+1)} \equiv F_{\ell'}^{j'}, \quad (3.3.21)$$

so that

$$\mathcal{F}_n^{(k)} = \prod_{\ell=k+3}^n \left( \prod_{j=1}^{k-2} F_\ell^j \right) \xrightarrow[k \mapsto (n-k)]{i \mapsto (n+1)-i} \mathcal{F}_n^{(n-k)} = \prod_{\ell=k+3}^n \left( \prod_{j=1}^{k-2} \widetilde{F}_\ell^j \right) = \prod_{j'=1}^{k'-2} \left( \prod_{\ell'=k'+3}^n F_{\ell'}^{j'} \right) = \prod_{\ell'=k'+3}^n \left( \prod_{j'=1}^{k'-2} F_{\ell'}^{j'} \right), \quad (3.3.22)$$

where  $k' \equiv (n - k)$ , which is that which it was required to demonstrate.

## Manifest Soft-Limits and the Particle Interpretation

As we have seen, the contour integral giving the  $n - 1$ -particle  $N^{(k-2)}$ MHV scattering amplitude, is related to that giving the  $n$ -particle  $N^{(k-2)}$ MHV scattering amplitude by a single overall factor which relates  $\mathcal{H}_n^{(k)}$  to  $\mathcal{H}_{n-1}^{(k)}$ , together with a partial contour

specification,

$$\begin{aligned}
\mathcal{A}_n^{(k)} &= \frac{1}{\text{vol}[\text{GL}(k)]} \oint_{\mathcal{F}_n^{(k)} = \vec{0}} dC_{\alpha a} \frac{\mathcal{H}_n^{(k)}}{(n-1)(1)(3) \mathcal{F}_n^{(k)}} \\
&= \frac{1}{\text{vol}[\text{GL}(k)]} \oint_{\mathcal{F}_{n-1}^{(k)} = \vec{0}} dC_{\alpha \hat{a}} \frac{\mathcal{H}_{n-1}^{(k)}}{(1)(3) \mathcal{F}_{n-1}^{(k)}} \times \oint_{\substack{F_n^1 = 0 \\ \vdots \\ F_n^{k-2} = 0}} dC_{\alpha n} \frac{\mathcal{H}_n^{(k)} / \mathcal{H}_{n-1}^{(k)}}{(n-1) F_n^1 \cdot F_n^2 \cdots F_n^{k-2}}, \\
\end{aligned} \tag{3.3.23}$$

where  $\hat{a} = 1, \dots, n-1$  and the ratio  $\mathcal{H}_n^{(k)} / \mathcal{H}_{n-1}^{(k)}$  was given explicitly after equation (3.2.3) in section 2. This separation of the integral is warranted because only the maps  $F_n^1, \dots, F_n^{k-2}$  involve the variables of the  $n^{\text{th}}$  column of  $C_{\alpha a}$ . We can anticipate which contour should be specified for these  $k-2$  variables to extract the soft-limit by considering the duality between the geometry of the columns of  $C_{\alpha a}$ , viewed as points in  $\mathbb{P}^{k-1}$ , and  $\mathcal{Z}$ -twistor-space geometry [10]. In twistor space, the soft-limit is achieved when the three twistors  $\mathcal{Z}_{n-1}, \mathcal{Z}_n$ , and  $\mathcal{Z}_1$  become (projectively) collinear, and so we can extract the soft limit from  $\mathcal{A}_n^{(k)}$  by choosing a contour for which the column-vectors  $C_{\alpha n-1}, C_{\alpha n}$ , and  $C_{\alpha 1}$  become linearly-dependent. This fixes exactly  $(k-2)$  variables of integration, and so should completely specify the integral factor in (3.3.23) relating  $\mathcal{A}_n^{(k)}$  to  $\mathcal{A}_{n-1}^{(k)}$ .

Recalling the definition of the maps  $F_n^1, F_n^2, \dots, F_n^{k-1}$ , it is easy to see that when the columns  $n-1, n, 1$  become linearly-dependent,  $F_n^2, \dots, F_n^{k-2}$  all vanish, while  $F_n^1$  factorizes into simply the product of four minors. Importantly, notice that  $\mathcal{H}_n^{(k)}, \mathcal{H}_{n-1}^{(k)}$ , and all the factors of  $\mathcal{F}_{n-1}^{(k)}$  are regular in this limit. Because of this, we can apply the global residue theorem in (3.3.23) to trade  $F_n^1$  for the minor

$(n - 1)$ —which does vanish in this limit.

This allows us to view the contour integral for the twistor string entirely in  $\mathcal{L}_{n,k}$ , and refer to some well-known facts [10] relating residues in  $\mathcal{L}_{n,k}$  to those of  $\mathcal{L}_{n-1,k}$  to see how the soft-factor arises. It turns out that the contour which sets three consecutive columns of the Grassmannian to be linearly dependent is particularly nice, and is nothing but a holomorphic inverse soft-factor times the ratio of the  $k$  consecutive minors containing  $n$  to the  $k - 1$  minors which were consecutive only prior to ‘adding particle  $n$ ’ to  $G(k, n - 1)$ . Recall that this ratio of minors is explicitly built-into the definition of  $\mathcal{H}_n^{(k)}$

### 3.4 Transformation to the Twistor String in Link Variables

In this section we demonstrate the equivalence of the twistor string amplitude [21] (when expressed in link variables as in [22, 23]) to our main formula (3.2.1) above. This is accomplished via repeated application of the identity transformation

$$\delta(S_{ijkrst})\delta(S_{ijkrsu}) \sim \frac{(jkt)(irt)}{(jks)(irs)}\delta(S_{ijkrst})\delta(S_{ijkrtu}); \quad (3.4.1)$$

here,  $\sim$  is used to indicate that the replacement may be made at the level of the integrand only strictly for *physical configurations* along the contour of integration. This transformation has played an important role in the analysis of [9], [31]. Note that this relation indicates a specific change in the contour prescription: the  $\delta(S_{ijkrsu})$  on the left-hand side may localize the integral on fewer (or more) poles than the

$\delta(S_{ijkrtu})$  on the right, in which case the extra (or missing) poles on the right-hand side are provided by zeros the minors in the denominator (or cancelled by zeros of the minors in the numerator).

In the next two subsections we first focus on following the transformation of the  $\delta(F_\ell^i)$ 's from equation (3.2.1) to the formula (4.12) in [23]. We then collect all the pre-factors which pile-up along the way and demonstrate precise agreement with [23]. It is very easy to check the agreement between our formula and that of [23] for NMHV using [9]. We may proceed by induction at step  $n$ , beginning with the assumption that equation (3.2.1) agrees with [23] for the  $(n-1)$ -point amplitudes.

### 3.4.1 Transforming the $\delta(F_\ell^j)$ 's

Let us first transform the  $\delta(F_\ell^j)$ 's from equation (3.2.1) to the corresponding ones in [23]. Because we will use induction, we only need to consider  $F_n^j$  and for the simplicity we will denote it as  $F_j$ . In order to compare with the formula in [23] we must first change the common piece in  $F_j$ , namely  $\sigma_n^j = [1, \dots, j-1] \cup [j+n-k, \dots, n-3]$  in (3.2.4), into a subset of the columns  $[1, 2, \dots, k]$ .<sup>8</sup> In this sense  $F_1$  is the ‘worst’ of the  $F$ 's and  $F_{k-2}$  is the ‘best’, so the strategy will be to first make all transformations on  $F_1$ , then to make all transformations on  $F_2$ , and continue in the same way (as far as possible) until  $F_{k-3}$ . In this way we gradually transform all of the original  $\delta(F_j)$ 's into ‘real sextics’ (objects which are indeed sextics in a certain gauge). In the following we show a first few steps and then move on to the final conclusion.

---

<sup>8</sup>The meaning of this will become clear by looking at the final result, equation (3.4.11).

- Let us first show how to transform  $F_1$  to  $F_1''$ ,

$$\begin{aligned} F_1 &= [n-k+1 \ \cdots \ n-3] \bowtie S_{1 \ 2 \ 3 \ n-2 \ n-1 \ n} \\ \rightarrow F_1'' &= [n-k+2 \ \cdots \ n-3 \ 2] \bowtie S_{1 \ 3 \ 4 \ n-2 \ n-1 \ n}. \end{aligned} \tag{3.4.2}$$

Step one is to use the identity

$$\delta(F_1)\delta(F_2') \sim J_1^{(1)}\delta(F_1')\delta(F_2'), \tag{3.4.3}$$

where the sextics and the Jacobian are

$$\begin{aligned} F_2' &= [n-k+2 \ \cdots \ n-3 \ 1] \bowtie S_{2 \ 3 \ n-k+1 \ n-2 \ n-1 \ n} \\ F_1' &= [n-k+2 \ \cdots \ n-3 \ 2] \bowtie S_{1 \ 3 \ n-k+1 \ n-2 \ n-1 \ n} \\ J_1^{(1)} &= [n-k+2 \ \cdots \ n-3] \bowtie \frac{(n \ 1 \ 2 \ 3)(n-2 \ n-1 \ 1 \ 2)}{(n \ 1 \ 3 \ n-k+1)(n-2 \ n-1 \ 1 \ n-k+1)}. \end{aligned} \tag{3.4.4}$$

This identity follows from (3.4.1) by setting a particular gauge, namely to use  $GL(k)$  symmetry to set  $k$  columns  $[1, 2, 3, n-k+1, \dots, n-3]$  of  $k \times n$  matrix  $(C_{\alpha a})$  to be an identity square matrix, and we will denote the gauge as  $\{1, 2, 3, n-k+1, \dots, n-3\}$ .

Note that we also transformed  $F_2$  into  $F_2'$  which generated a Jacobian  $J$  which will end up canceling, so we will not write it explicitly.

Next we further transform  $F_1'$  by using

$$\delta(F_1')\delta(F_1^{(n-1)}) \sim J_1^{(2)}\delta(F_1'')\delta(F_1^{(n-1)}), \tag{3.4.5}$$

where

$$\begin{aligned}
 F_1^{(n-1)} &= [n-k+2 \ \cdots \ n-3 \ 2] \bowtie S_{1 \ 3 \ n-k+1 \ n-2 \ n-1 \ 4}, \\
 F_1'' &= [n-k+2 \ \cdots \ n-3 \ 2] \bowtie S_{1 \ 3 \ 4 \ n-2 \ n-1 \ n}, \\
 J_{1_j}^{(2)} &= [n-k+2 \ \cdots \ n-3 \ \bar{j}] \bowtie \frac{(n-1 \ 4 \ j)(3 \ n-2 \ 4)}{(n-1 \ n-k+1 \ j)(3 \ n-2 \ n-k+1)}, \tag{3.4.6}
 \end{aligned}$$

with  $j = 1$  and  $\bar{j} = 2$ . Note that in carrying out this transformation we have made use of the constrain  $\delta(F_1^{(n-1)})$  which can be obtained by transforming  $F_{n-1}^j$  of the  $(n-1)$ -point amplitudes.

The third step is to transform  $F_2'$  back to  $F_2$ , which generates a Jacobian  $J^{-1}$ .

To summarize the construction so far, we have shown how to transform the original  $F_1$  into a “better” quantity  $F_1''$  at the cost of inserting the Jacobain factor  $J_1^{(1)} J_{1_1}^{(2)}$  into the integrand.

- Next we would like to similarly process  $F_2$  with  $F_1''$ . By applying (3.4.1) for the new  $F_1''$  and the old  $F_2$

$$\begin{aligned}
 F_1'' &= [n-k+2 \ \cdots \ n-3 \ 2] \bowtie S_{1 \ 3 \ 4 \ n-2 \ n-1 \ n}, \\
 F_2 &= [n-k+2 \ \cdots \ n-3 \ 1] \bowtie S_{2 \ 3 \ 4 \ n-2 \ n-1 \ n}, \tag{3.4.7}
 \end{aligned}$$

we get the new quantities

$$\begin{aligned}
 F_1''' &= [n-k+3 \ \cdots \ n-3 \ 2 \ 3] \bowtie S_{1 \ 4 \ 5 \ n-2 \ n-1 \ n}, \\
 F_2''' &= [n-k+3 \ \cdots \ n-3 \ 1 \ 3] \bowtie S_{2 \ 4 \ 5 \ n-2 \ n-1 \ n}. \tag{3.4.8}
 \end{aligned}$$

The Jacobians generated from this step are

$$J_2^{(1)} J_{2_1}^{(2)} J_2^{(1)} J_{2_2}^{(2)}, \quad (3.4.9)$$

where

$$\begin{aligned} J_2^{(1)} &= [n - k + 3 \ \cdots \ n - 3] \bowtie \frac{(n \ 1 \ 2 \ 3 \ 4)(n - 2 \ n - 1 \ 1 \ 2 \ 3)}{(n \ 1 \ 2 \ 4 \ n - k + 2)(n - 2 \ n - 1 \ 1 \ 2 \ n - k + 2)}, \\ J_{2_j}^{(2)} &= [n - k + 3 \ \cdots \ n - 3 \ \bar{j}] \bowtie \frac{(n - 1 \ 5 \ j)(4 \ n - 2 \ 5)}{(n - 1 \ n - k + 2 \ j)(4 \ n - 2 \ n - k + 2)}, \end{aligned} \quad (3.4.10)$$

with  $j = 1, 2$  and  $\bar{1} \equiv (2, 3)$ ,  $\bar{2} \equiv (1, 3)$ .

- We proceed by transforming the original  $F_3$  together with the new  $F_1''', F_2'''$  into three new quantities  $F_1''''$ ,  $F_2''''$ ,  $F_3''''$ . We continue in this manner until we reach  $F_{k-3}''''\dots''$ . In each step we will always make two-type transformations like the ones described above. At the end of the day, we have new quantities

$$F_j = [1, 2, \cdots, \bar{j}, \cdots, k - 2] \bowtie S_{j \ k-1 \ k \ n-2 \ n-1 \ n}, \quad (3.4.11)$$

where  $1 \leq j \leq k - 2$ . The Jacobians generated during the whole process are products of

$$\begin{aligned} J_l^{(1)} &= [n - k + \ell + 1 \ \cdots \ n - 3] \bowtie \frac{(n \ 1 \ 2 \ \cdots \ \ell + 2)(n - 2 \ n - 1 \ 1 \ \cdots \ \ell + 1)}{(n \ 1 \ \cdots \ \ell \ \ell + 2 \ n - k + \ell)(n - 2 \ n - 1 \ 1 \ \cdots \ \ell \ n - k + \ell)}, \\ J_{\ell_j}^{(2)} &= [n - k + \ell + 1 \ \cdots \ n - 3 \ \bar{j}] \bowtie \frac{(n - 1 \ \ell + 3 \ j)(\ell + 2 \ n - 2 \ \ell + 3)}{(n - 1 \ n - k + \ell \ j)(\ell + 2 \ n - 2 \ n - k + \ell)}, \end{aligned} \quad (3.4.12)$$

where  $\bar{j} \equiv (1, 2, \cdots, \bar{j}, \cdots, \ell + 1)$ ,  $1 \leq \ell \leq k - 3$  and  $1 \leq j \leq \ell$ .

Finally let us choose a gauge  $\{1, 2, 3, \cdots, k\}$ , in which case  $F_j = S_{j \ k-1 \ k \ n-2 \ n-1 \ n}$

may be found in (3.4.11). Thus we have mapped our  $F_n^j$ 's to the sextics in [23], and all we are left to compare is the corresponding prefactor.

### 3.4.2 Collecting Prefactors

Let us now verify that performing the above procedure on our formula (3.2.1) leads to precisely the same prefactor inside the integral as in [23]. We only need to compare the ratio between  $n$ -point amplitude and  $(n-1)$ -point amplitude which for our formula (3.2.1) reads

$$A_n = \frac{\mathcal{H}_n^{(k)}}{\mathcal{H}_{n-1}^{(k)}} = \frac{1}{(n-1 \ n \ 1 \ \dots \ k-2)} \left[ \prod_{j=1}^{k-1} (n-k+j \ \dots \ n-1 \ 1 \ \dots \ j) \right. \\ \times (n-k+j \ \dots \ n-3 \ n \ 1 \ \dots \ j+1) (n-k+j \ \dots \ n-2 \ 1 \ \dots \ j-1 \ j+1 \ j+2) \\ \left. \times (n-k+i \ \dots \ n-3 \ n-1 \ 1 \ \dots \ j \ j+2) \right]. \quad (3.4.13)$$

The corresponding ratio in twistor string is given by the formula (4.12) of [23]. Taking into account all the Jacobians from the transformations described in the previous subsection, we find the ratio of our formula (3.2.1) to that in [23] is precisely equal to one. This completes the proof.

# Chapter 4

## Five point three-loop amplitude in $\mathcal{N} = 4$ SYM

### 4.1 Introduction

Much of the recent-year interest in multi-loop scattering amplitudes has been stimulated by the ABDK/BDS ansatz [11, 12] which suggested that multi-loop MHV amplitudes satisfy a powerful iteration relation implying a simple exponential form for the full all-loop amplitude. Now, it is well known that the ansatz is incomplete starting from the two-loop six-particle amplitude [15, 16, 17, 18].

In this chapter we study the three-loop BDS ansatz

$$M_n^{(3)}(\epsilon) + \frac{1}{3}(M_n^{(1)}(\epsilon))^3 - M_n^{(1)}(\epsilon)M_n^{(2)}(\epsilon) - f^{(3)}(\epsilon)M_n^{(1)}(3\epsilon) = C^{(3)} + \mathcal{O}(\epsilon) \quad (4.1.1)$$

where  $C^{(3)}$  is a previously undetermined numerical constant. In sections II and III we use the leading singularity method [32] to determine the (four-dimensional cut-constructible part of the) 3-loop 5-particle amplitude  $M_5^{(3)}$  in terms of a simple basis of integrals. In section IV we then numerically evaluate enough pieces of these amplitudes (the pieces called ‘obstructions’ in [33, 34]) to determine  $C^{(3)} = 17.8241$ . Although current developments strongly suggest that the quantity appearing on the right-hand side of (4.1.1) will in general be non-constant (but still dual conformally invariant) for  $n > 5$ , there is some utility in knowing the precise number  $C^{(3)} = 17.8241$  since for any  $n$ , whatever appears on the right-hand side of (4.1.1) must approach this same number in any collinear limit.

## 4.2 Outline of the Calculation

Our goal is to find a compact expression for the planar 3-loop 5-particle amplitude in  $\mathcal{N} = 4$  SYM as a linear combination of some basic integrals. Several powerful and related techniques for carrying out calculations such as these include unitarity based methods [1, 35, 36, 37, 38, 39, 40] and more recently, building on [41, 42], maximal cuts [43] and the leading singularity method [32]. For the present calculation we find it convenient to use the leading singularity method (see also [44, 45]) since it allows for all integral coefficients to be determined analytically by solving simple linear equations. In this section we provide a detailed outline of the steps involved in setting up the calculation.

### 4.2.1 Review of the Leading Singularity Method

Suppose we are interested in calculating some  $L$ -loop scattering amplitude  $A$ . On the one hand, the amplitude may of course be represented as a sum over Feynman diagrams  $F_j$ ,

$$A(k) = \sum_j \int \prod_{a=1}^L d^d \ell_a F_j(k, \ell), \quad (4.2.1)$$

where  $k$  are external momenta and  $\ell_a$  are the loop momenta. However it is frequently the case, especially in theories as rich as  $\mathcal{N} = 4$  SYM, that directly calculating the sum over Feynman diagrams would be impractical. Rather the calculation proceeds by expressing  $A$  as a linear combination of relatively simple integrals in some appropriate basis  $\{I_i\}$ ,

$$A(k) = \sum_i c_i(k) \int \prod_{a=1}^L d^d \ell_a I_i(k, \ell), \quad (4.2.2)$$

and then determining the coefficients  $c_i$  by other means.

With the leading singularity method we equate (4.2.1) and (4.2.2) and perform the integral

$$\sum_i c_i(k) \int_{\Gamma} d^4 \ell I_i(k, \ell) = \int_{\Gamma} d^4 \ell \sum_j F_j(k, \ell) \quad (4.2.3)$$

over contours  $\Gamma \in \mathbb{C}^{4L}$  other than the real  $\ell$ -axis. At  $L$  loops each contour is a  $T^{4L}$  inside  $\mathbb{C}^{4L}$ . For each contour  $\Gamma$  we obtain one linear equation on the coefficients  $c_i$ . Of course if  $\Gamma$  is a random contour then we would generally get the useless equation  $0 = 0$ , so we should choose contours such that the integral on the right-hand side of (4.2.3) evaluates the residue on the isolated singularities of Feynman diagrams, which are associated with the locus where internal propagators become on-shell.

Since the number of isolated singularities in a generic  $L$ -loop diagram can be as high as  $2^L$  (simple diagrams can have fewer isolated singularities), the leading singularity method gives rise to an exponentially large (in  $L$ ) number of linear equations for the coefficients  $c_i$ . We note that the homogeneous part of these linear equations (the left-hand side of (4.2.3)) depends only on the set of integrals  $\{I_i\}$  and the choice of contours, while the details of which particular helicity configuration is under consideration enters only into the inhomogeneous terms on the right-hand side.

#### 4.2.2 Integration Strategy: Collapse and Expand

Here we briefly review from [42, 43, 44, 32, 45] the integration rules which make it simple to evaluate the contour integrals appearing in (4.2.3) in the cases relevant to the present calculation. Let us focus on a box with loop momentum  $p$  and external momenta  $k_i$ . The box may be sitting inside a higher-loop diagram, in which case the  $k_i$  may involve other loop momenta. The sum over Feynman diagrams contains poles at the locus

$$S = \{p \in \mathbb{C}^4 : p^2 = 0, (p - k_1)^2 = 0, (p - k_{12})^2 = 0, (p + k_4)^2 = 0\}, \quad (4.2.4)$$

which, for generic  $k_i$ , consists of two distinct points. To each of these points there is an associated contour  $\Gamma_p$  such that integrating  $p$  over  $\Gamma_p$  calculates the residue at the associated point.

The residue of a one-loop amplitude at one of these poles is computed by removing the four internal propagators and evaluating the product of on-shell tree amplitudes at the four corners (summed over all helicities of internal states). In the simplest

application, when all four  $k_i$  satisfy  $k_i^2 = 0$ , this product evaluates on either contour  $\Gamma_p$  to a four-particle tree amplitude, leading to the ‘collapse rule’ graphically depicted as

$$\int_{\Gamma_p} d^4 p \quad \begin{array}{c} \text{Diagram:} \\ \text{Two horizontal lines. Top line: } k_2 \text{ to } k_3, \text{ bottom line: } k_1 \text{ to } k_4. \text{ They are connected by a vertical line } p \text{ at the center.} \end{array} = \quad \begin{array}{c} \text{Diagram:} \\ \text{A single shaded circle with four external lines: } k_2 \text{ (top-left), } k_3 \text{ (top-right), } k_1 \text{ (bottom-left), } k_4 \text{ (bottom-right).} \end{array} \quad (4.2.5)$$

The figure on the left indicates the sum over that subset of all one-loop Feynman diagrams in which all four of the indicated propagators are present. Of course it may as well be the sum over *all* one-loop Feynman diagrams since those that do not contain all four of the indicated propagators contribute zero to the residue.

When one of the  $k_i^2$  is non-zero, the result (4.2.5) holds on only one of the two  $\Gamma_p$  contours, while the integral over the other contour gives zero. Given a helicity assignment for the external particles it is a simple matter to determine which of the two solutions leads to the non-zero result.

It is frequently the case that after collapsing a box in some loop momentum  $p$  there are less than four exposed propagators in some other loop momentum, which would apparently indicate a codimension 1 singularity rather than an isolated singularity. In this case one can use the ‘expand rule’

$$\begin{array}{c} \text{Diagram:} \\ \text{A shaded circle with four external lines: } k_2 \text{ (top-left), } k_3 \text{ (top-right), } k_1 \text{ (bottom-left), } k_4 \text{ (bottom-right).} \end{array} = \quad \begin{array}{c} \text{Diagram:} \\ \text{Two horizontal lines. Top line: } k_2 \text{ to } k_3, \text{ bottom line: } k_1 \text{ to } k_4. \text{ They are connected by a vertical line } p \text{ at the center.} \end{array} + \text{ terms non-singular at } (k_1 + k_2)^2 = 0$$

$$\begin{array}{c}
 \text{Diagram: Two shaded circles connected by a vertical line. Arrows on the top line point to } k_2 \text{ and } k_3. \text{ Arrows on the bottom line point to } k_1 \text{ and } k_4. \\
 = \quad \quad \quad + \text{ terms non-singular at } (k_2 + k_3)^2 = 0
 \end{array}$$

to expose additional propagators inside a tree amplitude. The choice of how to expand is correlated with the choice of integration contour for the next loop momentum. In the example shown here, the terms isolated on the first line are those which survive a contour integration around the singularity at  $(k_1 + k_2)^2 = 0$  while the second expansion displays those terms isolated by a contour integration around the singularity at  $(k_2 + k_3)^2 = 0$ .

These two simple rules are sufficient for evaluating all contour integrals appearing on the right-hand side of (4.2.3) in this paper. Finally, scalar integrals appearing on the left-hand side are integrated via the simple rule

$$\int_{\Gamma_p} d^4p \frac{1}{p^2(p - k_1)^2(p - k_{12})^2(p + k_4)^2} = \frac{1}{(k_1 + k_2)^2(k_2 + k_3)^2}, \quad (4.2.6)$$

which is valid as long as at least three of the  $k_i$  satisfy  $k_i^2 = 0$  (we will not encounter any other cases in the present calculation). We have chosen a simple normalization factor of 1 on the right-hand side of (4.2.6); this will be adjusted below in (4.3.3) to match standard conventions for normalizing amplitudes.

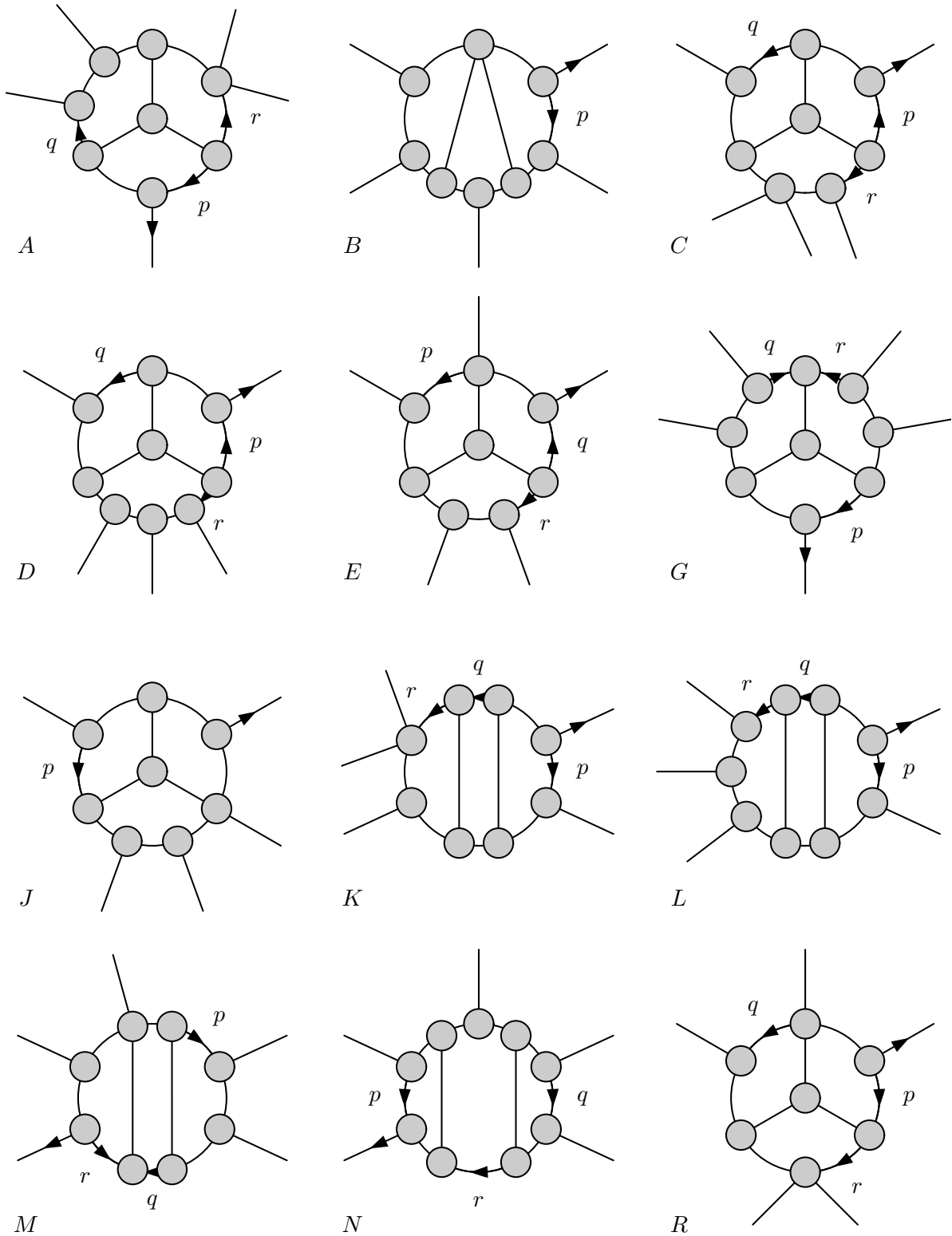


Figure 4.1: The planar 3-loop 5-particle topologies associated to leading singularities. Each figure represents a sum over that subset of Feynman diagrams in which all of the indicated propagators are present. We label the external momenta clockwise with  $k_1$  at the leg indicated with the arrow.

### 4.2.3 Choosing a Sufficient Set of Contours

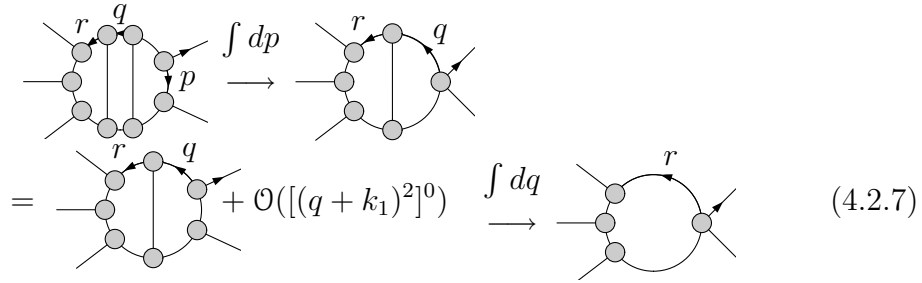
In order to proceed systematically we begin by enumerating all planar 3-loop 5-particle topologies which are free of tadpoles, bubbles, and triangles, since such diagrams are unnecessary due to  $\mathcal{N} = 4$  supersymmetry (see [47] for a thorough discussion). This leaves 17 topologies, of which 5 do not have any associated leading singularities and are therefore of no interest to us. The remaining 12 topologies are shown in Fig. 4.1.

Each topology in Fig. 4.1 has several distinct associated leading singularities, each of which gives rise to an equation via (4.2.3). The information contained in this collection of equations is highly redundant—the equations obtained from only a small subset of the leading singularities are sufficient to determine all coefficients, while the remaining equations serve as consistency checks. We now present a few details explaining how to extract a set of equations sufficient for determining all coefficients. We have verified a number of the additional equations to check consistency, but have not performed an exhaustive search for all possible leading singularities.

The topologies fall naturally into three different categories according to how we choose to implement the collapse and expand rules. Let us now address each category in turn, giving in each case the details of the simplest topology as an example.

### Example 1: Topology $L$

Topology  $L$  has several leading singularities, but the simplest ones can be isolated as indicated in the following cartoon:



In words: we first integrate the sum of Feynman diagrams over a  $p$  contour which collapses the associated massless box, then expand around  $(q + k_1)^2 = 0$  keeping only the singular terms indicated. Integrating  $q$  over an appropriate contour isolates these singular terms while collapsing the massless box. The final integral over  $r$  is again accomplished using the collapse rule.

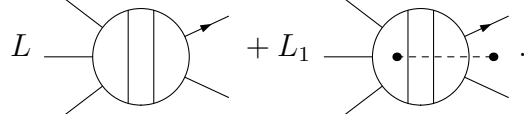
The leading singularities exposed by these steps are those located at the locus

$$\begin{aligned}
 S_L = \{ (p, q, r) \in \mathbb{C}^{12} : & p^2 = 0, q^2 = 0, r^2 = 0, (p + k_1)^2 = 0, (r - k_5)^2 = 0, \\
 & (r - k_{45})^2 = 0, (r + k_{12})^2 = 0, (q + k_{12})^2 = 0, (p - k_2)^2 = 0, \\
 & (q - r)^2 = 0, (p + q + k_1)^2 = 0, (q + k_1)^2 = 0 \}.
 \end{aligned} \tag{4.2.8}$$

For generic external momenta the set  $S_L$  consists of 8 distinct points in  $\mathbb{C}^{12}$ . For each point in  $S_L$  there is an associated contour which computes the residue at the point and hence leads to an equation via (4.2.3).

It remains only to construct an appropriate ansatz for the left-hand side of (4.2.3).

We try a linear combination of the two most natural integrals of topology  $L$ ,


(4.2.9)

Here and in what follows we use pictures as shorthand for the corresponding scalar integrands, so for example the first term in (4.2.9) represents

$$L \frac{1}{p^2 q^2 r^2 (p + k_1)^2 (r - k_5)^2 (r - k_{45})^2 (r + k_{12})^2 (q + k_{12})^2 (p - k_2)^2 (q - r)^2 (p + q + k_1)^2} \quad (4.2.10)$$

while the dotted line in the second picture in (4.2.9) indicates a factor of  $(r + k_1)^2$  in the numerator of the integrand.

Integrating (4.2.9) over the contours detailed above leads to the expression

$$\frac{L + L_1(r + k_1)^2}{s_{12}^2 s_{34} s_{45} (r + k_1)^2}, \quad (4.2.11)$$

where the denominator factors arise from the Jacobians in (4.2.6). Equating this to the result of (4.2.7) and choosing a particular helicity configuration leads to the equation

$$\frac{L + L_1(r + k_1)^2}{s_{12}^2 s_{34} s_{45} (r + k_1)^2} = A_{\text{tree}}(1^-, 2^-, 3^+, 4^+, 5^+) \delta_{\langle r, 5 \rangle}. \quad (4.2.12)$$

Of course this must be evaluated on the locus  $S_L$ , and it is easy to check that  $S_L$  contains only two different values of  $r$ :

$$r_1 = \lambda_5 \left( \tilde{\lambda}_5 + \frac{\langle 4, 3 \rangle}{\langle 5, 3 \rangle} \tilde{\lambda}_4 \right), \quad r_2 = \left( \lambda_5 + \frac{[4, 3]}{[5, 3]} \lambda_4 \right) \tilde{\lambda}_5, \quad (4.2.13)$$

giving us two distinct equations which are sufficient to determine the coefficients  $L$

and  $L_1$  uniquely.

Topologies  $D$ ,  $G$ , and  $N$  proceed in exactly the same manner, except that in these cases more than two integrals appear on the left-hand side. Topologies  $A$ ,  $C$ ,  $E$  and  $K$  are also very similar, except that since these three topologies only have 10 exposed propagators (rather than 11) it is necessary to isolate a second hidden singularity by performing a second expansion prior to integrating over  $r$ .

### Example 2: Topology $M$

For topology  $M$  it is sufficient to consider even simpler contours. We first collapse and expand the  $p$  box as done above for topology  $L$ , arriving at



At this stage it is convenient to integrate over a symmetric contour of the type considered in [32] where we require that  $\langle q, r \rangle$  and  $[q, r]$  separately vanish instead of just  $(q + r)^2 = 0$ . This leads us to consider the locus

$$\begin{aligned} S_M = \{ (p, q, r) \in \mathbb{C}^{12} : & p^2 = 0, q^2 = 0, r^2 = 0, (p - k_4)^2 = 0, (r + k_1)^2 = 0, \\ & (q + k_{45})^2 = 0, (r + k_{12})^2 = 0, (p - q - k_{45})^2 = 0, \\ & (p - k_{45})^2 = 0, (q + k_5)^2 = 0, \langle q, r \rangle = 0, [q, r] \neq 0 \} \end{aligned} \quad (4.2.15)$$

For generic external momenta  $S_M$  consists of 4 isolated points, each of which leads to one linear equation for the integral coefficients. Note that the right-hand side

of (4.2.3) always vanishes for such symmetric contours since the associated product of tree amplitudes must vanish when  $\langle q, r \rangle = 0 = [q, r]$ .

For topologies  $B$ ,  $J$  and  $G$  we proceed along exactly the same lines (we already treated  $G$  in the first example, but additional equations are needed to fix all of the coefficients which appear for this topology). It turns out that for topology  $J$  an interesting and very useful feature emerges: here we model the left-hand side as the linear combination

$$J \quad \text{Diagram} + J_1 \quad \text{Diagram} + \text{several other integrals.} \quad (4.2.16)$$

We will not display all of the relevant integrals explicitly, but they all have the property that they either vanish on the locus  $S_J$  (so that they do not enter the associated equations), or they contain the same numerator factor as  $J_1$  shown here, which we denote by  $\ell^2$ . Now when we perform the  $q$  integral one of the Jacobian factors is  $1/\ell^2$ , so we obtain the equation

$$\frac{J}{\ell^2} + J_1 + \text{several other coefficients} = 0. \quad (4.2.17)$$

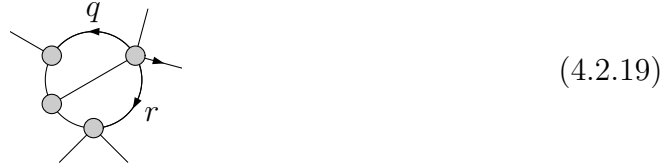
Since  $\ell^2 = 0$  on the locus  $S_J$ , we immediately see that the coefficient  $J$  must vanish in order to avoid a contradiction. Perhaps a safer way to express this is to say that we can consider an equation obtained by multiplying both sides of (4.2.3) by  $\ell^2$  before performing the contour integrals. Having determined that  $J = 0$ , we then see that (4.2.17) gives an equation relating  $J_1$  to the other coefficients. This trick is also useful for other topologies, in particular for  $C$  and  $E$ .

### Example 3: Topology $R$

There are five different triple-box 9-propagator topologies, of which topology  $R$  is the only one with associated leading singularities. These are situated on the locus

$$S_R = \{(p, q, r) \in \mathbb{C}^{12} : p^2 = 0, (p + q + k_{15})^2 = 0, q^2 = 0, (q - k_4)^2 = 0, (p - r)^2 = 0, (r - k_{23})^2 = 0, r^2 = 0, (r + q + k_{15})^2 = 0, (p + k_1)^2 = 0, (q + k_{15})^2 = 0, (r + k_1)^2 = 0, (r + k_{15})^2 = 0\}. \quad (4.2.18)$$

Here the first nine conditions are the visible propagators, while the last three are hidden singularities. In order to see what the right-hand side of (4.2.3) should be let us begin by integrating out  $q$  to collapse the first box. This leads to



For the first time we find a triangle-triangle diagram rather than a triangle-box or box-box. The Jacobian factor from integrating the corresponding scalar integral is  $1/(q+k_{15})^2(r+k_1)^2$ , suggesting that we expand (4.2.19) to expose either  $1/(q+k_{15})^2$  or the  $1/(r+k_1)^2$  propagator, but it is clearly impossible to expand both simultaneously. Either choice leaves us with a sum over triangle-box Feynman diagrams, which vanishes due to  $\mathcal{N} = 4$  supersymmetry. The right-hand side of (4.2.3) is therefore zero for the  $R$  topology leading singularities in eq. (4.2.18).

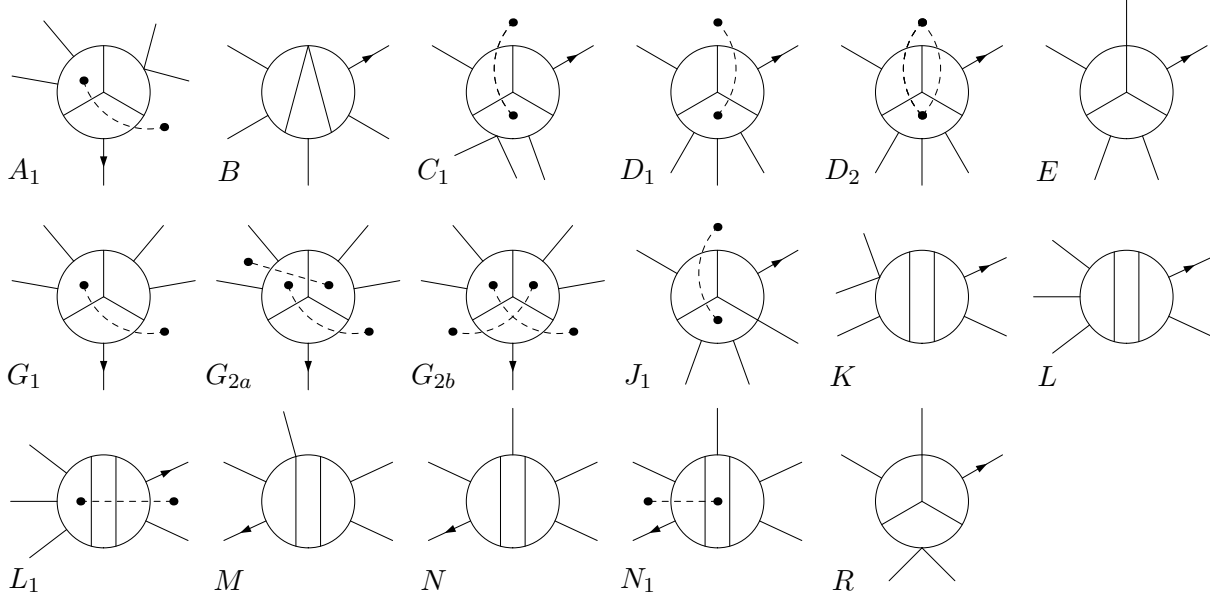


Figure 4.2: The 17 independent integrals appearing in the ansatz. Other integrals can be obtained by rotations or reflections. As in Fig. 4.1 we label the external momenta clockwise with  $k_1$  at the position indicated by the arrow.

### 4.3 The 3-loop 5-particle Amplitude

A basis of integrals which is sufficient for representing all of the leading singularities of the amplitude is shown in Fig. 4.2. By solving the collection of linear equations as explained in the previous section we find their coefficients

$$\begin{aligned}
 A_1 &= -s_{12}s_{23}^2 \frac{1 - \gamma_3}{\gamma_3 - \tilde{\gamma}_3}, \\
 B &= -s_{12}s_{23}s_{34}s_{45} \frac{\gamma_5}{\gamma_5 - \tilde{\gamma}_5}, \\
 C_1 &= -s_{12}s_{51}^2 \frac{\tilde{\gamma}_3}{\gamma_3 - \tilde{\gamma}_3}, \\
 D_1 &= s_{12}s_{23}s_{51}^2 \frac{1}{\gamma_3 - \tilde{\gamma}_3}, \\
 D_2 &= -s_{23}s_{34}s_{15} \frac{1 - \gamma_4}{\gamma_4 - \tilde{\gamma}_4}, \\
 E &= -s_{12}s_{23}^2 s_{51} \frac{1}{\gamma_3 - \tilde{\gamma}_3},
 \end{aligned}$$

$$\begin{aligned}
G_1 &= s_{12}s_{23}^2s_{51} \frac{1}{\gamma_3 - \tilde{\gamma}_3}, \\
G_{2a} &= -s_{23}s_{45}s_{51} \frac{\tilde{\gamma}_2}{\gamma_2 - \tilde{\gamma}_2}, \\
G_{2b} &= -s_{23}s_{34}s_{45} \frac{1}{\gamma_5 - \tilde{\gamma}_5}, \\
J_1 &= -s_{34}s_{45}s_{51} \frac{1}{\gamma_1 - \tilde{\gamma}_1}, \\
K &= -s_{12}^3s_{23} \frac{1 - \gamma_3}{\gamma_3 - \tilde{\gamma}_3}, \\
L &= s_{12}^3s_{23}s_{51} \frac{1}{\gamma_3 - \tilde{\gamma}_3}, \\
L_1 &= -s_{12}^2s_{34}s_{45} \frac{\tilde{\gamma}_1}{\gamma_1 - \tilde{\gamma}_1}, \\
M &= -s_{12}s_{45}^2s_{51} \frac{1}{\gamma_2 - \tilde{\gamma}_2}, \\
N &= s_{51}s_{12}s_{34}s_{45}^2 \frac{1}{\gamma_1 - \tilde{\gamma}_1}, \\
N_1 &= -s_{12}s_{34}s_{45}^2 \frac{\tilde{\gamma}_1}{\gamma_1 - \tilde{\gamma}_1}, \\
R &= s_{23}s_{45}s_{51} \frac{1 - \gamma_1}{\gamma_1 - \tilde{\gamma}_1}
\end{aligned} \tag{4.3.1}$$

where we have introduced the quantity

$$\gamma_i = \left( 1 + \frac{\langle i+2, i+3 \rangle [i+3, i]}{\langle i+2, i+4 \rangle [i+4, i]} \right)^{-1}, \tag{4.3.2}$$

and  $\tilde{\gamma}$  is given by the parity conjugate of this expression (i.e.,  $\langle a, b \rangle \leftrightarrow [a, b]$ ). In each case we have suppressed an overall factor of  $A_5^{\text{tree}}$ . In order to connect to the standard normalization conventions used in the study of the BDS ansatz it is necessary to multiply by an overall factor of  $(-1/2)^L$ . The complete amplitude is therefore assembled via the formula

$$M_5^{(3)} = A_5^{(3)}/A_5^{\text{tree}} = -\frac{1}{8} \sum_{\text{permutations}} \sum_{\text{integrals}} \frac{1}{S_i} \text{coefficient}_i \times \text{integral}_i. \tag{4.3.3}$$

The first sum runs over the 10 cyclic and anti-cyclic orderings of the labels 1, 2, 3, 4, 5 of the external particles and the second sum runs over the 17 integrals in Fig. 4.2.  $S_i$  is a symmetry factor to compensate for possible overcounting:  $S = 2$  for integrals  $B$ ,  $D_1$ ,  $D_2$ ,  $G_{2b}$ ,  $L$ ,  $L_1$ ,  $N$ , and  $R$ , and  $S = 1$  for the others.

The presentation (4.3.1) makes it simple to read off the parity-even parts of the coefficients, which will be useful in the following section. We find the parity-even parts

$$\begin{aligned}
 A_1 &= \frac{1}{2} s_{12} s_{23}^2, & B &= -\frac{1}{2} s_{12} s_{23} s_{34} s_{45}, \\
 C_1 &= \frac{1}{2} s_{12} s_{51}^2, & D_2 &= \frac{1}{2} s_{23} s_{34} s_{51}, \\
 G_{2a} &= \frac{1}{2} s_{23} s_{45} s_{51}, & K &= \frac{1}{2} s_{12}^3 s_{23}, \\
 L_1 &= \frac{1}{2} s_{12}^2 s_{34} s_{45}, & N_1 &= \frac{1}{2} s_{12} s_{34} s_{45}^2, \\
 R &= -\frac{1}{2} s_{23} s_{45} s_{51}. & & (4.3.4)
 \end{aligned}$$

with all others vanishing. We note that only the coefficients associated to dual conformal integrals have non-vanishing parity-even parts, as expected based on the pattern of previously studied amplitudes [12, 13, 14, 47, 18].

## 4.4 The Three-Loop BDS Ansatz

The infrared divergences of higher loop scattering amplitudes in gauge theory are very simply related to those of lower loop amplitudes [48]. In [11, 12], it was conjectured that in  $\mathcal{N} = 4$  SYM this simplicity persists, at least for MHV amplitudes, to the finite terms as well. Although the explicit  $n = 6$  calculation of [18] has now demonstrated,

following earlier doubts raised in [15, 16, 17] (see also [49]), that these relations are not true for all  $n$ , it is believed that they should hold for four and five particles at any number of loops since for these cases the amplitudes are determined up to a few constants by dual conformal invariance [15, 19].

The precise form of the BDS ansatz at three loops, in dimensional regularization to  $D = 4 - 2\epsilon$ , is

$$M_n^{(3)}(\epsilon) = -\frac{1}{3}(M_n^{(1)}(\epsilon))^3 + M_n^{(1)}(\epsilon)M_n^{(2)}(\epsilon) + f^{(3)}(\epsilon)M_n^{(1)}(3\epsilon) + C^{(3)} + \mathcal{O}(\epsilon) \quad (4.4.1)$$

where

$$f^{(3)}(\epsilon) = \frac{11\pi^4}{180} + (5\zeta(2)\zeta(3) + 6\zeta(5))\epsilon + a\epsilon^2, \quad C^{(3)} = b \quad (4.4.2)$$

in terms of two previously undetermined numerical constants  $a$  and  $b$ . BDS verified by explicit calculation that the 3-loop 4-particle amplitude satisfies (4.4.1), but the structure of the equation for  $n = 4$  is insensitive to the values of  $a$  and  $b$  as long as they obey the linear relation

$$2a - 9b = -\frac{341}{24}\zeta(6) + 17\zeta(3)^2. \quad (4.4.3)$$

Here we will use our 3-loop 5-particle amplitude to extract a second linear equation from (4.4.1) which will finally fix the constants  $a$  and  $b$ .

The calculation of  $a$  and  $b$  benefits from two simplifications. The first is that we may restrict our attention to the parity-even part of (4.4.1). If we write each amplitude as a sum of its parity-even and parity-odd parts,  $M_5^{(L)} = M_{5+}^{(L)} + M_{5-}^{(L)}$ , then taking

the parity-even part of (4.4.1) for  $n = 5$  gives

$$\begin{aligned} M_{5+}^{(3)}(\epsilon) = & -\frac{1}{3}(M_{5+}^{(1)}(\epsilon))^3 + M_{5+}^{(1)}(\epsilon)M_{5+}^{(2)}(\epsilon) + f^{(3)}(\epsilon)M_{5+}^{(1)}(3\epsilon) + C^{(3)} \\ & + M_{5-}^{(1)}(\epsilon) \left( M_{5-}^{(2)}(\epsilon) - M_{5+}^{(1)}(\epsilon)M_{5-}^{(1)}(\epsilon) \right) + \mathcal{O}(\epsilon). \end{aligned} \quad (4.4.4)$$

In [14] it was shown that  $M_{5-}^{(2)}(\epsilon) - M_{5+}^{(1)}(\epsilon)M_{5-}^{(1)}(\epsilon) = \mathcal{O}(\epsilon)$ . Since  $M_{5-}^{(1)}(\epsilon)$  itself is also  $\mathcal{O}(\epsilon)$ , we see that the entire last line of (4.4.4) can be replaced simply by  $+\mathcal{O}(\epsilon)$ . A consequence of the result of [14] is therefore that the parity-even part of the three-loop BDS ansatz can be obtained by making the naive replacement  $M_5^{(3)} \rightarrow M_{5+}^{(3)}$  in (4.4.1).

The second simplification is to make use of the notion of obstructions introduced in [33] and exploited in the four-loop calculations [34, 46]. We refer the reader to [34] for all of the necessary details, including a detailed algorithm for calculating obstructions. Here we simply remind the reader that for an amplitude  $A(x, \epsilon)$  depending on a single kinematic variable  $x$ , the obstruction  $P(\epsilon)$  is defined to be the coefficient of the simple pole at  $y = 0$  in the inverse Mellin transform transform, so that

$$A(x, \epsilon) = \int_{-i\infty}^{+i\infty} dy \ x^y \left[ (\text{higher order singularities}) + \frac{P(\epsilon)}{y} + (\text{regular at } y = 0) \right]. \quad (4.4.5)$$

As explained in [34] it is important to understand this relation as holding order by order in  $\epsilon$ , rather than at finite  $\epsilon$ . The prime advantage of dealing with  $P(\epsilon)$  rather than the full  $A(x, \epsilon)$  is that it is much simpler to compute. Furthermore it is important that obstructions satisfy a product algebra—the obstruction in any product of amplitudes is equal to the product of the individual obstructions.

This concept generalizes straightforwardly to integrals depending on more than

one kinematic variable. In the case at hand we have 5-particle integrals depending on five independent variables  $s_{i,i+1}$ , and we can extract the obstruction  $P(\epsilon)$  by applying the above procedure five times in succession. Equivalently, we define  $P(\epsilon)$  to be the coefficient of the  $1/(y_1 y_2 y_3 y_4 y_5)$  pole in the 5-fold inverse Mellin transform of  $A(s_{12}, s_{23}, s_{34}, s_{45}, s_{51})$ . By applying the algorithm outlined in [34] it is straightforward to find that the obstructions in the one- and two-loop five particle amplitudes are given by

$$\begin{aligned} P_5^{(1)}(\epsilon) &= -\frac{5}{2} \frac{1}{\epsilon^2} + \frac{5\pi^2}{8} + \frac{179\zeta(3)}{24}\epsilon + \frac{97\pi^4}{1440}\epsilon^2 - \left( \frac{51\pi^2\zeta(3)}{32} - \frac{137\zeta(5)}{8} \right) \epsilon^3 \\ &\quad - \left( \frac{763\zeta(3)^2}{72} - \frac{23\pi^6}{3780} \right) \epsilon^4 + \mathcal{O}(\epsilon^5), \\ P_5^{(2)}(\epsilon) &= \frac{25}{8} \frac{1}{\epsilon^4} - \frac{35\pi^2}{24} \frac{1}{\epsilon^2} - \frac{865\zeta(3)}{48} \frac{1}{\epsilon} - \frac{97\pi^4}{1152} + 21.494969\epsilon \\ &\quad - 64.357473\epsilon^2 + \mathcal{O}(\epsilon^3). \end{aligned} \quad (4.4.6)$$

For simplicity we have restricted  $P_5^{(L)}$  here to the parity-even parts of the amplitudes.

Note that these expressions satisfy the two-loop ABDK relation

$$P_5^{(2)}(\epsilon) = \frac{1}{2}(P_5^{(1)}(\epsilon))^2 + (-\zeta(2) - \zeta(3)\epsilon - \zeta(4)\epsilon^2)P_5^{(1)}(2\epsilon) - \frac{\pi^4}{72} + \mathcal{O}(\epsilon) \quad (4.4.7)$$

as expected.

At three loops, we have found that there are nine independent integrals which contribute to the parity-even part of the 5-particle amplitude. The obstructions for each of these types of integrals, through  $\mathcal{O}(\epsilon^0)$ , are

$$\begin{aligned} P_{A_1} &= \frac{20}{9} \frac{1}{\epsilon^6} + \frac{20\pi^2}{27} \frac{1}{\epsilon^4} - \frac{43\zeta(3)}{2} \frac{1}{\epsilon^3} + \frac{73\pi^4}{432} \frac{1}{\epsilon^2} - 850.242028 \frac{1}{\epsilon} + 34.239832, \\ P_B &= \frac{70}{3} \frac{1}{\epsilon^6} - \frac{45\pi^2}{2} \frac{1}{\epsilon^4} - \frac{1495\zeta(3)}{6} \frac{1}{\epsilon^3} - \frac{76\pi^4}{135} \frac{1}{\epsilon^2} + 1589.962798 \frac{1}{\epsilon} + 2824.770745, \end{aligned}$$

$$\begin{aligned}
P_{C_1} &= \frac{20}{9} \frac{1}{\epsilon^6} - \frac{25\pi^2}{54} \frac{1}{\epsilon^4} - \frac{557\zeta(3)}{36} \frac{1}{\epsilon^3} + \frac{17137\pi^4}{12960} \frac{1}{\epsilon^2} + 221.894995 \frac{1}{\epsilon} + 1030.164974, \\
P_{D_2} &= \frac{35}{3} \frac{1}{\epsilon^6} - \frac{355\pi^2}{36} \frac{1}{\epsilon^4} - \frac{645\zeta(3)}{4} \frac{1}{\epsilon^3} + \frac{767\pi^4}{2160} \frac{1}{\epsilon^2} + 231.123687 \frac{1}{\epsilon} - 4141.657880, \\
P_{G2a} &= 20 \frac{1}{\epsilon^6} - \frac{155\pi^2}{9} \frac{1}{\epsilon^4} - \frac{563\zeta(3)}{4} \frac{1}{\epsilon^3} - \frac{487\pi^4}{288} \frac{1}{\epsilon^2} + 1294.520402 \frac{1}{\epsilon} + 2938.6610 \pm 0.0036, \\
P_K &= \frac{20}{9} \frac{1}{\epsilon^6} - \frac{5\pi^2}{18} \frac{1}{\epsilon^4} - \frac{1177\zeta(3)}{36} \frac{1}{\epsilon^3} + \frac{719\pi^4}{4320} \frac{1}{\epsilon^2} + 178.487460 \frac{1}{\epsilon} - 2387.290195, \\
P_{L_1} &= \frac{35}{3} \frac{1}{\epsilon^6} - \frac{85\pi^2}{12} \frac{1}{\epsilon^4} - \frac{1411\zeta(3)}{12} \frac{1}{\epsilon^3} - \frac{1195\pi^4}{432} \frac{1}{\epsilon^2} - 673.319831 \frac{1}{\epsilon} - 2845.889639, \\
P_{N_1} &= 15 \frac{1}{\epsilon^6} - \frac{455\pi^2}{36} \frac{1}{\epsilon^4} - 136\zeta(3) \frac{1}{\epsilon^3} + \frac{983\pi^4}{1440} \frac{1}{\epsilon^2} + 625.875398 \frac{1}{\epsilon} + 437.509754 \\
P_R &= -\frac{80\zeta(3)}{3} \frac{1}{\epsilon^3} + \frac{107\pi^4}{108} \frac{1}{\epsilon^2} - 395.562804 \frac{1}{\epsilon} + 923.415196. \tag{4.4.8}
\end{aligned}$$

Each expression displays the result obtained after summing over all 10 permutations of the corresponding integral (including in each case the appropriate dual conformal numerator). The estimated error in the numerical results is much smaller than the precision indicated in all cases except for the last term in  $P_{G2a}$ , which is the overwhelmingly dominant source of numerical error.

Using the parity-even parts of the coefficients obtained in the previous section, and including the necessary factors of 1/2 to avoid overcounting those integrals with flip symmetries, we find the total three-loop obstruction

$$\begin{aligned}
P_5^{(3)} &= -\frac{1}{16} \left( P_{A_1} - \frac{1}{2} P_B + P_{C_1} + \frac{1}{2} P_{D_2} + P_{G2a} + P_K + \frac{1}{2} P_{L_1} + P_{N_1} - \frac{1}{2} P_R \right) \\
&= -\frac{125}{48} \frac{1}{\epsilon^6} + \frac{325\pi^2}{192} \frac{1}{\epsilon^4} + \frac{4175\zeta(3)}{192} \frac{1}{\epsilon^3} + \frac{499\pi^4}{10368} \frac{1}{\epsilon^2} \\
&\quad - 40.764885 \frac{1}{\epsilon} + 207.1613 \pm 0.0002 + \mathcal{O}(\epsilon) \tag{4.4.9}
\end{aligned}$$

Using the results (4.4.9) and (4.4.6), we find that the BDS relation (4.4.1) is satisfied

provided that  $a$  and  $b$  satisfy the linear relation

$$5a - 18b = 105.482 \pm 0.004. \quad (4.4.10)$$

Together with (4.4.3) this implies the solution

$$a = 85.263 \pm 0.004, \quad b = 17.8241 \pm 0.0009. \quad (4.4.11)$$

Based on the transcendentality hypothesis, it is expected that each of these numbers should be a linear combination of  $\zeta(6)$  and  $\zeta(3)^2$  with rational coefficients. However given the limited numerical accuracy of our calculation it seems prudent to avoid speculating on possible exact values for  $a$  and  $b$  at this time.

## 4.5 Summary

We have used the leading singularity method to obtain an ansatz for the four-dimensional cut-constructible part of the 3-loop 5-particle amplitude in  $\mathcal{N} = 4$  SYM theory. This means that we have determined the coefficients of the integrals shown in Fig. 4.2 by comparing residues of the ansatz to those of the amplitude on various leading singularities. Although it has not yet been proven that determination of only leading singularities completely determines an amplitude (in principle one might have to add additional integrals that vanish on all leading singularities but that have subleading singularities), the method so far has been found to give the complete answer in all cases where comparison with alternate methods was possible.

Dimensionally regulated amplitudes occasionally contain so-called ‘ $\mu$ -terms’ which are

defined as terms in the integrand which vanish in  $D = 4$  but not in  $D = 4 - 2\epsilon$  (note that this statement is, in general, completely unrelated to whether or not these terms vanish in  $D = 4 - 2\epsilon$  after integration; indeed  $\mu$ -terms can easily be IR divergent). Since the leading singularity method itself works with strictly four-dimensional loop momenta, it is insensitive to possible  $\mu$  terms, although it seems that in principle they could be determined by considering leading singularities in integer dimensions other than 4. However, in all cases that have been studied so far it has been observed that  $\mu$ -terms separately cancel out of the BDS relation, leaving  $C^{(3)}$  unaffected. We can therefore hope that even if the 3-loop 5-particle amplitude contains such terms which we have missed, they would not contribute to the constants  $a$  and  $b$  computed in section IV.

Finally we emphasize that since our goal in section IV was to streamline the calculation of  $a$  and  $b$  as much as possible, we have only evaluated the obstructions, not the full amplitude. Consequently we have not checked (even numerically) that the quantity  $+C^{(3)}$  appearing in (4.2.3) is a numerical constant; in principle it could depend on the kinematic variables  $s_{i,i+1}$ . The method of obstructions is efficient for quickly extracting the ‘constant part’ of  $C^{(3)}$  (defined as the coefficient of  $1/y$  in the inverse Mellin transform) but is insensitive to any other potential terms in  $C^{(3)}$  that depend on the  $s_{i,i+1}$ . It remains an interesting open problem to verify that there are no such terms.

# Chapter 5

## Tree formula for MHV gravity amplitude

### 5.1 Introduction

Now, we turn to study various aspects of the tree-level amplitudes in  $\mathcal{N} = 8$  SUGRA. It has recently been pointed out [20] that there are reasons to suspect  $\mathcal{N} = 8$  supergravity (SUGRA) to have even richer structure and to be ultimately even simpler than SYM. Despite great progress has been made, however, our understanding of SUGRA amplitudes is still poor compared to SYM, suggesting that we are still missing some key insights into this problem. Much of the progress on gluon amplitudes can be easily recycled and applied to graviton amplitudes due ultimately to the KLT relations [50] which roughly speaking state that “gravity is Yang-Mills squared”. Slightly more precisely, the KLT relations express an  $n$ -graviton amplitude as a sum

over permutations of the square of the color-ordered  $n$ -gluon subamplitude times some simple extra factors (see [52] for a review). There are several indications that maximal supergravity may be an extraordinarily remarkable theory and possibly even ultraviolet finite, but our feeling is that even at tree level we are still far from fully unlocking the structure of graviton amplitudes.

To illustrate this disparity we need look no further than the simplest graviton amplitudes. The original BGK (Berends, Giele and Kuijf) formula for the  $n$ -graviton MHV amplitude [51] is now over 20 years old. For later convenience we review here a different form due to Mason and Skinner [53], who proved the equivalence of the original BGK formula to the expression

$$\mathcal{M}_n^{\text{MHV}} = \sum_{P(1, \dots, n-3)} \frac{1}{\langle n \, n-2 \rangle \langle n-2 \, n-1 \rangle \langle n-1 \, n \rangle} \frac{1}{\langle 1 \, 2 \rangle \dots \langle n \, 1 \rangle} \prod_{k=1}^{n-3} \frac{[k|p_{k+1} + \dots + p_{n-2}|n-1\rangle}{\langle k \, n-1 \rangle}, \quad (5.1.1)$$

where the sum indicates a sum over all  $(n-3)!$  permutations of the labels  $1, \dots, n-3$  and we use the convention

$$[a|p_i + p_j + \dots |b\rangle = [a \, i] \langle i \, b\rangle + [a \, k] \langle j \, b\rangle + \dots. \quad (5.1.2)$$

The fact that any closed form expression exists at all for this quantity, the calculation of which would otherwise be vastly more complicated even than the corresponding one for  $n$  gluons, is an amazing achievement. Nevertheless the formula has some features which strongly suggest that it is not the end of the story.

First of all, the formula (5.1.1) does not manifest the requisite permutation symmetry of an  $n$ -graviton superamplitude. Specifically, any superamplitude  $\mathcal{M}_n$  must be fully

symmetric under all  $n!$  permutations of the labels  $1, \dots, n$  of the external particles, but only an  $S_{n-3}$  subgroup of this symmetry is manifest in (5.1.1) (several formulas which manifest a slightly larger  $S_{n-2}$  subgroup are known [4, 54]). Of course one can check, numerically if necessary, that (5.1.1) does in fact have this symmetry, but it is far from obvious. Moreover, even the  $S_{n-3}$  symmetry arises in a somewhat contrived way, via an explicit sum over permutations. Undoubtedly the summand in (5.1.1) contains redundant information which is washed out by taking the sum.

Secondly, one slightly disappointing feature of all previously known MHV formulas including (5.1.1) is the appearance of “ $\dots$ ”, which indicates that a particular cyclic ordering of the particles must be chosen in order to write the formula, even though a graviton amplitude ultimately cannot depend on any such ordering since gravitons do not carry any color labels. This vestigial feature usually traces back to the use of the KLT relations to calculate graviton amplitudes by recycling gluon amplitudes.

An important feature of graviton amplitudes is that they fall off like  $1/z^2$  as the supermomenta of any two particles are taking to infinity in a particular complex direction unlike in Yang-Mills theory where the falloff is only  $1/z$ . As we noted in previous Chapter, this seeming simple fact can be greatly used for simplifying the tree-level amplitudes. And this exceptionally soft behavior of graviton tree amplitudes is of direct importance for the remarkable ultraviolet cancellations in supergravity loop amplitudes (see e.g. [55] and related references).

It is difficult to imagine that it might be possible to improve upon the Parke-Taylor formula for the  $n$ -gluon MHV amplitude. However, for the reasons just reviewed, we feel that (5.1.1) cannot be the end of the story for gravity. Ideally one would like to have a formula for  $n$ -graviton scattering that (1) is manifestly  $S_n$  symmetric without

the need for introducing an explicit sum over permutations to impose the symmetry *vi et armis*; (2) makes no vestigial reference to any cyclic ordering of the  $n$  gravitons, and (3) manifests  $1/z^2$  falloff term by term, making it unsqueezable by the bonus relations.

In this chapter we present and prove an new formula for the MHV scattering amplitude which addresses the second and third points but only manifests  $S_{n-2}$  symmetry. In section 2 we introduce the tree formula and discuss several special cases as well as the general soft limit. In section 3 we work out the simple link representation of the amplitude in twistor space, from which new physical space formula follows. Finally the proof is in section 4.

## 5.2 The MHV Tree Formula

### 5.2.1 Statement of the Tree Formula

Here we introduce a formula for the  $n$ -graviton MHV scattering amplitude which we call the “tree formula” since it consists of a sum of terms, each of which is conveniently represented by a tree diagram. The tree formula manifests an  $S_{n-2}$  subgroup of the full permutation group. For the moment we choose to treat particles  $n-1$  and  $n$  as special. With this arbitrary choice the formula is:

$$\mathcal{M}_n^{\text{MHV}} = \frac{1}{\langle n-1 n \rangle^2} \sum_{\text{trees}} \left( \prod_{\text{edges } ab} \frac{[a b]}{\langle a b \rangle} \right) \left( \prod_{\text{vertices } a} (\langle a n-1 \rangle \langle a n \rangle)^{\deg(a)-2} \right). \quad (5.2.1)$$

It is interesting to note that the expression for the  $n$ -point amplitude can actually be represented as all inequivalent connected tree graphs with vertices labelled  $1, 2, \dots, n - 2$ . (It was proven by Cayley long time ago that there are precisely  $(n - 2)^{n-4}$  such diagrams.)

### 5.2.2 Examples

We defer to section IV a formal proof of the tree formula as the impatient reader may be sufficiently convinced by seeing the formula in action here for small  $n$  and by noting that it has the correct soft limits for all  $n$ , as we discuss shortly.

For each of the trivial cases  $n = 3, 4$  there is only a single tree diagram,

$$\mathcal{M}_3^{\text{MHV}} = \frac{1}{(\langle 12 \rangle \langle 13 \rangle \langle 23 \rangle)^2} \quad (5.2.2)$$

and

$$\mathcal{M}_4^{\text{MHV}} = \frac{[12]}{\langle 12 \rangle \langle 13 \rangle \langle 14 \rangle \langle 23 \rangle \langle 24 \rangle \langle 34 \rangle^2} \quad (5.2.3)$$

respectively, which immediately reproduce the correct expressions.

For  $n = 5$  there are three tree diagrams

$$\begin{aligned} A_5 = & \frac{[12][23]}{\langle 12 \rangle \langle 14 \rangle \langle 15 \rangle \langle 23 \rangle \langle 34 \rangle \langle 35 \rangle \langle 45 \rangle^2} \\ & + \frac{[13][23]}{\langle 13 \rangle \langle 14 \rangle \langle 15 \rangle \langle 23 \rangle \langle 24 \rangle \langle 25 \rangle \langle 45 \rangle^2} \\ & + \frac{[12][13]}{\langle 12 \rangle \langle 13 \rangle \langle 24 \rangle \langle 25 \rangle \langle 34 \rangle \langle 35 \rangle \langle 45 \rangle^2} \end{aligned} \quad (5.2.4)$$

which can easily be verified by hand to sum to the correct expression. Agreement

between the tree formula and other known formulas such as (5.1.1) may be checked numerically for slightly larger values of  $n$  by assigning random values to all of the spinor helicity variables.

### 5.2.3 Soft Limit of the Tree Formula

Let us consider for a moment the component amplitude

$$M(1^+, \dots, (n-2)^+, (n-1)^-, n^-) = \langle n-1 n \rangle^8 \mathcal{M}_n^{\text{MHV}} \quad (5.2.5)$$

with particles  $n-1$  and  $n$  having negative helicity. The universal soft factor for gravitons is [51]

$$\lim_{p_1 \rightarrow 0} \frac{M(1^+, \dots, (n-2)^+, (n-1)^-, n^-)}{M(2^+, \dots, (n-2)^+, (n-1)^-, n^-)} = \sum_{i=2}^{n-2} g(i^+), \quad g(i^+) = \frac{\langle i n-1 \rangle}{\langle 1 n-1 \rangle} \frac{\langle i n \rangle}{\langle 1 n \rangle} \frac{[1 i]}{\langle 1 i \rangle}. \quad (5.2.6)$$

It is simple to see that the MHV tree formula satisfies this property: the tree diagrams which do not vanish in the limit  $p_1 \rightarrow 0$  are those in which vertex 1 is connected by a propagator to a single other vertex  $i$ . Such diagrams remain connected when vertex 1 is chopped off, leaving a contribution to the  $n-1$ -graviton amplitude times the indicated factor  $g(i^+)$ .

Thinking about this process in reverse therefore suggests a simple interpretation of (5.2.6) in terms of tree diagrams—it is a sum over all possible places  $i$  where the vertex 1 may be attached to the  $n-1$ -graviton amplitude. This structure is exactly that of the “inverse soft factors”, and we have checked that the MHV tree formula may be built up by recursively applying the rule proposed there.

### 5.3 The MHV Tree Formula in Twistor Space

Before turning to the formal proof of the tree formula in the next section, here we work out the link representation of the MHV graviton amplitude in twistor space, which was one of the steps which led to the discovery of the tree formula. Two papers [56, 24] have recently constructed versions of the BCF on-shell recursion relation directly in twistor space variables. We follow the standard notation where  $\mu$ ,  $\tilde{\mu}$  are respectively Fourier transform conjugate to the spinor helicity variables  $\lambda$ ,  $\tilde{\lambda}$ , and assemble these together with a four-component Grassmann variable  $\eta$  and its conjugate  $\tilde{\eta}$  into the  $4|8$ -component supertwistor variables

$$\mathcal{Z} = \begin{pmatrix} \lambda \\ \mu \\ \eta \end{pmatrix}, \quad \mathcal{W} = \begin{pmatrix} \tilde{\mu} \\ \tilde{\lambda} \\ \tilde{\eta} \end{pmatrix}. \quad (5.3.1)$$

In the approach of [24], in which variables of both chiralities  $\mathcal{Z}$  and  $\mathcal{W}$  are used simultaneously, an apparently important role is played by the link representation which expresses an amplitude  $\mathcal{M}$  in the form

$$\mathcal{M}(\mathcal{Z}_i, \mathcal{W}_J) = \int dc U(c_{iJ}, \lambda_i, \tilde{\lambda}_J) \exp \left[ i \sum_{i,J} c_{iJ} \mathcal{Z}_i \cdot \mathcal{W}_J \right]. \quad (5.3.2)$$

Here one splits the  $n$  particles into two groups, one of which (labeled by  $i$ ) one chooses to represent in  $\mathcal{Z}$  space and the other of which (labeled by  $J$ ) one chooses to represent in  $\mathcal{W}$  space. The integral runs over all of the aptly-named link variables  $c_{iJ}$  and we refer to the integrand  $U(c_{iJ}, \lambda_i, \tilde{\lambda}_J)$  as the link representation of  $\mathcal{M}$ . It was shown in [24] that the BCF on-shell recursion in twistor space involves nothing more

than a simple integral over  $\mathcal{Z}$ ,  $\mathcal{W}$  variables with a simple (and essentially unique) measure factor.

The original motivation for our investigation was to explore the structure of link representations for graviton amplitudes. We will always adopt the convenient convention of expressing an  $N^k$ MHV amplitude in terms of  $k + 2$   $\mathcal{Z}$  variables and  $n - k - 2$   $\mathcal{W}$  variables. The three-particle MHV and  $\overline{\text{MHV}}$  amplitudes

$$U_3^{\text{MHV}} = \frac{|\langle 1 2 \rangle|}{c_{13}^2 c_{23}^2}, \quad U_3^{\overline{\text{MHV}}} = \frac{|[1 2]|}{c_{31}^2 c_{32}^2} \quad (5.3.3)$$

seed the on-shell recursion, which is then sufficient (in principle) to determine the link representation for any desired amplitude.

For example, the four-particle amplitude is the sum of two contributing BCF diagrams

$$U_4^{\text{MHV}} = \frac{\langle 1 2 \rangle [3 4]}{c_{13}^2 c_{24}^2 c_{12:34}} + \frac{\langle 1 2 \rangle [3 4]}{c_{13}^2 c_{24}^2 c_{14} c_{23}} \quad (5.3.4)$$

where we use the notation

$$c_{i_1 i_2: J_1 J_2} = c_{i_1 J_1} c_{i_2 J_2} - c_{i_1 J_2} c_{i_2 J_1}. \quad (5.3.5)$$

Remarkably the two terms in (5.3.4) combine nicely into the simple result presented already in [24]:

$$U_4^{\text{MHV}} = \frac{\langle 1 2 \rangle [3 4]}{c_{13} c_{14} c_{23} c_{24} c_{12:34}}. \quad (5.3.6)$$

This simplification seems trivial at the moment but it is just the tip of an iceberg. For larger  $n$  the enormous simplifications discussed in the previous section, which are apparently non-trivial in physical space, occur automatically in the link

representation.

For example the five particle MHV amplitude is the sum of three BCF diagrams,

$$U_5^{\text{MHV}} = \left\{ \frac{|\langle 1 2 \rangle| [4 5] (c_{24}[3 4] + c_{25}[3 5])}{c_{13} c_{23} c_{14} c_{25}^2 c_{12:34} c_{12:45}} + (3 \leftrightarrow 4) \right\} + \frac{|\langle 1 2 \rangle| [3 4] (c_{24}[4 5] + c_{23}[3 5])}{c_{13} c_{14} c_{15} c_{23} c_{24} c_{25}^2 c_{12:34}} \quad (5.3.7)$$

which nicely simplifies to

$$\frac{1}{|\langle 1 2 \rangle|} U_5^{\text{MHV}} = \frac{[3 4][4 5]}{c_{13} c_{15} c_{23} c_{25} c_{12:34} c_{12:45}} + \frac{[3 5][4 5]}{c_{13} c_{14} c_{23} c_{24} c_{12:35} c_{12:45}} + \frac{[3 4][3 5]}{c_{14} c_{15} c_{24} c_{25} c_{12:34} c_{12:35}}. \quad (5.3.8)$$

This expression already exhibits the structure of the MHV tree formula (except that here particles 1 and 2 are singled out, and the vertices of the trees are labeled by  $\{3, 4, 5\}$ ).

Subsequent investigations for higher  $n$  reveal the general pattern which is as follows. Returning to the convention where particles  $n - 1$  and  $n$  are treated as special, the link representation for any desired MHV amplitude may be written down by drawing all tree diagrams with vertices labeled by  $\{1, \dots, n - 2\}$  and then assigning

1. an overall factor of  $\langle n - 1 \ n \rangle \text{sign}(\langle n - 1 \ n \rangle)^n$ ,
2. for each propagator connecting nodes  $a$  and  $b$ , a factor of  $[a \ b]/c_{n-1,n:a,b}$ ,
3. for each vertex  $a$ , a factor of  $(c_{n-1,a} c_{n,a})^{\deg(a)-2}$ , where  $\deg(a)$  is the degree of the vertex labeled  $a$ .

It is readily verified by direct integration over the link variables that these rules are precisely the link-space representation of the physical space rules for the MHV tree formula given in the previous section.

## 5.4 Proof of the MHV Tree Formula

Here we present a proof of the MHV tree formula. One way one might attempt to prove the formula would be to show directly that it satisfies the BCF on-shell recursion relation [2, 3] for gravity [4, 5], but the structure of the formula is poorly suited for this task. Instead we proceed by considering the usual BCF deformation of the formula  $M_n^{\text{MHV}}$  by a complex parameter  $z$  and demonstrating that  $M_n^{\text{MHV}}(z)$  has the same residue at every pole (and behavior at infinity) as the similarly deformed graviton amplitude, thereby establishing equality of the two for all  $z$ .

In this section we return to singling out particles 1 and 2, letting the vertices in the tree diagrams carry the labels  $\{3, \dots, n\}$ . Then the MHV tree formula (5.2.1) can be written as

$$M_n^{\text{MHV}} = \langle 1 2 \rangle^6 \sum_{\text{trees}} \frac{[\cdot] \cdots [\cdot]}{\langle \cdot \rangle \cdots \langle \cdot \rangle} \prod_{a=3}^n (\langle 1 a \rangle \langle 2 a \rangle)^{\deg(a)-2} \quad (5.4.1)$$

(note that we continue to work with the component amplitude (5.2.5)) where the factors  $[\cdot] \cdots [\cdot] / \langle \cdot \rangle \cdots \langle \cdot \rangle$  associated with the propagators of a diagram are independent of 1 and 2. Let us now make the familiar BCF shift [3]

$$\lambda_1 \rightarrow \lambda_1(z) = \lambda_1 - z\lambda_2, \quad \tilde{\lambda}_2 \rightarrow \tilde{\lambda}_2(z) = \tilde{\lambda}_2 + z\tilde{\lambda}_1 \quad (5.4.2)$$

which leads to the  $z$ -deformed MHV tree formula

$$M_n^{\text{MHV}}(z) = \langle 1 2 \rangle^6 \sum_{\text{trees}} \frac{[\cdot] \cdots [\cdot]}{\langle \cdot \rangle \cdots \langle \cdot \rangle} \prod_{a=3}^n [(\langle 1 a \rangle - z\langle 2 a \rangle) \langle 2 a \rangle]^{\deg(a)-2}. \quad (5.4.3)$$

Here we are in a position to observe a nice fact: since each tree diagram is connected,

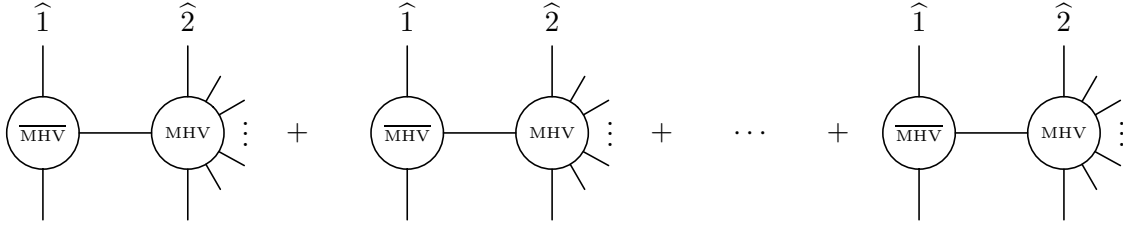


Figure 5.1: All factorizations contributing to the on-shell recursion relation for the  $n$ -point MHV amplitude. Only the first diagram contributes to the residue at  $z = \langle 13 \rangle / \langle 23 \rangle$ .

the degrees satisfy the sum rule

$$\sum_{a=3}^n (\deg(a) - 2) = -2, \quad (5.4.4)$$

which guarantees that each individual term in (5.4.3) manifestly behaves like  $1/z^2$  at large  $z$ . This exceptionally soft behavior of graviton amplitudes is completely hidden in the usual Feynman diagram expansion.

A complex function of a single variable which vanishes at infinity is uniquely determined by the locations of its poles as well as its residues. Having noted that (5.4.3) has the correct behavior at large  $z$ , we can conclude the proof of the MHV tree formula by demonstrating that (5.4.3) has precisely the expected residues at all of its poles. In order to say what the expected residues are we shall use induction on  $n$ . As discussed above the tree formula is readily verified for sufficiently small  $n$ , so let us assume that it has been established up through  $n - 1$ . We can then use BCF on-shell recursion (whose terms are displayed graphically in Fig. 5.1) to determine what the residues in the deformed  $n$ -point amplitude ought to be.

Without loss of generality let us consider just the pole at  $z = z_3 \equiv \langle 13 \rangle / \langle 23 \rangle$ . The only tree diagrams which contribute to the residue at this pole are those with

$\deg(3) = 1$ , meaning that the vertex labeled 3 is connected to the rest of the diagram by a single propagator. Chopping off vertex 3 gives a subdiagram with vertices labeled  $\{4, \dots, n\}$ . Clearly all diagrams which contribute to this residue can be generated by first considering the collection of tree diagrams with vertices labeled  $\{4, \dots, n\}$  and then attaching vertex 3 in all possible ways to the  $n - 3$  vertices of the subdiagram. We therefore have

$$M_n^{\text{MHV}}(z) \sim \langle 1 2 \rangle^6 \sum_{\text{subdiagrams}} \frac{[ ] \cdots [ ]}{\langle \rangle \cdots \langle \rangle} \left( \sum_{b=4}^n \frac{[3 b]}{\langle 3 b \rangle} \langle \hat{1} b \rangle \langle 2 b \rangle \right) \frac{1}{\langle \hat{1} 3 \rangle \langle 2 3 \rangle} \prod_{a=4}^n \left( \langle \hat{1} a \rangle \langle 2 a \rangle \right)^{\deg(a)-2} \quad (5.4.5)$$

where  $\sim$  denotes that we have dropped terms which are nonsingular at  $z = z_3$ , the sum over  $b$  runs over all the places where vertex 3 can be attached to the subdiagram, and  $[ ] \cdots [ ] / \langle \rangle \cdots \langle \rangle$  indicates all edge factors associated the subdiagram, necessarily independent of 3. Using the Schouten identity we find that  $\langle \hat{1} b \rangle = \langle 1 2 \rangle \langle b 3 \rangle / \langle 2 3 \rangle$  so we have after a couple of simple steps (and using (5.4.4))

$$M_n^{\text{MHV}}(z) \sim \langle 1 2 \rangle^6 \frac{[1 3]}{\langle 1 3 \rangle - z \langle 2 3 \rangle} \sum_{\text{subdiagrams}} \frac{[ ] \cdots [ ]}{\langle \rangle \cdots \langle \rangle} \prod_{a=4}^n \left( \langle 2 a \rangle \langle 3 a \rangle \right)^{\deg(a)-2}. \quad (5.4.6)$$

On the other hand we know from the on-shell recursion for the  $n$ -point amplitude that the residue at  $z = z_3$  comes entirely from the first BCFW diagram in Fig. 5.1, whose value is

$$M_3^{\overline{\text{MHV}}}(z_3) \times \frac{1}{P^2(z)} \times M_{n-1}^{\text{MHV}}(z_3) \quad (5.4.7)$$

where

$$P(z) = p_1 + p_3 - z \lambda_2 \tilde{\lambda}_1. \quad (5.4.8)$$

Assuming the validity of the MHV tree formula for the  $n - 1$ -point amplitude on the

right, the expression (5.4.7) evaluates to

$$\frac{[\hat{P} 3]^6}{[3 1]^2 [1 \hat{P}]^2} \times \frac{1}{[1 3](\langle 1 3 \rangle - z \langle 2 3 \rangle)} \times \langle \hat{P} 2 \rangle^6 \sum_{\text{subdiagrams}} \frac{[ ] \cdots [ ]}{\langle \rangle \cdots \langle \rangle} \prod_{a=4}^n \left( \langle \hat{P} a \rangle \langle 2 a \rangle \right)^{\deg(a)-2} \quad (5.4.9)$$

where  $\hat{P} = P(z_3)$ . After simplifying this result with the help of (5.4.8) we find precise agreement with (5.4.5), thereby completing the proof of the MHV tree formula.

## 5.5 Discussion and Open Questions

The tree formula introduced in this paper has several conceptually satisfying features and almost completely fulfills the wish-list outlined in the introduction. It appears to be a genuinely gravitational formula, rather than a recycled Yang-Mills result.

The new MHV tree formula can be very naturally translated into “link” representation, we hope that the new MHV tree formula might provide a more appropriate starting point for this purpose and perhaps shed some more light on a twistor-string-like (or Grassmannian formulation) description, as we discussed earlier, for supergravity.

Another interesting fact is that the tree formula apparently can neither be easily derived from BCF, nor usefully used as an input to BCF, suggests the possible existence of some kind of new rules for the efficient calculation of more general gravity amplitudes.

# Chapter 6

## All tree-level amplitudes in $\mathcal{N} = 8$ SUGRA

### 6.1 Introduction

Previously we have presented a new formula for gravity MHV amplitude, which has many nice properties as a gravity amplitude. Now we would like to go beyond MHV level to study all tree-level amplitudes in SUGRA. The natural weapon we will use is BCFW recursion relations.

In this chapter we present an algorithm for writing down an arbitrary tree-level SUGRA amplitude. Our result was largely made possible by combining and extending the results of two recent papers. In [7] an explicit formula for all tree amplitudes in SYM was found by solving the supersymmetric version [20] of the on-shell recursion relation [2, 3]. We will review all appropriate details in a moment, but for now it

suffices to write their formula for the color-ordered SYM amplitude  $A(1, \dots, n)$  very schematically as

$$A(1, \dots, n) = A^{\text{MHV}}(1, \dots, n) \sum_{\{\alpha\}} R_\alpha(\lambda_i, \tilde{\lambda}_i, \eta_i), \quad (6.1.1)$$

where the sum runs over a collection of dual superconformal [57, 58, 59] invariants  $R_\alpha$ . The set  $\{\alpha\}$  is dictated by whether  $A$  is MHV (in which case there is obviously only a single term, 1, in the sum), next-to-MHV (NMHV), next-to-next-to-MHV (NNMHV), etc.

Our second inspiration is an intriguing formula for the  $n$ -graviton MHV amplitude obtained by Elvang and Freedman [54] which has the feature of expressing the amplitude in terms of sums of squares of gluon amplitudes, in spirit similar to though in detail very different from the KLT relations. Their formula reads

$$\mathcal{M}_n^{\text{MHV}} = \sum_{\mathcal{P}(2, \dots, n-1)} [A^{\text{MHV}}(1, \dots, n)]^2 G^{\text{MHV}}(1, \dots, n), \quad (6.1.2)$$

where the sum runs over all permutations of the labels 2 through  $n - 1$  and  $G^{\text{MHV}}(1, \dots, n)$  is a particular ‘gravity factor’ reviewed below.

Our result involves a natural merger of (6.1.1) and (6.1.2), expressing an arbitrary  $n$ -graviton super-amplitude in the form

$$\mathcal{M}_n = \sum_{\mathcal{P}(2, \dots, n-1)} [A^{\text{MHV}}(1, \dots, n)]^2 \sum_{\{\alpha\}} [R_\alpha(\lambda_i, \tilde{\lambda}_i, \eta_i)]^2 G_\alpha(\lambda_i, \tilde{\lambda}_i). \quad (6.1.3)$$

Two important features worth pointing out are that the sum runs over precisely the same set  $\{\alpha\}$  that appears in the SYM case (6.1.1), rather than some kind of double

sum as one might have guessed, and that the ‘gravity dressing factors’  $G_\alpha$  do not depend on the fermionic coordinates  $\eta_i^A$  of the on-shell  $\mathcal{N} = 8$  superspace. All of the ‘super’ structure of the amplitudes is completely encoded in the same  $R$ -factors that appear already in the SYM amplitudes.

We begin in the next section by reviewing some of the necessary tools for carrying out our calculation. In section III we provide detailed derivations of explicit formulas for MHV, NMHV, and NNMHV amplitudes. Finally in section IV we discuss the structure of the gravity dressing factors  $G_\alpha$  for more general graviton amplitudes.

## 6.2 Setting up the Calculation

### 6.2.1 Supersymmetric Recursion

We will use the supersymmetric version [60, 20] of the on-shell recursion relation [2, 3]

$$\mathcal{M}_n = \sum_P \int \frac{d^8\eta}{P^2} \mathcal{M}_L(z_P) \mathcal{M}_R(z_P) \quad (6.2.1)$$

where we follow the conventions of [7] in choosing the supersymmetry preserving shift

$$\begin{aligned} \lambda_1^z(z) &= \lambda_1 - z\lambda_n, \\ \tilde{\lambda}_{\bar{n}}(z) &= \tilde{\lambda}_n + z\tilde{\lambda}_1, \\ \eta_{\bar{n}}(z) &= \eta_n + z\eta_1, \end{aligned} \quad (6.2.2)$$

so that the sum in (6.2.1) runs over all factorization channels of  $\mathcal{M}_n$  which separate particle 1 and particle  $n$  (into  $\mathcal{M}_L$  and  $\mathcal{M}_R$ , respectively). The value of the shift parameter

$$z_P = \frac{P^2}{[1|P|n]} \quad (6.2.3)$$

is chosen so that the shifted intermediate momentum

$$\hat{P}(z) = P + z\lambda_n\tilde{\lambda}_1, \quad P = -p_1 - \dots = \dots + p_n \quad (6.2.4)$$

goes on-shell at  $z = z_P$ . The recursion relation (6.2.1) can be seeded with the fundamental 3-particle amplitudes [20]

$$\mathcal{M}_3^{\overline{\text{MHV}}} = \frac{\delta^{(8)}(\eta_1[2\ 3] + \eta_2[3\ 1] + \eta_3[1\ 2])}{([1\ 2][2\ 3][3\ 1])^2}, \quad \mathcal{M}_3^{\text{MHV}} = \frac{\delta^{(16)}(q)}{(\langle 1\ 2 \rangle \langle 2\ 3 \rangle \langle 3\ 1 \rangle)^2}. \quad (6.2.5)$$

## 6.2.2 Gravity Subamplitudes

Color-ordered amplitudes in SYM have a cyclic structure such that only those factorizations preserving the cyclic labeling of the external particles appear in the analogous recursion (6.2.1).

In contrast, gravity amplitudes must be completely symmetric under the exchange of any particle labels, so vastly more factorizations contribute to (6.2.1). We can deal with this complication once and for all by introducing the notion of an ordered ‘gravity subamplitude’  $M(1, \dots, n)$ . These non-physical but mathematically useful

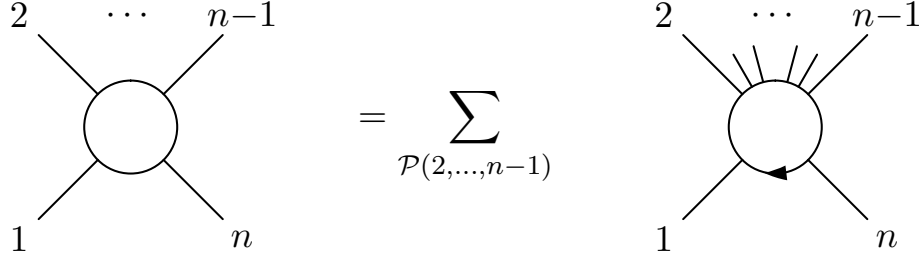


Figure 6.1: A diagrammatic representation of the relation (6.2.6) between a physical gravity amplitude  $\mathcal{M}_n$  and the sum over its ordered subamplitudes  $M(1, \dots, n)$ . We draw an arrow indicating the cyclic order of the indices between the special legs  $n$  and  $1$ .

objects are related to the complete, physical amplitudes  $\mathcal{M}_n$  via the relation

$$\mathcal{M}_n = \sum_{\mathcal{P}(2, \dots, n-1)} M(1, \dots, n), \quad (6.2.6)$$

depicted graphically in Fig. 6.1. This decomposition only makes a subgroup of the full permutation symmetry manifest. However it is the largest subgroup that the recursion (6.2.1) allows us to preserve since two external lines are singled out for special treatment.

The relation (6.2.6) does not uniquely determine the subamplitudes for a given  $\mathcal{M}_n$ , since one could add to  $M(1, \dots, n)$  any quantity which vanishes after summing over permutations. We choose to define the subamplitudes  $M$  recursively via (6.2.1) restricted to factorizations which preserve the cyclic ordering of the indices, just like in SYM theory:

$$M(1, \dots, n) \equiv \sum_{i=3}^{n-1} \int \frac{d^8 \eta}{P^2} M(\hat{1}, 2, \dots, i-1, \hat{P}) M(-\hat{P}, i, \dots, n-1, \bar{n}). \quad (6.2.7)$$

This recursion is also seeded with the three-point amplitudes (6.2.5) since there is no

distinction between  $M(1, 2, 3)$  and  $\mathcal{M}_3$ . Note however that unlike the color-ordered SYM amplitudes  $A(1, \dots, n)$ , the gravity subamplitude  $M(1, \dots, n)$  is *not* in general invariant under cyclic permutations of its arguments.

It remains to prove the consistency of this definition. That is, we need to check that the subamplitudes defined in (6.2.7), when substituted into (6.2.6), do in fact give correct expressions for the physical gravity amplitude  $\mathcal{M}_n$ . This straightforward combinatorics exercise proceeds by induction, beginning with the  $n = 3$  case which is trivial and then assuming that (6.2.6) is correct up to and including  $n - 1$  gravitons. For  $n$  gravitons we then have

$$\begin{aligned}
\mathcal{M}_n &= \sum_{A \cup B = \{2, \dots, n-1\}} \int \frac{d^8 \eta}{P^2} \mathcal{M}(\hat{1}, \{A\}, \hat{P}) \mathcal{M}(-\hat{P}, \{B\}, \bar{n}) \\
&= \frac{1}{(n-2)!} \sum_{\mathcal{P}(2, \dots, n-1)} \sum_{A \cup B = \{2, \dots, n-1\}} \int \frac{d^8 \eta}{P^2} \mathcal{M}(\hat{1}, \{A\}, \hat{P}) \mathcal{M}(-\hat{P}, \{B\}, \bar{n}) \\
&= \frac{1}{(n-2)!} \sum_{\mathcal{P}(2, \dots, n-1)} \sum_{j=3}^{n-1} \binom{n-2}{j-2} \int \frac{d^8 \eta}{P^2} \mathcal{M}(\hat{1}, 2, \dots, j-1, \hat{P}) \mathcal{M}(-\hat{P}, j, \dots, n-1, \bar{n}) \\
&= \sum_{\mathcal{P}(2, \dots, n-1)} \sum_{j=3}^{n-1} \int \frac{d^8 \eta}{P^2} M(\hat{1}, 2, \dots, j-1, \hat{P}) M(-\hat{P}, j, \dots, n-1, \bar{n}) \\
&= \sum_{\mathcal{P}(2, \dots, n-1)} M(1, 2, \dots, n).
\end{aligned} \tag{6.2.8}$$

The first line is the superrecursion for the physical amplitude, including a sum over all partitions of  $\{2, \dots, n-1\}$  into two subsets  $A$  and  $B$ , not just those which preserve a cyclic ordering. In the second line we have thrown in a spurious sum over all permutations of  $\{2, \dots, n-1\}$  at the cost of dividing by  $(n-2)!$  to compensate for the overcounting. This is allowed since we know that  $\mathcal{M}_n$  is completely symmetric under the exchange of any of its arguments. Inside the sum over permutations we

are then free to choose  $A = \{2, \dots, i-1\}$  and  $B = \{i, \dots, n-1\}$  as indicated on the third line, including the factor  $\binom{n-2}{i-2}$  to count the number of times this particular term appears. On the fourth line our prior assumption that (6.2.6) holds up to  $n-1$  particles allows us to replace  $\mathcal{M}_a \rightarrow (a-2)!M_a$  inside the sum over permutations. The last line invokes the definition (6.2.7) and completes the proof that the physical  $n$ -graviton amplitude may be recovered from the ordered subamplitudes via (6.2.6) and the definition (6.2.7).

### 6.2.3 From $\mathcal{N} = 4$ to $\mathcal{N} = 8$ Superspace

The astute reader may have objected already to (6.1.2) in the introduction. The SYM MHV amplitude involves the delta function  $\delta^{(8)}(q)$  expressing conservation of the total supermomentum

$$q = \sum_{i=1}^n \lambda_i^\alpha \eta_i^A, \quad \alpha = 1, 2, \quad A = 1, \dots, 4. \quad (6.2.9)$$

Since the square of a fermionic delta function is zero, it would seem that it makes no sense for the quantity  $[A^{\text{MHV}}(1, \dots, n)]^2$  to appear in (6.1.2).

Throughout this paper it will prove extremely convenient to adopt the convention that the square of an  $\mathcal{N} = 4$  superspace expression refers to an  $\mathcal{N} = 8$  superspace expression in the most natural way. For example, it should always be understood that

$$[\delta^{(8)}(q)]^2 = \delta^{(16)}(q), \quad (6.2.10)$$

where the  $q$  on the right-hand side is given by the same expression (6.2.9) but

with  $A = 1, \dots, 8$ . This notation will prove especially useful for lifting results of Grassmann integration from  $\mathcal{N} = 4$  to  $\mathcal{N} = 8$  superspace. This trick works because we can break the  $SU(8)$  symmetry of a  $d^8\eta$  integration into  $SU(4)_a \times SU(4)_b$  by taking  $\eta_1, \dots, \eta_4$  for  $SU(4)_a$  and  $\eta_5, \dots, \eta_8$  for  $SU(4)_b$ . Then every  $d^8\eta$  integral can be rewritten as a product of two SYM integrals and the  $SU(8)$  symmetry of the answer is restored simply by adopting the convention (6.2.10).

For a specific example consider the basic SYM integral

$$\int \frac{d^4\eta}{P^2} A^{\overline{\text{MHV}}}(\hat{1}, 2, \hat{P}) A^{\text{MHV}}(-\hat{P}, 3, \dots, \bar{n}) = \frac{\delta^{(8)}(q)}{\langle 1 2 \rangle \langle 2 3 \rangle \dots \langle n 1 \rangle} \quad (6.2.11)$$

which expresses the superrecursion for the case of MHV amplitudes. By ‘squaring’ this formula we immediately obtain the answer for a similar  $\mathcal{N} = 8$  Grassmann integral,

$$\int \frac{d^8\eta}{P^2} [A^{\overline{\text{MHV}}}(\hat{1}, 2, \hat{P})]^2 [A^{\text{MHV}}(-\hat{P}, 3, \dots, \bar{n})]^2 = P^2 \frac{\delta^{(16)}(p)}{(\langle 1 2 \rangle \langle 2 3 \rangle \dots \langle n 1 \rangle)^2}. \quad (6.2.12)$$

Note the extra factor of  $P^2$  which appears on the right-hand side because we have, for obvious reasons, chosen not to square the propagator  $1/P^2$  on the left.

### 6.2.4 Review of SYM Amplitudes

Given the above considerations it should come as no surprise that we will be able to import much of the structure of SYM amplitudes directly into our SUGRA results. Therefore we now review the results of [7] for tree amplitudes in SYM. Here and in

all that follows we use the standard dual superconformal [57, 58, 59] notation

$$\begin{aligned} x_{ij} &= p_i + p_{i+1} + \cdots + p_{j-1}, \\ \theta_{ij} &= \lambda_i \eta_i + \cdots + \lambda_{j-1} \eta_{j-1}, \end{aligned} \tag{6.2.13}$$

where all subscripts are understood mod  $n$ .

We will base our expression for the SUGRA amplitudes on an expression for the SYM amplitudes which is equivalent to, but not exactly the same as the one presented in [7]. The reason is that the cyclic symmetry of the Yang-Mills amplitudes implies certain identities for the invariants  $R_\alpha$  appearing in (6.1.1). This symmetry was used in [7] when solving the recursion relations. Instead it is helpful to have a different expression which is more suitable to the gravity case where the subamplitudes  $M$  do not have cyclic symmetry.

To be precise we need to return to the construction of [7] and make sure that when considering the right-hand side of the BCF recursion relation we always insert the lower point amplitudes so that leg 1 of the left amplitude factor corresponds to the shifted leg  $\hat{1}$ . We also need to have the leg  $n$  of the right amplitude factor corresponding to the shifted leg  $\bar{n}$ , but this was already the choice made in [7].

The expression for all  $\mathcal{N} = 4$  SYM amplitudes is given in terms of paths in a particular rooted tree diagram, these invariants appeared in (6.1.1) take the general form [59, 7]

$$R_{n;a_1b_1;a_2b_2;\dots;a_rb_r;ab} = \frac{\langle a a - 1 \rangle \langle b b - 1 \rangle \delta^{(4)}(\langle \xi | x_{b_r a} x_{ab} | \theta_{bb_r} \rangle + \langle \xi | x_{b_r b} x_{ba} | \theta_{ab_r} \rangle)}{x_{ab}^2 \langle \xi | x_{b_r a} x_{ab} | b \rangle \langle \xi | x_{b_r a} x_{ab} | b - 1 \rangle \langle \xi | x_{b_r b} x_{ba} | a \rangle \langle \xi | x_{b_r b} x_{ba} | a - 1 \rangle}, \tag{6.2.14}$$

where the chiral spinor  $\xi$  is given by

$$\langle \xi | = \langle n | x_{na_1} x_{a_1 b_1} x_{b_1 a_2} x_{a_2 b_2} \dots x_{a_r b_r} . \quad (6.2.15)$$

As in [7] this expression needs to be slightly modified when any  $a_i$  index attains the lower limit of its range<sup>1</sup>. We indicate by means of a superscript on  $R$  the nature of the appropriate modification. Specifically,  $R_{n;a_1 b_1; a_2 b_2; \dots; a_r b_r; ab}^{l_1, \dots, l_r}$  indicates the same quantity (6.2.14) but with the understanding that when  $a$  reaches its lower limit, we need to replace

$$\langle a-1 | \rightarrow \langle n | x_{nl_1} x_{l_1 l_2} \dots x_{l_{r-1} l_r} . \quad (6.2.16)$$

We now have all of the ingredients necessary to begin assembling the complete amplitude, which is given by the formula

$$A_n = A_n^{\text{MHV}} \mathcal{P}_n = \frac{\delta^{(8)}(q)}{\langle 1 2 \rangle \dots \langle n 1 \rangle} \mathcal{P}_n , \quad (6.2.17)$$

where  $\mathcal{P}_n$  is given by the sum over vertical paths in the rooted diagram [7]. To each such path we associate a nested sum of the product of the associated  $R$ -invariants in the vertices visited by the path. The last pair of labels in a given  $R$  are those which are summed first, these are denoted by  $a_p b_p$  in row  $p$  of the diagram. We always take the convention that  $a_p$  and  $b_p$  are separated by at least two ( $a_p < b_p - 1$ ) which is necessary for the  $R$ -invariants to be well-defined. The lower and upper limits for the summation variables  $a_p, b_p$  are indicated by the two numbers appearing adjacent to the line above each vertex.

---

<sup>1</sup> In [7] it was also necessary to sometimes take into account modifications when indices reached the upper limits of their ranges, but this feature does not arise in our reorganized presentation of the amplitude.

Given the complexity of this prescription it behooves us to illustrate a few cases explicitly. There is one path of length zero, whose value is simply 1 and this corresponds to the MHV amplitudes,

$$\mathcal{P}_n^{\text{MHV}} = 1. \quad (6.2.18)$$

Then there is one path of length one which gives the NMHV amplitudes. We get  $1 \times R_{n;a_1,b_1}$ , summed over the region  $2 \leq a_1, b_1 < n$ , as always with the convention that  $a_i < b_i - 1$ . There are no boundary replacements so we have

$$\mathcal{P}_n^{\text{NMHV}} = \sum_{2 \leq a_1, b_1 < n} R_{n;a_1,b_1}. \quad (6.2.19)$$

The two paths of length two give the NNMHV amplitudes. This time we get superscripts on the  $R$ -invariants as dictated by the rules in point 4 above,

$$\mathcal{P}_n^{\text{NNMHV}} = \sum_{2 \leq a_1, b_1 < n} R_{n;a_1,b_1} \left( \sum_{a_1 \leq a_2, b_2 < b_1} R_{n;a_1b_1;a_2b_2}^{b_1a_1} + \sum_{b_1 \leq a_2, b_2 < n} R_{n;a_2b_2}^{a_1b_1} \right). \quad (6.2.20)$$

Continuing to  $N^3$ MHV amplitudes we find five paths of length three, giving the following nested sums,

$$\begin{aligned} \mathcal{P}_n^{\text{N}^3\text{MHV}} = & \sum_{2 \leq a_1, b_1 < n} R_{n;a_1,b_1} \left[ \right. \\ & \sum_{a_1 \leq a_2, b_2 < b_1} R_{n;a_1b_1;a_2b_2}^{b_1a_1} \left( \sum_{a_2 \leq a_3, b_3 < b_2} R_{n;a_1b_1;a_2b_2;a_3b_3}^{a_1b_1b_2a_2} + \sum_{b_2 \leq a_3, b_3 < b_1} R_{n;a_1b_1;a_3b_3}^{a_1b_1a_2b_2} + \sum_{b_1 \leq a_3, b_3 < n} R_{n;a_3b_3}^{a_1b_1} \right) \\ & \left. + \sum_{b_1 \leq a_2, b_2 < n} R_{n;a_2b_2}^{a_1b_1} \left( \sum_{a_2 \leq a_3, b_3 < b_2} R_{n;a_2b_2;a_3b_3}^{b_2a_2} + \sum_{b_2 \leq a_3, b_3 < n} R_{n;a_3b_3}^{a_2b_2} \right) \right]. \end{aligned} \quad (6.2.21)$$

These examples hopefully serve to illustrate how to write a general SYM amplitude,

though a more thorough discussion may be found in [7].

## 6.3 Examples of Gravity Amplitudes

### 6.3.1 MHV Amplitudes

Elvang and Freedman have shown that the  $n$ -graviton MHV amplitude may be written in the form<sup>2</sup>

$$\mathcal{M}_n^{\text{MHV}} = \sum_{\mathcal{P}(2, \dots, n-1)} [A^{\text{MHV}}(1, \dots, n)]^2 G^{\text{MHV}}(1, \dots, n) \quad (6.3.1)$$

in terms of

$$G^{\text{MHV}}(1, \dots, n) = x_{13}^2 \prod_{s=2}^{n-3} \frac{\langle s | x_{s,s+2} x_{s+2,n} | n \rangle}{\langle s n \rangle}. \quad (6.3.2)$$

The formula (6.3.1) is valid for  $n > 3$ ;  $n = 3$  will always be treated as a special case with  $G^{\text{MHV}}(1, 2, 3) = 1$ .

Comparison of (6.3.1) with (6.2.6) suggests that we should identify the MHV ordered subamplitude as

$$M^{\text{MHV}}(1, \dots, n) = [A^{\text{MHV}}(1, \dots, n)]^2 G^{\text{MHV}}(1, \dots, n). \quad (6.3.3)$$

Let us now check that our definition (6.2.7) yields precisely the same expression for the subamplitude (they may have differed by terms which cancel out when one sums over all permutations in (6.2.6)).

---

<sup>2</sup> We have relabeled their indices according to  $i \rightarrow 2 - i \bmod n$  and have expressed the amplitude in  $\mathcal{N} = 8$  superspace.

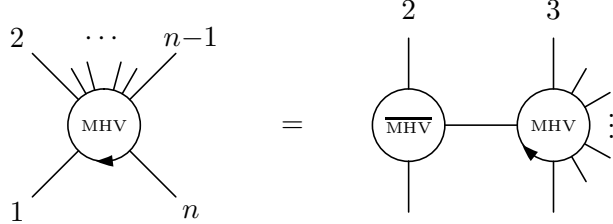


Figure 6.2: The recursion for MHV amplitudes.

We will again proceed by induction, assuming that (6.3.3) satisfies (6.2.7) for  $n - 1$  and fewer gravitons. To calculate  $M^{\text{MHV}}$  for  $n$  gravitons from the definition (6.2.7) we first note that only the single term  $i = 3$  contributes, giving

$$M^{\text{MHV}}(1, \dots, n) = \int \frac{d^8 \eta}{P^2} M^{\overline{\text{MHV}}}(\hat{1}, 2, \hat{P}) M^{\text{MHV}}(-\hat{P}, 3, \dots, \bar{n}) \quad (6.3.4)$$

as shown in Fig. 6.2. The calculation is rendered essentially trivial by plugging in the relations

$$\begin{aligned} M^{\overline{\text{MHV}}}(\hat{1}, 2, \hat{P}) &= [A^{\overline{\text{MHV}}}(\hat{1}, 2, \hat{P})]^2, \\ M^{\text{MHV}}(-\hat{P}, 3, \dots, \bar{n}) &= [A^{\text{MHV}}(-\hat{P}, 3, \dots, \bar{n})]^2 G^{\text{MHV}}(-\hat{P}, 3, \dots, \bar{n}) \end{aligned} \quad (6.3.5)$$

between ordered graviton and Yang-Mills amplitudes. The  $G$  factor in (6.3.4) comes along for the ride as we perform the  $d^8 \eta$  integral using the square of the analogous Yang-Mills calculation as explained above (6.2.12). Therefore with no effort we find that (6.3.4) gives

$$M^{\text{MHV}}(1, \dots, n) = [A^{\text{MHV}}(1, \dots, n)]^2 P^2 G^{\text{MHV}}(-\hat{P}, 3, \dots, \bar{n}). \quad (6.3.6)$$

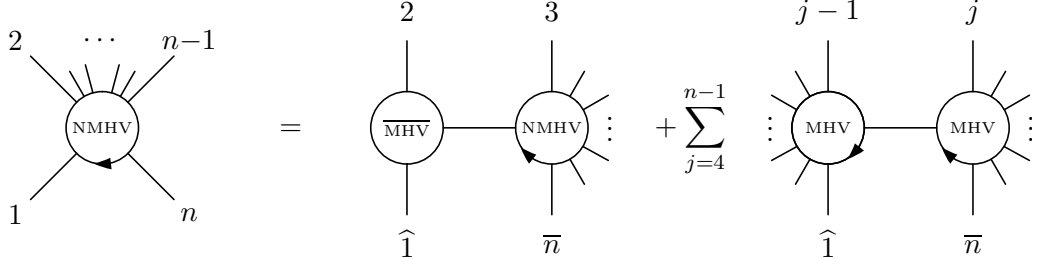


Figure 6.3: The two kinds of diagrams contributing to the recursion of NMHV amplitudes.

A simple calculation using the shift (6.2.2) now reveals that

$$\begin{aligned}
 P^2 G^{\text{MHV}}(-\hat{P}, 3, \dots, \bar{n}) &= x_{13}^2 (-\hat{P} + p_3)^2 \prod_{s=3}^{n-3} \frac{\langle s | x_{s,s+2} x_{s+2,\bar{n}} | \bar{n} \rangle}{\langle s n \rangle} \\
 &= x_{13}^2 \prod_{s=2}^{n-3} \frac{\langle s | x_{s,s+2} x_{s+2,n} | n \rangle}{\langle s n \rangle} \\
 &= G^{\text{MHV}}(1, \dots, n). \tag{6.3.7}
 \end{aligned}$$

This completes the inductive proof that the formula (6.3.3) obtained by Elvang and Freedman is precisely the MHV case of the ordered subamplitudes that we have defined in (6.2.7).

### 6.3.2 NMHV Amplitudes

Next we turn our attention to the NMHV amplitude. The two kinds of diagrams which contribute to the recursion are shown in Fig. 6.3. Let us begin with  $n = 5$ , in which case the first diagram is absent and only the term  $i = 4$  appears in the sum.

According to the definition (6.2.7) we then have

$$\begin{aligned}
M^{\text{NMHV}}(1, \dots, 5) &= \int \frac{d^8 \eta}{P^2} M^{\text{MHV}}(\hat{1}, 2, 3, \hat{P}) M^{\text{MHV}}(-\hat{P}, 4, \bar{5}) \\
&= [A^{\text{NMHV}}(1, \dots, 5)]^2 P^2 G^{\text{MHV}}(\hat{1}, 2, 3, \hat{P}) \\
&\equiv [A^{\text{NMHV}}(1, \dots, 5)]^2 G^{\text{NMHV}}(1, \dots, 5). \tag{6.3.8}
\end{aligned}$$

Here, following the example set in the previous subsection, evaluating the Grassmann integral leads to the square of the analogous SYM result, times the gravity factor

$$G^{\text{NMHV}}(1, \dots, 5) = P^2 G^{\text{MHV}}(\hat{1}, 2, 3, \hat{P}) = (p_4 + p_5)^2 (p_{\hat{1}} + p_2)^2 = (p_4 + p_5)^2 \frac{[4|p_3 p_2|1]}{[4|1]}. \tag{6.3.9}$$

One can check that this result it is consistent with the known answer (for example, from the KLT relation).

Let us now turn to the general NMHV case. In the previous section we recalled the SYM result obtained in [7],

$$A^{\text{NMHV}}(1, \dots, n) = A^{\text{MHV}}(1, \dots, n) \sum_{i=2}^{n-3} \sum_{j=i+2}^{n-1} R_{n;ij}. \tag{6.3.10}$$

It was shown in [7] that the  $i = 2$  term in (6.3.10) corresponds to the sum over  $\text{MHV} \times \text{MHV}$  diagrams in Fig. 6.3, while the  $i > 2$  terms arise iteratively from the  $\overline{\text{MHV}} \times \text{NMHV}$  diagram.

## Statement

Now we claim that the NMHV gravity subamplitude is given by

$$M^{\text{NMHV}}(1, \dots, n) = [A^{\text{MHV}}(1, \dots, n)]^2 \sum_{i=2}^{n-3} \sum_{j=i+2}^{n-1} R_{n;ij}^2 G_{n;ij}^{\text{NMHV}} \quad (6.3.11)$$

where  $R$  is the same dual superconformal invariant (6.2.14) as in SYM and the NMHV gravity factor can be split for future convenience into three parts as follows,

$$G_{n;ab}^{\text{NMHV}} = f_{n;ab} G_{n;ab}^L G_{n;ab}^R. \quad (6.3.12)$$

To express the gravity factor we introduce the notation

$$P_{a_1, \dots, a_r}^{l,u} = \prod_{k=l}^u \frac{\langle k|x_{k,k+2}x_{k+2,a_1}x_{a_1a_2}x_{a_2a_3} \dots x_{a_{r-1}a_r}|a_r\rangle}{\langle k|x_{a_1a_2}x_{a_2a_3} \dots x_{a_{r-1}a_r}|a_r\rangle}, \quad (6.3.13)$$

$$Z_{b_1, \dots, b_l; c_1, \dots, c_r}^{a_1, \dots, a_u} = \frac{\langle a_1|x_{a_1a_2}x_{a_2a_3} \dots x_{a_{u-1}a_u}|a_u\rangle}{\langle b_1|x_{b_1b_2}x_{b_2b_3} \dots x_{b_{l-1}b_l}x_{c_1c_2}x_{c_2c_3} \dots x_{c_{r-1}c_r}|c_r\rangle}, \quad (6.3.14)$$

which is overkill at the moment but will be fully utilized below when we move beyond the NMHV level. In the numerators only dual conformal chains of  $x$ -matrices appear, while in the denominators the chains are not dual conformal due to the break in the way the labels are arranged. The break is denoted by the semi-colon in the subscript of  $Z$  while in the denominator of  $P$  it is immediately after the left-most spinor  $\langle k|$ .

Then the first factor in (6.3.12) is given by

$$f_{n;2b} = x_{1b}^2, \quad (6.3.15)$$

$$f_{n;ab} = x_{13}^2 (-Z_{n;a-1}^{n,b,a-1}) P_n^{2,a-2} \quad \text{for } a > 2, \quad (6.3.16)$$

while the remaining two are

$$G_{n;ab}^L = -Z_{n;b,a,n}^{n,a+1,b,a,n} P_{b,a,n}^{a,b-3}, \quad (6.3.17)$$

$$G_{n;ab}^R = -Z_{n;b,a,n}^{n,b+1,b,a,n} P_n^{b,n-3}. \quad (6.3.18)$$

## Proof

To check that the formula (6.3.11) is correct it is useful to first have a general formula for  $x_{1v}^2$ , where the shift is defined so that  $\hat{P}_i^2 = x_{1i}^2 = 0$ . This tells us that the shift parameter is given by (6.2.3), i.e

$$z_P = \frac{x_{1i}^2}{\langle n|x_{1i}|1 \rangle}. \quad (6.3.19)$$

Then we have

$$x_{1v}^2 = x_{1v}^2 - z_P \langle n|x_{1v}|1 \rangle \quad (6.3.20)$$

$$= \frac{x_{1v}^2 \langle n|x_{1i}|1 \rangle - x_{1i}^2 \langle n|x_{1v}|1 \rangle}{\langle n|x_{1i}|1 \rangle} \quad (6.3.21)$$

$$= \frac{\langle n|x_{1v}(x_{1v} - x_{1i})x_{1i}|1 \rangle}{\langle n|x_{1i}|1 \rangle} \quad (6.3.22)$$

$$= \frac{\langle n|x_{1v}x_{iv}x_{1i}|1 \rangle}{\langle n|x_{1i}|1 \rangle} \quad (6.3.23)$$

$$= -\frac{\langle n|x_{nv}x_{vi}x_{i2}x_{2n}|n \rangle}{\langle n|x_{i2}x_{2n}|n \rangle} \equiv -Z_{n;i,2,n}^{n,v;i,2,n}. \quad (6.3.24)$$

Note that instead of writing (6.3.22) we could have alternatively written it as

$$x_{1v}^2 = \frac{\langle n|x_{1i}(x_{1v} - x_{1i})x_{1v}|1\rangle}{\langle n|x_{1i}|1\rangle} \quad (6.3.25)$$

$$= \frac{\langle n|x_{1i}x_{iv}x_{1v}|1\rangle}{\langle n|x_{1i}|1\rangle} \quad (6.3.26)$$

$$= \frac{\langle n|x_{ni}x_{iv}x_{v2}x_{2n}|n\rangle}{\langle n|x_{i2}x_{2n}|n\rangle} \equiv Z_{n;i,2,n}^{n,i,v,2,n}. \quad (6.3.27)$$

The freedom to write this factor in these two various forms is useful because in certain cases either one or the other form simplifies by cancelling factors from the numerator and denominator.

Finally we are set up to check our claim (6.3.12) for the NMHV  $G$ -factor. We first check the case  $a = 2$  which comes entirely from MHV  $\times$  MHV diagrams. From these diagrams we obtain

$$\sum_{i=4}^{n-1} R_{n;2,i}^2 G_{n;2,i}^{\text{NMHV}} = \sum_{i=4}^{n-1} R_{n;2,i}^2 P^2 G^{\text{MHV}}(\hat{1}, \dots, -\hat{P}) G^{\text{MHV}}(\hat{P}, \dots, \bar{n}), \quad (6.3.28)$$

from which we find

$$G_{n;2,i}^{\text{NMHV}} = x_{1i}^2 \left( x_{13}^2 \prod_{k=2}^{i-3} \frac{\langle k|x_{k,k+2}x_{k+2,i}|\hat{P}\rangle}{\langle k|\hat{P}\rangle} \right) \left( x_{1i+1}^2 \prod_{l=i}^{n-3} \frac{\langle l|x_{l,l+2}x_{l+2,n}|n\rangle}{\langle l|n\rangle} \right) \quad (6.3.29)$$

$$= x_{1i}^2 \left( -Z_{n;i,2,n}^{n,3,i,2,n} P_{i,2,n}^{2,i-3} \right) \left( -Z_{n;i,2,n}^{n,i+1,i,2,n} P_n^{i,n-3} \right), \quad (6.3.30)$$

which is in agreement with equations (6.3.12) to (6.3.18) for the case  $a = 2$ .

For the case  $a > 2$  we must consider diagrams of the form  $\overline{\text{MHV}}_3 \times \text{NMHV}_{n-1}$ . From

these diagrams we obtain

$$\sum_{3 \leq a, b \leq n-1} R_{n;ab}^2 G_{n;ab}^{\text{NMHV}} = \sum_{3 \leq a, b \leq n-1} R_{n;ab}^2 P^2 G^{\text{NMHV}}(\hat{P}, 3, \dots, \bar{n}) . \quad (6.3.31)$$

The sum splits into two contributions,  $a = 3$  and  $a > 3$ . The first gives

$$G_{n;3b}^{\text{NMHV}} = x_{13}^2 x_{1b}^2 \left( -Z_{n;b,3,n}^{n,4,b,3,n} P_{b,a,n}^{a,b-3} \right) \left( -Z_{n;b,3,n}^{n,b+1,b,3,n} P_n^{b,n-3} \right) \quad (6.3.32)$$

$$= x_{13}^2 \left( -Z_{n;2}^{n,b,2} \right) \left( -Z_{n;b,3,n}^{n,4,b,3,n} P_{b,a,n}^{a,b-3} \right) \left( -Z_{n;b,3,n}^{n,b+1,b,3,n} P_n^{b,n-3} \right) , \quad (6.3.33)$$

in agreement with equations (6.3.12) to (6.3.18) for the case  $a = 3$ . To go from (6.3.32) to (6.3.33) we have used the fact that  $x_{1b}^2 = -Z_{n;3,2,n}^{n,b,3,2,n} = -Z_{n;2}^{n,b,2}$  where the simplification of the  $Z$ -factor is due to a cancellation between its numerator and denominator.

For the contributions to (6.3.31) where  $a > 3$  we find

$$G_{n;ab}^{\text{NMHV}} = x_{13}^2 x_{14}^2 \left( -Z_{n;a-1}^{n,b,a-1} \right) P_n^{3,a-2} \left( -Z_{n;b,a,n}^{n,a+1,b,a,n} P_{b,a,n}^{a,b-3} \right) \left( -Z_{n;b,a,n}^{n,b+1,b,a,n} P_n^{b,n-3} \right) \quad (6.3.34)$$

$$= x_{13}^2 \left( -Z_{n;a-1}^{n,b,a-1} \right) P_n^{2,a-2} \left( -Z_{n;b,a,n}^{n,a+1,b,a,n} P_{b,a,n}^{a,b-3} \right) \left( -Z_{n;b,a,n}^{n,b+1,b,a,n} P_n^{b,n-3} \right) , \quad (6.3.35)$$

which is again in agreement with equations (6.3.12) to (6.3.18). The factor  $x_{14}^2$  completes the factor  $P_n^{3,a-2}$  to  $P_n^{2,a-2}$  just as in the MHV case. This completes the verification of the formula (6.3.11) for NMHV graviton amplitudes. Appendix B contains some notes on extracting NMHV graviton amplitudes from the super-amplitude (6.3.11).

### 6.3.3 NNMHV Amplitudes

In this section we consider the NNMHV case as an exercise towards finding the general algorithm for all tree-level gravity amplitudes.

#### Statement

The structure of the result is just like in Yang-Mills and similar to the NMHV case (6.3.11) except that we now have two more subscripts on both the Yang-Mills  $R$ -factors and the gravity factors,

$$\frac{M^{\text{NNMHV}}(1, \dots, n)}{[A^{\text{MHV}}(1, \dots, n)]^2} = \sum_{2 \leq a, b \leq n-1} R_{n;ab}^2 \left[ \sum_{a \leq c, d < b} (R_{n;ab;cd}^{ba})^2 H_{n;ab;cd}^{(1)} + \sum_{b \leq c, d < n} (R_{n;cd}^{ab})^2 H_{n;ab;cd}^{(2)} \right]. \quad (6.3.36)$$

The factors  $H^{(1)}$  and  $H^{(2)}$  can be written in the form

$$H_{n;ab;cd}^{(1)} = f_{n;ab} G_{n;ab}^R \tilde{f}_{n;ab;cd} G_{n;ab;cd}^L G_{n;ab;cd}^R, \quad (6.3.37)$$

$$H_{n;ab;cd}^{(2)} = f_{n;ab} G_{n;ab}^L \hat{f}_{n;ab;cd} G_{n;cd}^L G_{n;cd}^R. \quad (6.3.38)$$

In this formula  $f_{n;ab}$ ,  $G_{n;ab}^L$  and  $G_{n;ab}^R$  are defined as before in the case of the NMHV amplitude (see formulae (6.3.16), (6.3.17) and (6.3.18)). The factor  $\tilde{f}$  in  $H^{(1)}$  is given by

$$\tilde{f}_{n;ab,ad} = -Z_{n;b,a,n}^{n,b,d,a,n}, \quad (6.3.39)$$

$$\tilde{f}_{n;ab;cd} = \left( -Z_{n;b,a,n}^{n,b,a+1,a,n} \right) \left( -Z_{c-1;b,a,n}^{c-1,d,b,a,n} \right) P_{b,a,n}^{a,c-2} \quad \text{for } c > a, \quad (6.3.40)$$

and the factor  $\hat{f}$  in the second term in the parentheses is given by

$$\hat{f}_{n;ab;bd} = -Z_{n;b,a,n}^{n,d,b,a,n} \quad (6.3.41)$$

$$\hat{f}_{n;ab;cd} = \left(-Z_{n;b,a,n}^{n,b+1,b,a,n}\right) \left(-Z_{n;c-1}^{n,d,c-1}\right) P_n^{b,c-2} \quad \text{for } c > b. \quad (6.3.42)$$

Finally the new  $G$ -factors are given by

$$G_{n;ab;cd}^L = -Z_{n,a,b;d,c,b,a,n}^{n,a,b,c+1,d,c,b,a,n} P_{d,c,b,a,n}^{c,d-3}, \quad (6.3.43)$$

$$G_{n;ab;cd}^R = -Z_{n,a,b;d,c,b,a,n}^{n,a,b,d+1,d,c,b,a,n} P_{b,a,n}^{d,n-3}. \quad (6.3.44)$$

## Proof

Let us now check the claim (6.3.36). As before we begin with the case  $a = 2$  which comes purely from  $\text{NMHV} \times \text{MHV}$  diagrams and  $\text{MHV} \times \text{NMHV}$  diagrams. We start by calculating the former kind. From these diagrams we obtain

$$\begin{aligned} & \sum_{i=5}^{n-1} R_{n;2i}^2 \sum_{2 \leq c,d < i} (R_{n;2i;cd}^{i2})^2 H_{n;2i,cd}^{(1)} \\ &= \sum_{i=5}^{n-1} R_{n;2i}^2 \sum_{2 \leq c,d < i} (R_{n;2i;cd}^{i2})^2 P^2 G^{\text{NMHV}}(\hat{1}, \dots, -\hat{P}) G^{\text{MHV}}(\hat{P}, \dots, \bar{n}). \end{aligned} \quad (6.3.45)$$

The sum over  $c$  splits into two pieces,  $c = 2$  and  $c > 2$ . For the terms where  $c = 2$  we have

$$H_{n;2i;2d}^{(1)} = x_{1i}^2 \left[ x_{1d}^2 \left( -Z_{n,2,i;d,2,n}^{n,2,i,3,d,2,n} P_{d,2,n}^{2,d-3} \right) \left( -Z_{n,2,i;d,2,n}^{n,2,i,d+1,d,2,n} P_{i,2,n}^{d,i-3} \right) \right] \left[ x_{1,i+1}^2 P_n^{i,n-3} \right]. \quad (6.3.46)$$

Here as in the previous subsection we have used the fact that certain  $Z$ -factors simplify. For example, reading the  $Z$ -factor from the formula (6.3.17) and taking into account the fact that the spinor  $\langle \hat{P} |$  can be replaced in both the numerator and denominator of  $Z$  by  $\langle n | x_{n2} x_{2i}$ , we would obtain  $Z_{n,2,i;d,2,i,2,n}^{n,2,i,3,d,2,i,2,n}$ . The sequence of indices  $2, i, 2$  implies however that one can factor out  $x_{2i}^2$ . Since the sequence is present in both the numerator and the denominator, it can simply be replaced by 2. Thus we arrive at the form of the  $Z$ -factor in the first set of parentheses in (6.3.46).

To verify that equation (6.3.46) is consistent with (6.3.37) it remains to substitute the  $Z$ -factors appropriate to the factors  $x_{1d}^2$  and  $x_{1,i+1}^2$ . Doing so we obtain

$$H_{n;2i;2d}^{(1)} = x_{1i}^2 \left[ -Z_{n;i,2,n}^{n,d,i,2,n} \left( -Z_{n,2,i;d,2,n}^{n,2,i,3,d,2,n} P_{d,2,n}^{2,d-3} \right) \left( -Z_{n,2,i;d,2,n}^{n,2,i,d+1,d,2,n} P_{i,2,n}^{d,i-3} \right) \right] \left[ -Z_{n;i,2,n}^{n,i+1,i,2,n} P_n^{i,n-3} \right]. \quad (6.3.47)$$

The factor  $x_{1i}^2$  gives the required contribution  $f_{n;2i}$ , while the factor in the second factor in square brackets is  $G_{n;2i}^R$ . The remaining factor in the first set of square brackets is the contribution from  $\tilde{f}_{n;2i,2d}$  and the other  $Z$  and  $P$  factors in (6.3.37).

Now let us look at the terms where  $c > 2$ . We have

$$H_{n;2i;cd}^{(1)} = x_{1i}^2 \left[ x_{13}^2 \left( -Z_{n,2,i;c-1}^{n,2,i,d,c-1} P_{i,2,n}^{2,c-2} \right) \left( -Z_{n,2,i;d,c,i,2,n}^{n,2,i,c+1,d,c,i,2,n} P_{d,c,i,2,n}^{c,d-3} \right) \left( -Z_{n,2,i;d,c,i,2,n}^{n,2,i,d+1,d,c,i,2,n} P_{i,2,n}^{d,i-3} \right) \right] \left[ x_{1,i+1}^2 P_n^{i,n-3} \right]. \quad (6.3.48)$$

Again, substituting for  $x_{13}^2$  and  $x_{1,i+1}^2$  we find agreement with (6.3.37).

Now let us turn our attention to the latter kind of diagrams, namely the MHV  $\times$

NMHV diagrams. From these diagrams we find

$$\begin{aligned} & \sum_{i=4}^{n-3} R_{n;2i}^2 \sum_{2 \leq c, d < i} (R_{n;cd}^{2i})^2 H_{n;2i,cd}^{(2)} \\ &= \sum_{i=4}^{n-3} R_{n;2i}^2 \sum_{2 \leq c, d < i} (R_{n;cd}^{2i})^2 P^2 G^{\text{NMHV}}(\hat{1}, \dots, -\hat{P}) G^{\text{MHV}}(\hat{P}, \dots, \bar{n}). \end{aligned} \quad (6.3.49)$$

As before the sum over  $c$  splits into two pieces. For  $c = i$  we find

$$H_{n;2i;2d}^{(2)} = x_{1i}^2 \left[ x_{13}^2 P_{i,2,n}^{2,i-3} \right] \left[ x_{1d}^2 \left( -Z_{n;d,i,n}^{n,i+1,d,i,n} P_{d,i,n}^{i,d-3} \right) \left( -Z_{n;d,i,n}^{n,d+1,d,i,n} P_n^{d,n-3} \right) \right], \quad (6.3.50)$$

while for  $c > i$  we find

$$H_{n;2i;cd}^{(2)} = x_{1i}^2 \left[ x_{13}^2 P_{i,2,n}^{2,i-3} \right] \left[ x_{1,i+1}^2 \left( -Z_{n;c-1}^{n,d,c-1} P_n^{i,c-2} \right) \left( -Z_{n;d,c,n}^{n,c+1,d,c,n} P_{d,c,n}^{c,d-3} \right) \left( -Z_{n;d,c,n}^{n,d+1,d,c,n} P_n^{d,n-3} \right) \right]. \quad (6.3.51)$$

Making the usual substitutions for the factors of the form  $x_{1v}^2$  we find agreement with (6.3.38) in both cases.

To check the terms for  $a > 2$  we need to consider  $\overline{\text{MHV}}_3 \times \text{NNMHV}_{n-1}$  diagrams.

These diagrams give us

$$\begin{aligned} & \sum_{3 \leq a, b < n} R_{n;ab}^2 \left[ \sum_{a \leq c, d < b} (R_{n;ab;cd}^{ba})^2 H_{n;ab,cd}^{(1)} + \sum_{b \leq c, d < n} (R_{n;cd}^{ab})^2 H_{n;ab;cd}^{(2)} \right] \\ &= \sum_{3 \leq a, b < n} R_{n;ab}^2 \left[ \sum_{a \leq c, d < b} (R_{n;ab;cd}^{ba})^2 P^2 H^{(1)}(\hat{P}, \dots, \bar{n}) + \sum_{b \leq c, d < n} (R_{n;cd}^{ab})^2 H^{(2)}(\hat{P}, \dots, \bar{n}) \right]. \end{aligned} \quad (6.3.52)$$

As in the NMHV case, the sum over  $a$  splits into a part where  $a = 3$  and a part where  $a > 3$ . The calculation is essentially the same as in the NMHV case, with

the factor of  $P^2 = x_{13}^2$  providing the necessary piece of  $f_{n;ab}$  in both cases. This completes the verification of the formula (6.3.36) for NNMHV amplitudes.

## 6.4 Discussion of General Tree-Level Amplitudes

Because of the association between vertices in the rooted tree diagram Fig. ?? with individual terms appearing in the iterative solution of the recursion relation (6.2.1), it is clear that the procedure applied in the previous section can be generalized to express an arbitrary  $N^p$ MHV  $n$ -graviton super-amplitude in the form

$$\mathcal{M}_n = \sum_{\mathcal{P}(2, \dots, n-1)} [A^{\text{MHV}}(1, \dots, n)]^2 \sum_{\{\alpha\}} [R_\alpha(\lambda_i, \tilde{\lambda}_i, \eta_i)]^2 G_\alpha(\lambda_i, \tilde{\lambda}_i), \quad (6.4.1)$$

where  $R_\alpha$  are precisely the same dual superconformal invariants (6.2.14) that appear in SYM and  $G_\alpha$  are some additional, non-dual conformally invariant, dressing factors. Explicit formulas for the MHV, NMHV, and NNMHV gravity factors are given respectively in (6.3.2), (6.3.12), and (6.3.37)–(6.3.38).

The gravity factors  $G_\alpha$  for a general amplitude can be worked out on a case-by-case basis. They always have the form

$$G_{n;a_1b_1;\dots} = f_{n;a_1b_1} \dots, \quad (6.4.2)$$

where  $\dots$  is some combination of  $f$ ,  $G^R$  and  $G^L$  factors. The iterative construction of any desired amplitude is no more difficult than the examples we have already studied in detail. Actually one only needs to take care of the factor  $f_{n;a_1b_1}$ , because the other parts just go from lower points to higher points automatically under the

usual rules

$$\langle n | x_{ny} \rightarrow \langle \hat{p} | x_{iy} \rightarrow \langle n | x_{nj} x_{ji} x_{iy} , \quad (6.4.3)$$

and

$$\langle n | x_{kl} \rightarrow \langle \hat{p} | x_{kl} \rightarrow \langle n | x_{nj} x_{ji} x_{kl} , \quad (6.4.4)$$

as, for example, in going from the NMHV formula (6.3.12) to the NNMHV formula (6.3.37) and (6.3.38). The  $f$  factors arise at each level for the simple reason that an extra propagator  $P^2$  appears in on-shell recursion for gravity as compared to the ‘square’ of the corresponding Yang-Mills result, a fact which we noted already back in (6.2.12). As we already explained carefully in previous section for the NMHV case, the factor  $f_{n;a_1 b_1}$  is needed to satisfy the recursion relation.

Although it is simple to describe the algorithm for a general amplitude in words and by appealing to the examples detailed above, we have not identified a pattern which would allow us to write down a general explicit formula, as was done for SYM in [7]. As noted above each  $R_\alpha$  invariant comes with its own  $f$ -type factor, and each path in rooted diagrams which ends on a vertex with indices  $a_1 b_1; \dots; a_p b_p$  leads to an associated factor of the form

$$G_{a_1, b_1; \dots; a_p b_p}^R G_{a_1 b_1; \dots; a_p b_p}^L , \quad (6.4.5)$$

where the general  $f$ ,  $G^R$  and  $G^L$  are suitably defined following the examples in the previous section. Specifically we have

$$G_{n; a_1 b_1; \dots; a_r b_r; ab}^L = - Z_{n, a_1, b_1, \dots, a_r, b_r; b, a, b_r, a_r, \dots, b_1, a_1, n}^{n, a_1, b_1, \dots, a_r, b_r, a+1, b, a, b_r, a_r, \dots, b_1, a_1, n} P_{b, a, b_r, a_r, \dots, b_1, a_1, n}^{a, b-3} , \quad (6.4.6)$$

$$G_{n; a_1 b_1; \dots; a_r b_r; ab}^R = - Z_{n, a_1, b_1, \dots, a_r, b_r; b, a, b_r, a_r, \dots, b_1, a_1, n}^{n, a_1, b_1, \dots, a_r, b_r, b+1, b, a, b_r, a_r, \dots, b_1, a_1, n} P_{b_r, a_r, \dots, b_1, a_1, n}^{b, n-3} . \quad (6.4.7)$$

The  $f$  factors can be of two types,  $\tilde{f}$  and  $\hat{f}$ . The first type are defined as follows,

$$\tilde{f}_{n;a_1b_1;...;a_rb_r;a_r} = -Z_{n,a_1,b_1,...,a_{r-1},b_{r-1};b_r,a_r,...,b_1,a_1,n}^{n,a_1,b_1,...,a_r,b_r,b,a_r,b_{r-1},a_{r-1},...,b_1,a_1,n}, \quad (6.4.8)$$

$$\begin{aligned} \tilde{f}_{n;a_1b_1;...;a_rb_r;ab} &= \left( -Z_{n,a_1,b_1,...,a_{r-1},b_{r-1};b_r,a_r,...,b_1,a_1,n}^{n,a_1,b_1,...,b_r,a_r+1,a_r,b_{r-1},a_{r-1},...,b_1,a_1,n} \right) \\ &\quad \left( -Z_{a-1;b_r,a_r,...,b_1,a_1,n}^{a-1,b,b_r,a_r,...,b_1,a_1,n} \right) P_{b_r,a_r,...,b_1,a_1,n}^{a_r,a-2} \quad \text{for } a > a_r. \end{aligned} \quad (6.4.9)$$

The second type are given by

$$\hat{f}_{n;a_1b_1;...;a_rb_r;b_r} = -Z_{n,a_1,b_1,...,a_{r-1},b_{r-1};b_r,a_r,...,b_1,a_1,n}^{n,a_1,b_1,...,a_{r-1},b_{r-1},b,b_r,a_r,...,b_1,a_1,n}, \quad (6.4.10)$$

$$\begin{aligned} \hat{f}_{n;a_1b_1;...;a_rb_r;ab} &= \left( -Z_{n,a_1,b_1,...,a_{r-1},b_{r-1};b_r,a_r,...,b_1,a_1,n}^{n,a_1,b_1,...,a_{r-1},b_{r-1},b_r+1,b_r,a_r,...,b_1,a_1,n} \right) \\ &\quad \left( -Z_{n,a_1,b_1,...,a_{r-1},b_{r-1};a-1}^{n,a_1,b_1,...,a_{r-1},b_{r-1},b,a-1} \right) P_{b_{r-1},a_{r-1},...,b_1,a_1,n}^{b_r,a-2} \quad \text{for } a > b_r. \end{aligned} \quad (6.4.11)$$

In addition to the factors (6.4.5), other  $G^R$  and  $G^L$  factors also appear. We emphasize that we have attempted here only to illustrate some features of the general structure; in order to determine precisely the factors which appear for a given path it seems necessary to work out recursively which kinds of  $N^a$ MHV  $\times$   $N^b$ MHV factorizations that particular path corresponds to.

To stress that the algorithm can be simply exploited to generate higher and higher

$N^p$ MHV amplitudes, we give here the formula for  $N^3$ MHV amplitudes:

$$\begin{aligned}
M^{N^3\text{MHV}}(1, \dots, n) = & [A^{\text{MHV}}(1, \dots, n)]^2 \sum_{2 \leq a_1, b_1 < n} R_{n; a_1 b_1}^2 \left[ \right. \\
& \sum_{a_1 \leq a_2, b_2 < b_1} (R_{n; a_1 b_1; a_2 b_2}^{b_1 a_1})^2 \left( \sum_{a_2 \leq a_3, b_3 < b_2} (R_{n; a_1 b_1; a_2 b_2; a_3 b_3}^{a_1 b_1 b_2 a_2})^2 G_{n; a_1 b_1; a_2 b_2; a_3 b_3}^{(1)} \right. \\
& \quad \left. + \sum_{b_2 \leq a_3, b_3 < b_1} (R_{n; a_1 b_1; a_3 b_3}^{a_1 b_1 a_2 b_2})^2 G_{n; a_1 b_1; a_2 b_2; a_3 b_3}^{(2)} + \sum_{b_1 \leq a_3, b_3 < n} (R_{n; a_3 b_3}^{a_1 b_1})^2 G_{n; a_1 b_1; a_2 b_2; a_3 b_3}^{(3)} \right) \\
& \left. + \sum_{b_1 \leq a_2, b_2 < n} (R_{n; a_2 b_2}^{a_1 b_1})^2 \left( \sum_{a_2 \leq a_3, b_3 < b_2} (R_{n; a_2 b_2; a_3 b_3}^{b_2 a_2})^2 G_{n; a_1 b_1; a_2 b_2; a_3 b_3}^{(4)} + \sum_{b_2 \leq a_3, b_3 < n} (R_{n; a_3 b_3}^{a_2 b_2})^2 G_{n; a_1 b_1; a_2 b_2; a_3 b_3}^{(5)} \right) \right]. \tag{6.4.12}
\end{aligned}$$

The five different  $G$ -factors are in correspondence with the five different vertical paths from the root node to the vertices on the lowest row explicitly shown in Fig. ??.

Explicitly they are given by

$$G_{n; a_1 b_1; a_2 b_2; a_3 b_3}^{(1)} = f_{n; a_1 b_1} \tilde{f}_{n; a_1 b_1; a_2 b_2} \tilde{f}_{n; a_1 b_1; a_2 b_2; a_3 b_3} G_{n; a_1 b_1}^R G_{n; a_1 b_1; a_2 b_2}^R G_{n; a_1 b_1; a_2 b_2; a_3 b_3}, \tag{6.4.13}$$

$$G_{n; a_1 b_1; a_2 b_2; a_3 b_3}^{(2)} = f_{n; a_1 b_1} \tilde{f}_{n; a_1 b_1; a_2 b_2} \tilde{f}_{n; a_1 b_1; a_2 b_2; a_3 b_3} G_{n; a_1 b_1}^R G_{n; a_1 b_1; a_2 b_2}^L G_{n; a_1 b_1; a_3 b_3}, \tag{6.4.14}$$

$$G_{n; a_1 b_1; a_2 b_2; a_3 b_3}^{(3)} = f_{n; a_1 b_1} \tilde{f}_{n; a_1 b_1; a_2 b_2} \hat{f}_{n; a_1 b_1; a_3 b_3} G_{n; a_1 b_1; a_2 b_2} G_{n; a_3 b_3}, \tag{6.4.15}$$

$$G_{n; a_1 b_1; a_2 b_2; a_3 b_3}^{(4)} = f_{n; a_1 b_1} \hat{f}_{n; a_1 b_1; a_2 b_2} \hat{f}_{n; a_1 b_1; a_2 b_2; a_3 b_3} G_{n; a_1 b_1}^L G_{n; a_2 b_2}^R G_{n; a_2 b_2; a_3 b_3}, \tag{6.4.16}$$

$$G_{n; a_1 b_1; a_2 b_2; a_3 b_3}^{(5)} = f_{n; a_1 b_1} \hat{f}_{n; a_1 b_1; a_2 b_2} \hat{f}_{n; a_1 b_1; a_2 b_2; a_3 b_3} G_{n; a_1 b_1}^L G_{n; a_2 b_2}^L G_{n; a_3 b_3}, \tag{6.4.17}$$

where  $G$  is shorthand for  $G^L \times G^R$  (with the same subscripts on both).

The expressions we have found can certainly be used in the calculation of loop amplitudes in supergravity. It is straightforward to apply the generalized unitarity

technique in a manifestly supersymmetric way [61, 60, 20]; the basic ingredients in this procedure are the tree-level super-amplitudes.

# Chapter 7

## Bonus relations in gravity amplitudes

### 7.1 Review of tree amplitudes in SUGRA and bonus relations

In last chapter, we obtained all tree-level amplitudes in  $\mathcal{N} = 8$  SUGRA by solving supersymmetric BCFW recursion relations. In this chapter, we will simplify the obtained results by applying the extra relations between gravity tree-level amplitude, which will be called bonus relations.

As we noted from last chapter that SUGRA tree amplitude can be written as a summation of  $(n - 2)!$  ordered gravity subamplitudes, and each of them has a structure similar to SYM ordered amplitude. In the following we shall use bonus

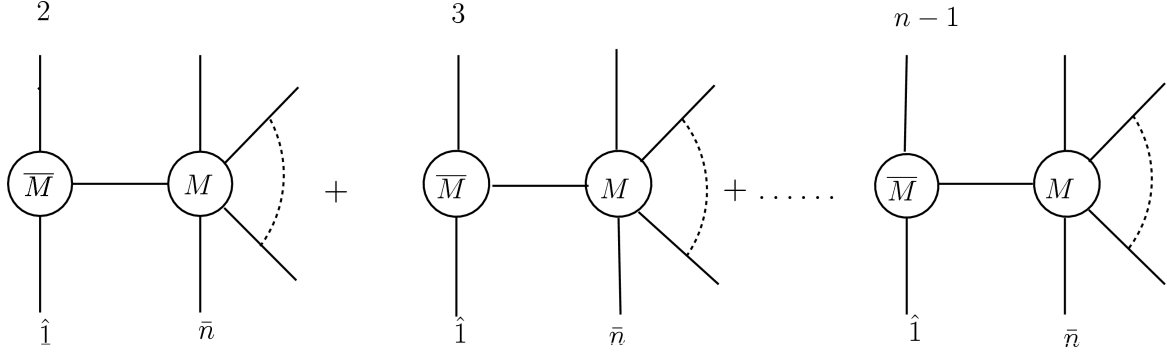


Figure 7.1: All factorizations contributing to (7.1.2) for the MHV amplitude.

relations to reduce this form to a simpler,  $(n - 3)!$  form, and first we recall the simplest MHV case.

### 7.1.1 Applying Bonus Relations to MHV Amplitudes

Applying bonus relation to MHV SUGRA tree-level amplitudes was well understood in [62]. From Eq. (6.3.2), we have the MHV amplitudes as a summation of  $(n - 2)!$  terms,

$$\mathcal{M}_n^{\text{MHV}} = G^{\text{MHV}}(1, \dots, n)[A^{\text{MHV}}(1, \dots, n)]^2 + \mathcal{P}(2, 3, \dots, n - 1). \quad (7.1.1)$$

From Fig. 7.1, we see that there are  $(n - 2)$  BCFW factorizations and thus the formula can be expressed as,

$$\mathcal{M}_n^{\text{MHV}} = M_2 + M_3 + \dots + M_{n-1}, \quad (7.1.2)$$

where each  $M_i$  is a BCFW term from  $\overline{\text{MHV}}(\hat{1}, i, \hat{P}(z_i)) \times \text{MHV}_{n-1}$  with  $z_i = -\frac{\langle 1i \rangle}{\langle ni \rangle}$ .

Now since the amplitude has  $1/z^2$  fall off, we have a bonus relation which is simple in the MHV case,

$$0 = z_2 M_2 + z_3 M_3 + \dots + z_{n-1} M_{n-1}. \quad (7.1.3)$$

Using this relation, we can express the last diagram  $M_{n-1}$  in terms of the other  $n-3$  diagrams, and a simple manipulation gives us a  $(n-3)!$ -term formula,

$$\begin{aligned} \mathcal{M}_n^{\text{MHV}} = & B^{\text{MHV}} G^{\text{MHV}}(1, 2, \dots, n) [A^{\text{MHV}}(1, 2, \dots, n)]^2 \\ & + \mathcal{P}(2, 3, \dots, n-2). \end{aligned} \quad (7.1.4)$$

where we have defined the MHV bonus coefficient  $B^{\text{MHV}} = \frac{\langle 1 \ n \rangle \langle n-1 \ n-2 \rangle}{\langle 1 \ n-1 \rangle \langle n \ n-2 \rangle}$ . Beyond MHV, we have many more types of BCFW diagrams with complicated structures and the application of bonus relations becomes trickier. In the next section, we shall work out the NMHV and  $N^2$ MHV cases, and then move on to general amplitudes in section 4.

## 7.2 Applying Bonus Relations to Non-MHV Gravity Tree Amplitudes

### 7.2.1 General Strategy

Before moving on to examples, we first explain the general strategy for applying bonus relations to non-MHV gravity tree amplitudes. For a  $N^k$ MHV amplitude, inhomogeneous contributions of the form  $N^p$ MHV  $\times$   $N^q$ MHV are needed ( $p+q+1 =$

$k$ )<sup>1</sup>. Naively one would like to use “bonus-simplified”<sup>2</sup> lower-point amplitudes for both  $M_L$  and  $M_R$  in the BCFW recursion relations, but this is not compatible with the fact that we can only delete one diagram (not two) by applying the bonus relations, if we want to preserve the structure of ordered BCFW recursion relations.

To keep the advantages of the ordered BCFW recursion relations, which are crucial to solve for all tree-level amplitudes, instead we shall apply bonus relations selectively.

The idea is illustrated in Fig. 7.2. Similar to the MHV case, we shall delete Fig. 7.2(d) by using bonus relations. To compute the inhomogeneous parts of the amplitudes, we shall use the bonus-simplified amplitude only on one side of a BCFW diagram, namely the lower-point amplitude with the leg  $(n-1)$  in it, as indicated in Fig. 7.2(a) and Fig. 7.2(b). In this way, the amplitude splits into two types, one type coming from the diagrams of the form as in Fig. 7.2(a), which has the leg  $(n-1)$  adjacent to the leg  $n$  and will be called the normal, or type I contributions, and the other one coming from those having the form as in Fig. 7.2(b), which has the leg  $(n-1)$  exchanged with another leg  $(b_1-1)$ , and will be called the exchanged, or type II contributions,

$$\mathcal{M}_n = \left[ A_n^{\text{MHV}} \right]^2 \left( \sum_{\alpha} B_{\alpha}^{(1,m_1)} G_{\alpha} R_{\alpha}^2 + \sum_{\beta} B_{\beta}^{(2,m_2)} [G_{\beta} R_{\beta}^2 (b_1-1 \leftrightarrow n-1)] \right) + \mathcal{P}(2, 3, \dots, n-2), \quad (7.2.1)$$

where  $(b_1-1 \leftrightarrow n-1)$  denotes the exchanges of momenta  $(p_{b_1-1} \leftrightarrow p_{n-1})$  as well as the fermionic coordinates  $(\eta_{b_1-1} \leftrightarrow \eta_{n-1})$ , and we have used square bracket to indicate that the exchanges act only on the expression inside the bracket. The

<sup>1</sup>We follow the notations of reference [7] to call the contributions from diagrams of type Fig. 7.2(a) or Fig. 7.2(b) as inhomogeneous contributions, while those from Fig. 7.2(c) as homogeneous ones.

<sup>2</sup>Here “bonus-simplified” means that these lower-point amplitudes used in the BCFW diagrams are simplified by using bonus relations.

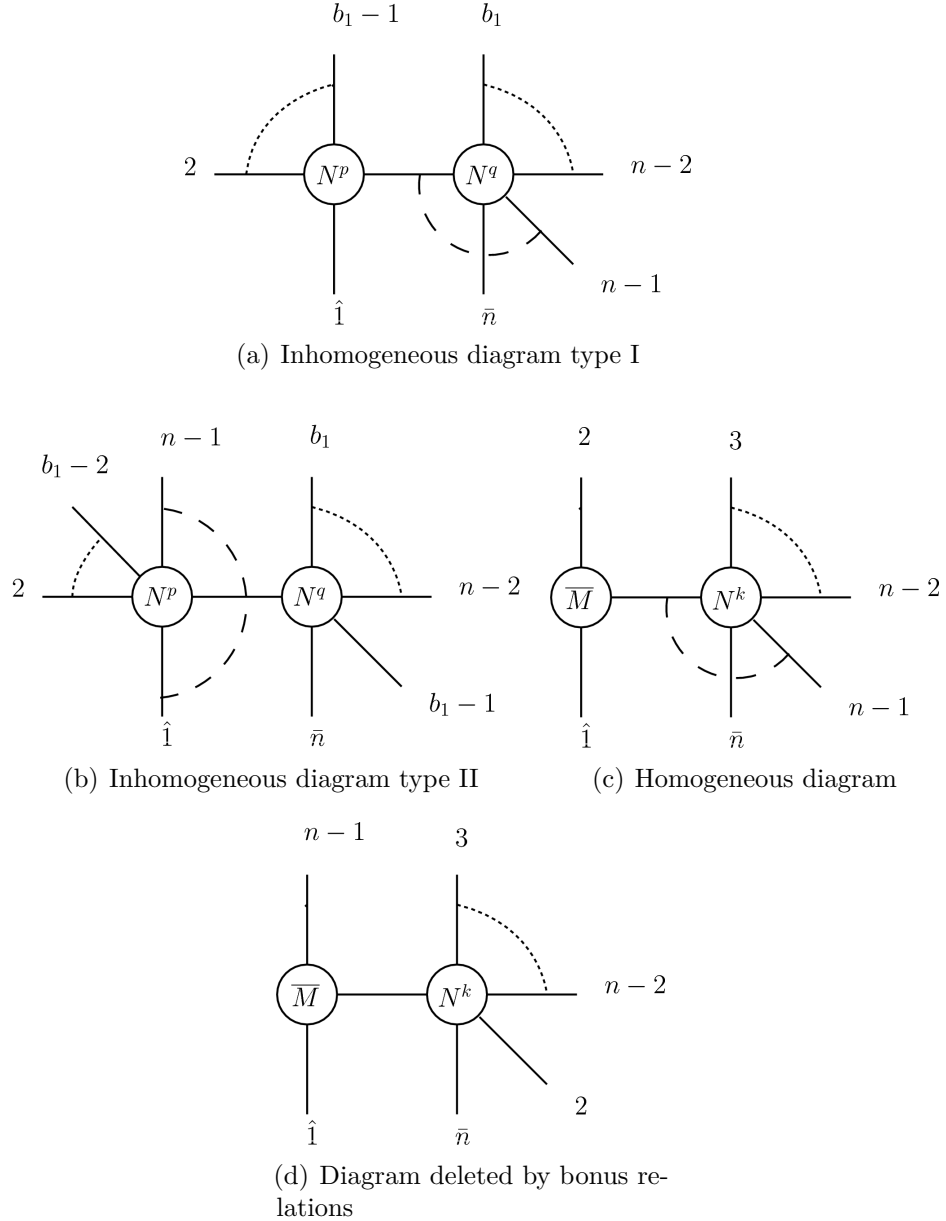


Figure 7.2: Different types of diagrams for a general  $N^k$ MHV amplitude, where  $k = p + q + 1$ . We use a dashed line  $---$  connecting three legs to denote a bonus-simplified lower-point amplitude, in which these three legs are kept fixed. For lower-point amplitudes without dashed lines, we use the usual  $(n - 2)!$  form.

superscript  $(i, m_i)$  in  $B_\alpha^{(i, m_i)}$  is used to show the type of this contribution, which will become clear in the examples.

Thus we have seen that, by using bonus relations, any amplitude can be written as a summation of  $(n - 3)!$  permutations with the coefficients  $B_\alpha^{(i, m_i)}$ , which will be called bonus coefficients. In this section, we shall calculate all bonus coefficients for NMHV and  $N^2$ MHV cases, and generalize the pattern observed in these examples to general  $N^k$ MHV amplitudes in the next section. Once bonus coefficients are calculated, we obtain explicitly all simplified SUGRA tree amplitudes.

### 7.2.2 NMHV Amplitudes

Here we use bonus relations to simplify the  $(n - 2)!$  form of NMHV amplitudes. First we state the general simplified form of NMHV amplitudes, and then prove it by induction. To be concise, we abbreviate the combinations

$$\{n; a_1 b_1\} \equiv G_{n; a_1 b_1} \left[ R_{n; a_1 b_1} A^{\text{MHV}}(1, 2, \dots, n) \right]^2 \quad (7.2.2)$$

and similar notations will be used in the following sections.

As mentioned above generally, we delete the contributions corresponding to Fig. 7.2(d) by using the bonus relation. It is straightforward to compute the inhomogeneous contributions from the two  $\text{MHV} \times \text{MHV}$  diagrams, Fig. 7.3(a) and Fig. 7.3(b). Firstly, let us consider the contribution from Fig. 7.3(a), which corresponds to terms

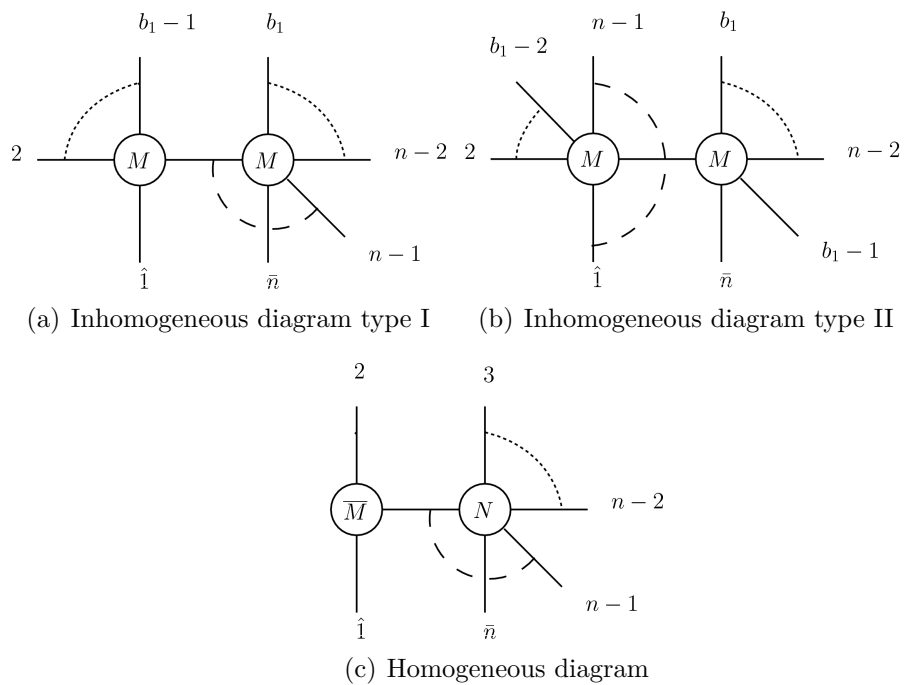


Figure 7.3: Diagrams for NMHV amplitudes.

with  $a_1 = 2$ , and we have

$$M_1 = B_{n;2b_1}^{(1)} \{n; 2b_1\}, \quad \text{with } 4 \leq b_1 \leq n-1, \quad (7.2.3)$$

where  $B_{n;2b_1}^{(1)}$  are the special cases of the general bonus coefficients  $B_{n;a_1b_1}^{(1)}$ . We have used the superscript (1) to indicate that this is the contribution coming from type-I diagram, and similar notations will be used below.

When  $b_1 \neq n-1$ , the bonus coefficients are given by,

$$B_{n;a_1b_1}^{(1)} = B^{\text{MHV}} \frac{\langle n-1|x_{b_1a_1}x_{b_1n}|n\rangle}{\langle n-1|x_{b_1a_1}x_{a_1n}|n\rangle}. \quad (7.2.4)$$

Here we note that we can get the above coefficients from the previous ones, namely the bonus coefficients of MHV amplitude, multiplied by the factor  $\frac{\langle n-1|x_{b_1a_1}x_{b_1n}|n\rangle}{\langle n-1|x_{b_1a_1}x_{a_1n}|n\rangle}$ . It is a general feature of this type of coefficients for  $N^k$ MHV case, which are given by  $N^{k-1}$ MHV coefficients multiplied by the same factor, as we will see explicitly again in the  $N^2$ MHV case.

However when  $b_1 = n-1$ , no bonus relation can be used for the right-hand-side 3-point MHV amplitude in Fig. 7.3(a), and we find

$$B_{n;a_1n-1}^{(1)} = \frac{\langle 1\ n\rangle}{\langle 1\ n-1\rangle} \frac{\langle n-1|x_{n-1a_1}|n-1\rangle}{\langle n|x_{na_1}|n-1\rangle}. \quad (7.2.5)$$

For the exchanged diagrams, Fig. 7.3(b), the contribution can be similarly written as

$$M_2 = B_{n;2b_1}^{(2)} [\{n; 2a_1\}(b_1 - 1 \leftrightarrow n - 1)], \quad \text{with } 4 \leq b_1 \leq n-1, \quad (7.2.6)$$

where the bonus coefficients  $B_{n;a_1b_1}^{(2)}$  are given by

$$B_{n;a_1b_1}^{(2)} = \frac{\langle 1|n\rangle}{\langle 1|n-1\rangle} \frac{\langle n-1|b_1-2\rangle (x'_{a_1b_1})^2}{\langle n|x_{na_1}x'_{a_1b_1}|b_1-2\rangle}, \quad (7.2.7)$$

and we have defined  $x'_{a_i b_i}$  as,

$$\begin{aligned} x'_{a_i b_i} &\equiv x_{a_i b_i - 1} + x_{n-1 n} \\ &= x_{a_i b_i} (p_{b_i - 1} \leftrightarrow p_{n-1}). \end{aligned} \quad (7.2.8)$$

All the above calculations do not include the boundary case  $a_1 = n - 3, b_1 = n - 1$ , which needs special treatment. This boundary case is special because it recursively reduces to the special 5-point NMHV ( $\overline{\text{MHV}}$ ) amplitude. It does not have the diagram with the type of  $\overline{\text{MHV}}_3 \times \text{NMHV}$ , and one has to treat it separately. We apply the bonus relations to this case in the following way: we use the bonus relation to delete the contribution from Fig. 7.4(a), and compute Fig. 7.4(b), and we find

$$\mathcal{M}_5 = -\frac{[24][34][51]}{[23][45][41]} [\{5; 24\}(3 \leftrightarrow 4)] + \mathcal{P}(2, 3). \quad (7.2.9)$$

By plugging the above 5-point result in Fig. 7.4(c), we get the boundary term of the 6-point NMHV amplitude

$$M_6^{(\text{boundary})} = \frac{\langle 16\rangle\langle 25\rangle[35][45]x_{36}^2}{\langle 15\rangle[34]\langle 2|1+6|5\rangle\langle 6|1+2|5\rangle} [\{6; 35\}(4 \leftrightarrow 5)]. \quad (7.2.10)$$

A generic form for the boundary term of the  $n$ -point NMHV amplitudes can be

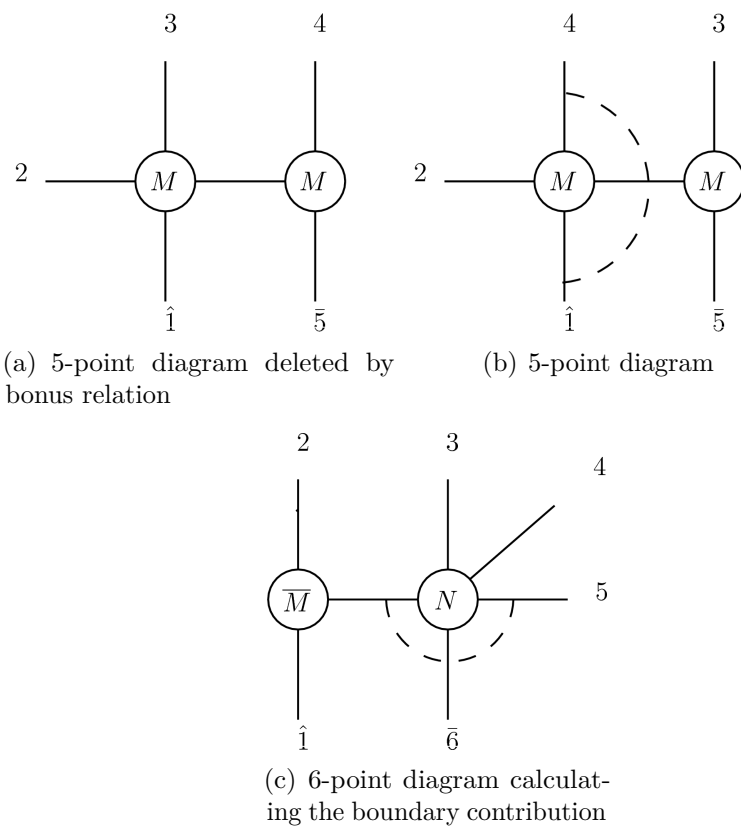


Figure 7.4: Diagrams for 5-point NMHV amplitude and the boundary term of 6-point NMHV amplitude. Fig. 6(a) and Fig. 6(b) are used to calculate the bonus-simplified 5-point right-hand-side amplitude of Fig. 6(c).

obtained as a straightforward generalization of (7.2.9) and (7.2.10),

$$M_n^{(\text{boundary})} = B_{n;n-3 \ n-1}^{(\text{boundary})} \left[ \{n; n-3 \ n-1\} (n-2 \leftrightarrow n-1) \right], \quad (7.2.11)$$

where  $B_{n;n-3 \ n-1}^{(\text{boundary})}$  is given by,

$$B_{n;n-3 \ n-1}^{(\text{boundary})} = \frac{\langle 1n \rangle \langle n-4 \ n-1 \rangle [n-3 \ n-1][n-2 \ n-1] x_{n-3n}^2}{\langle 1 \ n-1 \rangle [n-3 \ n-2] \langle n-4 | x_{n-3 \ n-1} | n-1 \rangle \langle n | x_{n-1 \ n-3} | n-1 \rangle}. \quad (7.2.12)$$

Putting everything together, we obtain the general formula for NMHV amplitude and as promised, the amplitude indeed can be written as a sum of  $(n-3)!$  permutations

$$\begin{aligned} \mathcal{M}_n^{\text{NMHV}} = & \sum_{a_1=2}^{n-4} \sum_{b_1=a_1+2}^{n-1} \left( B_{n;a_1b_1}^{(1)} \{n; a_1b_1\} + B_{n;a_1b_1}^{(2)} [\{n; a_1b_1\} (b_1-1 \leftrightarrow n-1)] \right) + M_n^{(\text{boundary})} \\ & + \mathcal{P}(2, 3, \dots, n-2). \end{aligned} \quad (7.2.13)$$

## Proof by Induction

Here we shall give an inductive proof for the simplified NMHV formula. For  $a_1 = 2$ , as we explained above, the formula follows directly from Fig. 7.3(a) and Fig. 7.3(b). Therefore we shall focus on the cases when  $a_1 \geq 3$ , which correspond to the homogeneous contributions from Fig. 7.3(c). We shall prove that the formula satisfies the BCFW recursion relations.

First note that we have deleted one diagram of the form  $\text{MHV}_L(\hat{1}, n-1, \hat{P}) \times \text{MHV}_R$  by using bonus relations, this results in a multiplicative prefactor for the overall

amplitude, which is given by,

$$(1 - \frac{z_2}{z_{n-1}}) = \frac{\langle 1n \rangle \langle n-1 \ 2 \rangle}{\langle n2 \rangle \langle 1n-1 \rangle}. \quad (7.2.14)$$

Let us consider the bonus coefficient  $B_{n;a_1b_1}^{(1)}$ , other coefficients  $B_{n;a_1b_1}^{(2)}$  and  $B_{n;n-3 \ n-1}^{(\text{boundary})}$  can be treated similarly. By plugging formula (7.2.4) into the  $(n-1)$ -point amplitude  $M(-\hat{P}, 3, 4, \dots, n-1, \bar{n})$  in Fig. 7.3(c), it is straightforward to check that the second piece of  $B_{n;a_1b_1}^{(1)}$ ,  $\frac{\langle n-1|x_{b_1a_1}x_{b_1n}|n \rangle}{\langle n-1|x_{b_1a_1}x_{a_1n}|n \rangle}$ , is transformed back to itself under the recursion relations.

For the first piece  $B^{\text{MHV}} = \frac{\langle n-1 \ n-2 \rangle \langle 1 \ n \rangle}{\langle n \ n-2 \rangle \langle 1 \ n-1 \rangle}$  of  $B_{n;a_1b_1}^{(1)}$ , which is the MHV bonus coefficient, the proof is essentially the same as in the MHV case. Taking into account the factor in (7.2.14) coming from bonus relations, we have

$$\frac{\langle n-1 \ n-2 \rangle \langle \hat{p} \ n \rangle}{\langle n \ n-2 \rangle \langle \hat{p} \ n-1 \rangle} \times \frac{\langle 1 \ n \rangle \langle n-1 \ 2 \rangle}{\langle 1 \ n-1 \rangle \langle n \ 2 \rangle} = \frac{\langle n-1 \ n-2 \rangle \langle 1 \ n \rangle}{\langle n \ n-2 \rangle \langle 1 \ n-1 \rangle}. \quad (7.2.15)$$

Thus the contribution with  $B_{n;a_1b_1}^{(1)}$  indeed satisfies the recursion relations.

Finally we should remark that we have used the fact that  $\{n; a_1b_1\}$  by themselves satisfy the ordered BCFW recursion relations during the whole proof.

### 7.2.3 $N^2$ MHV amplitudes

In this subsection we consider  $N^2$ MHV amplitudes as one more example to show the general features of bonus-simplified gravity amplitudes. Similar to NMHV case, let

us denote the ordered gravity solutions in the following way

$$H_{n;a_1b_1,a_2b_2}^{(1)} \left[ R_{n;a_1b_1} R_{n;a_1b_1,a_2b_2}^{b_1a_1} A^{\text{MHV}}(1, 2, \dots, n) \right]^2 \equiv \{n; a_1b_1, a_2b_2\}_1,$$

$$H_{n;a_1b_1,a_2b_2}^{(2)} \left[ R_{n;a_1b_1} R_{n;a_2b_2}^{a_1b_1} A^{\text{MHV}}(1, 2, \dots, n) \right]^2 \equiv \{n; a_1b_1, a_2b_2\}_2.$$

There are four relevant types of diagrams (and a boundary case) which contribute to the general  $N^2\text{MHV}$  amplitudes. The general structure of  $N^2\text{MHV}$  is given in Fig. 7.5 and the corresponding contributions from each of the four diagrams can be calculated separately.

First we consider the contributions from the diagrams in Fig. 7.5(b), which are of the form  $\text{MHV} \times \text{NMHV}$ . We use bonus-simplified amplitude for the right-hand-side NMHV amplitude and we obtain<sup>3</sup>,

$$M_I = \sum_{2 \leq a_1, b_1 \leq n-1} \sum_{b_1 \leq a_2, b_2 < n} \left( B_{n;a_1b_1;a_2b_2}^{(1,1)} \{n; a_1b_1; a_2b_2\}_2 \right. \\ \left. + B_{n;a_1b_1;a_2b_2}^{(1,2)} [\{n; a_1b_1; a_2b_2\}_2 (b_2 - 1 \leftrightarrow n - 1)] \right) \\ + \sum_{2 \leq a_1, b_1 \leq n-1} B_{n;a_1b_1;n-3n-1}^{(1,\text{boundary})} [\{n; a_1b_1; n - 3n - 1\}_2 (n - 2 \leftrightarrow n - 1)] \quad [2.16]$$

where in the first sum  $a_2 \leq n - 4$  because of the range of summation of the first

---

<sup>3</sup>Here and in the following calculations we have included the corresponding homogeneous terms, for the case we consider the contributions are from Fig. 7.5(a).

term in Eq. (7.2.13). Here the bonus coefficients are given by

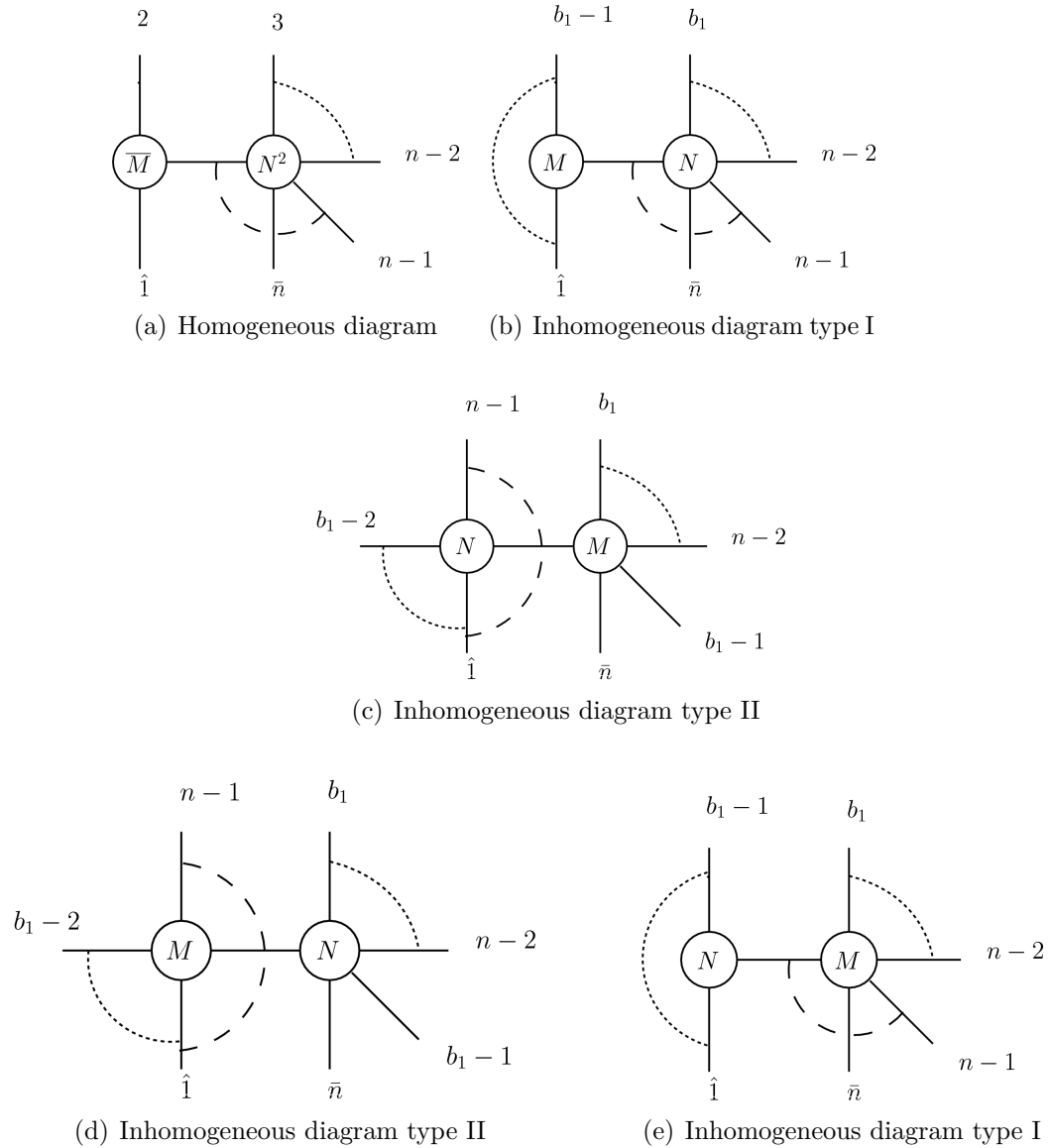
$$\begin{aligned}
B_{n;a_1b_1;a_2b_2}^{(1,1)} &= \frac{\langle 1n \rangle \langle n-1|n-2 \rangle \langle n-1|x_{a_2b_2}x_{b_2n}|n \rangle}{\langle 1n-1 \rangle \langle n|n-2 \rangle \langle n-1|x_{a_2b_2}x_{a_2n}|n \rangle} \frac{\langle n-1|x_{a_1b_1}x_{b_1n}|n \rangle}{\langle n-1|x_{a_1b_1}x_{a_1n}|n \rangle} \\
B_{n;a_1b_1;a_2b_2}^{(1,1)} &= \frac{\langle 1n \rangle \langle n-1|x_{n-1a_2}|n-1 \rangle}{\langle 1n-1 \rangle \langle n|x_{na_2}|n-1 \rangle} \frac{\langle n-1|x_{a_1b_1}x_{b_1n}|n \rangle}{\langle n-1|x_{a_1b_1}x_{a_1n}|n \rangle} \quad (b_2 = n-1) \\
B_{n;a_1b_1;a_2b_2}^{(1,2)} &= \frac{\langle 1n \rangle \langle n-1|b_2-2 \rangle (x'_{a_2b_2})^2}{\langle 1n-1 \rangle \langle n|x_{na_2}x'_{a_2b_2}|b_2-2 \rangle} \frac{\langle n-1|x_{a_1b_1}x_{b_1n}|n \rangle}{\langle n-1|x_{a_1b_1}x_{a_1n}|n \rangle} \\
B_{n;a_1b_1;n-3n-1}^{(1,\text{boundary})} &= B_{n;n-3\ n-1}^{(\text{boundary})} \frac{\langle n-1|x_{a_1b_1}x_{b_1n}|n \rangle}{\langle n-1|x_{a_1b_1}x_{a_1n}|n \rangle}, \tag{7.2.17}
\end{aligned}$$

where the last term  $B_{n;a_1b_1;n-3n-1}^{(1,\text{boundary})}$  comes from Eq. (7.2.12). Again the superscripts are used to show the types of the contributions. For instance, in the superscript  $(1, 1)$  of  $B_{n;a_1b_1;a_2b_2}^{(1,1)}$ , the first “1” means that it is the type-I contribution, while the second “1” implies that it is descendant from the NMHV case. A generalization to the  $N^k$ MHV case will be  $B_{n;a_1b_1;\dots;a_kb_k}^{(m)}$ , where  $m$  is a string composed of three kinds of labels, “1” “2” and “boundary”.

As we have mentioned in the NMHV case, and we want to stress it here again that the bonus coefficients of Fig. 7.5(b) are simply given as the previous ones, namely the coefficients of NMHV amplitudes, with replacements  $(a_1 \rightarrow a_2, b_1 \rightarrow b_2)$  and multiplied by the same factor  $\frac{\langle n-1|x_{a_1b_1}x_{b_1n}|n \rangle}{\langle n-1|x_{a_1b_1}x_{a_1n}|n \rangle}$ .

Next, we calculate the contributions from the diagrams in Fig. 7.5(c) which are of the form NMHV  $\times$  MHV and we get

$$\begin{aligned}
M_{\text{II}} &= \sum_{2 \leq a_1, b_1 \leq n-1} \sum_{a_1 \leq a_2, b_2 < b_1} \left( B_{n;a_1b_1;a_2b_2}^{(2,1)} \{n; a_1b_1; a_2b_2\}_1 (n-1 \leftrightarrow b_1-1) \right. \\
&\quad \left. + B_{n;a_1b_1;a_2b_2}^{(2,2)} [\{n; a_1b_1; a_2b_2\}_1 (b_2-1 \leftrightarrow b_1-1)] \right) \tag{7.2.18} \\
&\quad + \sum_{2 \leq a_1 \leq n-3} B_{n;a_1n-1;n-4n-2}^{(2,\text{boundary})} [\{n; a_1n-1; n-3n-1\}_1 (n-2 \leftrightarrow n-1)].
\end{aligned}$$

Figure 7.5: Diagrams for  $N^2MHV$  amplitudes.

In the above sum we do not include the boundary case  $(a_1, b_1, a_2, b_2) = (n-4, n-1, n-4, n-2)$ , which we shall study separately. The coefficients are given by

$$\begin{aligned}
 B_{n;a_1b_1;a_2b_2}^{(2,1)} &= \frac{\langle 1n \rangle \langle n-1 | b_1 - 2 \rangle \langle n-1 | x_{b_2a_2} x'_{b_2b_1} x'_{a_1b_1} x_{a_1n} | n \rangle (x'_{a_1b_1})^2}{\langle 1n-1 \rangle \langle b_1 - 2 | x'_{a_1b_1} x_{a_1n} | n \rangle \langle n-1 | x_{b_2a_2} x'_{a_2b_1} x'_{a_1b_1} x_{a_1n} | n \rangle} \\
 B_{n;a_1b_1;a_2b_2}^{(2,1)} &= \frac{\langle 1n \rangle \langle n-1 | x_{n-1a_2} | n-1 \rangle (x'_{a_1b_1})^2}{\langle 1n-1 \rangle \langle n | x_{na_1} x'_{a_1b_1} x'_{b_1a_2} | n-1 \rangle} \quad (b_2 = n-2) \\
 B_{n;a_1b_1;a_2b_2}^{(2,2)} &= \frac{\langle 1n \rangle \langle n-1 | b_2 - 2 \rangle (x'_{a_2b_2})^2 (x'_{a_1b_1})^2}{\langle 1n-1 \rangle \langle n | x_{na_1} x'_{a_1b_1} x'_{b_1a_2} x'_{a_2b_2} | b_2 - 2 \rangle} \\
 B_{n;a_1b_1;n-4n-2}^{(2,\text{boundary})} &= \frac{\langle 1n \rangle \langle b_1 - 4 | n-1 \rangle [b_1 - 3 | n-1 \rangle [b_1 - 2 | n-1 \rangle (x'_{b_1-3b_1})^2 (x'_{a_1b_1})^2}{\langle 1 | n-1 \rangle [b_1 - 3 | b_1 - 2 \rangle [b_1 - 4 | x_{b_1-4} | b_1 - 1 \rangle [n-1] \langle n | x_{na_1} x'_{a_1b_1} x_{b_1-1b_1-3} | n-1 \rangle}.
 \end{aligned} \tag{7.2.19}$$

By comparing the results with those of NMHV, now we are ready to see the patterns.

For this type of diagrams Fig. 7.5(c), the bonus coefficients can be obtained from the results of NMHV by doing the following replacements on the indices of region momenta  $x$ 's:  $n \rightarrow b_1, a_1 \rightarrow a_2, b_1 \rightarrow b_2$ , and  $x \rightarrow x'$  when  $x$  has the index  $n$  with it. Furthermore one should apply the changes on  $\langle n |$  as well as  $\langle n-i |$ , which read  $\langle n | \rightarrow \langle n | x_{na_1} x'_{a_1b_1}$ , and  $\langle n-i |$  (or  $[n-i |$ )  $\rightarrow \langle b_1 - i |$  (or  $[b_1 - i |$ ) for  $i > 1$ . Finally we multiply the obtained answers by a factor  $(x'_{a_1b_1})^2$ .

The bonus coefficients of the contributions from other diagrams are actually the same as those of the NMHV case. For the sake of completeness, let us write down these contributions: for the contribution from Fig. 7.5(d), we have

$$M_{\text{III}} = \sum_{2 \leq a_1, b_1 \leq n-1} \sum_{b_1 \leq a_2, b_2 < n} B_{n;a_1b_1;a_2b_2}^{(2)} [\{n; a_1b_1; a_2b_2\}_2 (b_1 - 1 \leftrightarrow n - 1)], \tag{7.2.20}$$

where the bonus coefficients  $B_{n;a_1b_1;a_2b_2}^{(2)}$  are given by Eq. (7.2.7); for the other

contributions coming from Fig. 7.5(e), we get

$$M_{\text{IV}} = \sum_{2 \leq a_1, b_1 \leq n-1} \sum_{a_1 \leq a_2, b_2 < b_1} B_{n; a_1 b_1; a_2 b_2}^{(1)} \{n; a_1 b_1; a_2 b_2\}_1, \quad (7.2.21)$$

and similarly the coefficients are given by Eq. (7.2.4) and Eq. (7.2.5).

Again as in the case of Eq. (7.2.18), this formula does not include the boundary case,  $\{n; a_1 b_1; a_2 b_2\}_1 = \{n; n-4n-1; n-4n-2\}_1$ , which should be considered separately, as we shall do below.

Similar to 5-point NMHV amplitude, the 6-point  $N^2\text{MHV}$  amplitude is special which only receives contributions from diagrams of  $\text{NMHV} \times \text{MHV}$  type and we must treat it separately. We can delete Fig. 7.6(a) by bonus relations, and the contribution from Fig. 7.6(b) gives,

$$\mathcal{M}_6 = -\frac{[16][25][45]}{[15][24][56]} [\{6; 25, 24\}_1 (3 \leftrightarrow 5)] + \mathcal{P}(2, 3, 4). \quad (7.2.22)$$

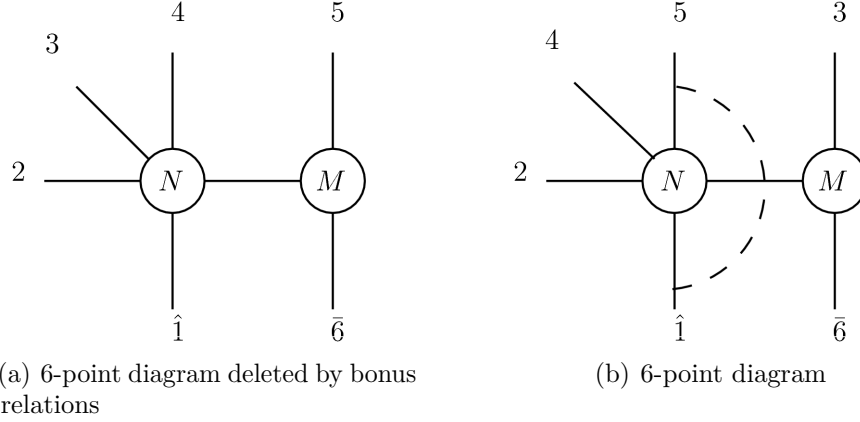
As the NMHV case (7.2.11), 6-point  $N^2\text{MHV}$  amplitude (7.2.22) can also be similarly generalized, and we obtain the boundary term of the full  $n$ -point  $N^2\text{MHV}$  amplitudes,

$$M_n^{(\text{boundary})} = B_{n; n-4 \ n-1; n-4 \ n-2}^{(\text{boundary})} [\{n; n-4 \ n-1; n-4 \ n-2\}_1 (n-3 \leftrightarrow n) \quad (7.2.23)]$$

where the bonus coefficients are given as

$$B_{n; n-4 \ n-1; n-4 \ n-2}^{(\text{boundary})} = \frac{\langle 1n \rangle \langle n-5 \ n-1 \rangle [n-4 \ n-1] [n-2 \ n-1] x_{n-4n}^2}{\langle 1n-1 \rangle [n-4 \ n-2] \langle n-5 | x_{n-4 \ n-1} | n-1 \rangle \langle n | x_{n-1 \ n-4} | n-1 \rangle} \quad (7.2.24)$$

Therefore we have calculated all the contributions for  $N^2\text{MHV}$  amplitudes and as in

Figure 7.6: Diagrams for 6-point  $N^2\text{MHV}$  amplitude.

the NMHV case, it can also be written as a sum of  $(n - 3)!$  permutations,

$$\mathcal{M}_n^{\text{N}^2\text{MHV}} = M_{\text{I}} + M_{\text{II}} + M_{\text{III}} + M_{\text{IV}} + M_n^{\text{(boundary)}} + \mathcal{P}(2, 3, \dots, n - 2). \quad (7.2.25)$$

The result can be proved very similarly by induction as in the NMHV case.

### 7.3 Generalization to all gravity tree amplitudes

Now we have all the ingredients for generalizing our results and stating the patterns for all tree-level gravity amplitudes. Our way of using bonus relations gives the simplified tree-level  $N^k\text{MHV}$  superamplitude as a sum of  $(n - 3)!$  permutations, and each of them contains normal and exchanged contributions,

$$\mathcal{M}_n^{\text{N}^k\text{MHV}} = \left[ A_n^{\text{MHV}} \right]^2 \left( \sum_{\alpha} B_{\alpha}^{(1, m_1)} G_{\alpha} R_{\alpha}^2 + \sum_{\beta} B_{\beta}^{(2, m_2)} [G_{\beta} R_{\beta}^2 (b_1 - 1 \leftrightarrow n - 1)] \right) + \mathcal{P}(2, 3, \dots, n - 2). \quad (7.3.1)$$

In both contributions, by reducing the homogeneous term recursively, we have  $k$  types of terms from  $k$  BCFW channels,  $N^p\text{MHV} \times N^q\text{MHV}$ , for  $p + q + 1 = k$  with  $0 \leq p, q < k$ . As we have stressed repeatedly, to respect the ordered structure, we have only used bonus relations on one lower-point amplitude, namely the right-hand-side  $N^q\text{MHV}$  for normal contribution, and the left-hand-side  $N^p\text{MHV}$  for exchanged contribution.

Before presenting all the bonus coefficients for general tree amplitudes, we pause to show by induction that bonus relations roughly reduce the number of terms from  $(n - 2)!$  in the original solution to  $(k + 1)(n - 3)!$  in the simplified one. To get the previous counting we note that in the  $N^p\text{MHV} \times N^q\text{MHV}$  channel of the normal contribution, by applying bonus relations to the  $N^q\text{MHV}$  lower-point amplitude we can reduce the number of terms from  $(n - 2)!/k$  to  $(q + 1)(n - 3)!/k$ . Taking into account all channels gives us  $(1 + 2 + \dots + k)(n - 3)!/k$  terms, with the same number from the exchanged contribution, thus the simplified form has only  $(k + 1)(n - 3)!$  terms. By parity, one only needs  $N^k\text{MHV}$  amplitudes with  $n > 2k + 2$  legs and thus the bonus relations can be used to delete at least half of the terms in tree amplitudes. The simplification becomes more significant when  $n \gg k$ .

Now we generalize the pattern found in the NMHV and  $N^2\text{MHV}$  cases to write down all the bonus coefficients for general tree amplitudes. As we have learned from the examples, once the bonus coefficients of  $N^{k-1}\text{MHV}$  amplitudes are calculated, then for the  $N^k\text{MHV}$  amplitudes, one only needs to compute two types of new contributions for  $N^k\text{MHV}$  amplitudes, namely the normal contribution from  $\text{MHV} \times N^{k-1}\text{MHV}$  channel ( $q = k - 1$ ) and the exchanged contribution from  $N^{k-1}\text{MHV} \times \text{MHV}$  channel ( $p = k - 1$ ) (see Fig. 7.7). All other bonus coefficients  $B_\alpha^{(m)}$  of  $N^p\text{MHV} \times N^q\text{MHV}$

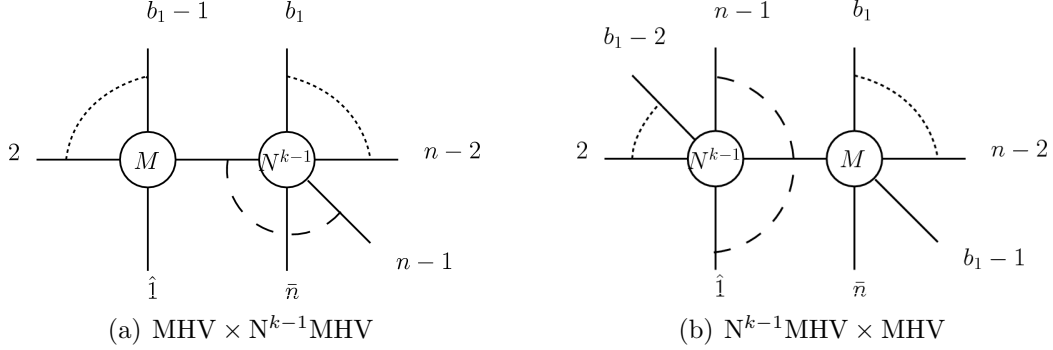


Figure 7.7: Two relevant diagrams for computing new bonus coefficients for  $n$ -point  $\text{N}^k\text{MHV}$  amplitude. The rest of the bonus coefficients can be obtained recursively from the  $\text{N}^{k-1}\text{MHV}$  case.

with  $q < k - 1$  and  $p < k - 1$ , are the same as those computed previously, namely the results from  $\text{N}^{k-1}\text{MHV}$  amplitudes. Since the summation variables of  $\text{N}^k\text{MHV}$  amplitude can be obtained by adding a pair of new labels  $a_k, b_k$  to the previous one,  $\alpha', \alpha = \{\alpha'; a_k, b_k\}$ , the result can be written as

$$B_{\alpha}^{(m)} = B_{\alpha'}^{(m)}, \quad (7.3.2)$$

for both normal contributions with  $q < k - 1$  and exchanged ones with  $p < k - 1$ .

Thus we only need to calculate two new contributions from Fig. 7.7(a) and Fig. 7.7(b). It is straightforward to confirm that all the observations we have made for the cases of NMHV and  $\text{N}^2\text{MHV}$  can be directly generalized to all tree-level amplitudes. We shall first state the rules and then justify them. Firstly, just like Eq. (7.2.4) and Eq. (7.2.17) for NMHV and  $\text{N}^2\text{MHV}$  cases, the bonus coefficients of Fig. 7.7(a),  $B_{\alpha}^{(1,m_1)}$ , can be similarly obtained by the replacements on the indices of the region momenta  $x$ 's,  $a_i \rightarrow a_{i+1}, b_i \rightarrow b_{i+1}$ , for  $B_{\alpha}^{(m_1)}$  of  $\text{N}^{k-1}\text{MHV}$  amplitudes, then multiplying with a simple common factor of the form  $\frac{\langle n-1|x_{a_1 b_1} x_{b_1 n}|n\rangle}{\langle n-1|x_{a_1 b_1} x_{a_1 n}|n\rangle}$ , which are the same for all tree-level

amplitudes,

$$B_{\alpha}^{(1,m_1)} = \frac{\langle n-1|x_{a_1b_1}x_{b_1n}|n\rangle}{\langle n-1|x_{a_1b_1}x_{a_1n}|n\rangle} B_{\alpha'}^{(m_1)}(a_i \rightarrow a_{i+1}, b_i \rightarrow b_{i+1}). \quad (7.3.3)$$

Secondly, the bonus coefficients for the new exchanged contributions Fig. 7.7(b),  $B_{\beta}^{(2,m_2)}$ , can be obtained by taking  $B_{\beta'}^{(m_2)}$  of  $N^{k-1}$ MHV amplitudes, and performing the following replacements on the indices of region momenta  $x$ 's, namely  $n \rightarrow b_1$ ,  $a_i \rightarrow a_{i+1}$ ,  $b_i \rightarrow b_{i+1}$ , and  $x \rightarrow x'$  when  $x$  has index  $n$  with it. And for the spinors, we have  $\langle n | \rightarrow \langle n | x_{na_1}x'_{a_1b_1}$  as well as  $|n-i\rangle$  (or  $|n-i]\rangle$ )  $\rightarrow |b_1-i\rangle$  (or  $|b_1-i]\rangle$ ) for  $i > 1$ . In addition, the obtained answers are further multiplied by a factor  $(x'_{a_1b_1})^2$ ,

$$B_{\beta}^{(2,m_2)} = (x'_{a_1b_1})^2 B_{\beta'}^{(m_2)}, \quad (7.3.4)$$

where the arguments of  $B_{\beta'}^{(m_2)}$  should be changed under the rules we described above.

All these rules can be understood in a simple way. For the rules of the normal contributions, the common factor is obtained in the following way,

$$(1 - \frac{z_i}{z_{n-1}}) \frac{\langle n1 \rangle}{\langle n-11 \rangle} \rightarrow (1 - \frac{z_i}{z_{n-1}}) \frac{\langle n\hat{P} \rangle}{\langle n-1\hat{P} \rangle} \rightarrow \frac{\langle n-1|x_{a_1b_1}x_{b_1n}|n\rangle}{\langle n-1|x_{a_1b_1}x_{a_1n}|n\rangle}, \quad (7.3.5)$$

where  $(1 - \frac{z_i}{z_{n-1}})$  comes from the fact that we delete one diagram using bonus relations, and  $\frac{\langle n1 \rangle}{\langle n-11 \rangle}$  is a factor that always appears in every bonus coefficient.

While for the rules of the exchanged contributions, we find that the factor  $(x'_{a_1b_1})^2$  appears because

$$\langle n1 \rangle \rightarrow \langle \hat{P}\hat{1} \rangle \rightarrow [\hat{P}\hat{1}]\langle \hat{P}\hat{1} \rangle \rightarrow (x'_{a_1b_1})^2, \quad (7.3.6)$$

and  $\langle n|$  changes in the following way under the recursion relations,

$$\langle n| \rightarrow \langle \hat{P}| \rightarrow \langle n1| [1\hat{P}] \langle \hat{P}| \rightarrow \langle n| x_{na_1} x'_{a_1 b_1}. \quad (7.3.7)$$

Besides, the transformation rule of  $x_{n\gamma_i}$  follows as

$$x_{n\gamma_i} \rightarrow x_{\hat{P}\gamma_{i+1}} \rightarrow x'_{b_1\gamma_{i+1}}, \quad (7.3.8)$$

where  $\gamma$  can be  $a$  or  $b$  and we have used the fact that  $p_{\hat{P}} = p_{b_1} + \dots + p_{n-2} + p_{b_1-1} + p_{\hat{n}}$ .

So in this way, we have a complete understanding of the rules we have proposed.

Finally, as shown in the examples a boundary contribution has to be considered separately because the special case  $(k+4)$ -point  $N^k$ MHV amplitude only has diagrams of  $N^{k-1}$ MHV  $\times$  MHV type. For this special contribution, it is straightforward to obtain a general form,

$$M_n^{(\text{boundary})} = B_{\beta_0}^{(\text{boundary})} \left[ \left( A_n^{\text{MHV}} \right)^2 G_{\beta_0} R_{\beta_0}^2 (n - k - 1 \leftrightarrow n - 1) \right], \quad (7.3.9)$$

where  $\beta_0 = \{n; n - k - 2 \ n - 1; n - k - 2 \ n - 2; \dots; n - k - 2 \ n - k\}$ , and the coefficients can be written as

$$B_{\beta_0}^{(\text{boundary})} = \frac{\langle 1n \rangle \langle n - k - 3 \ n - 1 \rangle [n - k - 2 \ n - 1] [n - k \ n - 1] x_{n-k-2 \ n}^2}{\langle 1n - 1 \rangle [n - k - 2 \ n - 2] \langle n - k - 3 | x_{n-k-3 \ n-1} | n - 1 \rangle \langle n | x_{n-1 \ n-k-2} | n - 1 \rangle} \quad (7.3.10)$$

Therefore, we have found a set of explicit rules to write down all the bonus coefficients for all tree amplitude in  $\mathcal{N} = 8$  supergravity.

## 7.4 Conclusion and outlook

In this chapter, we simplified tree-level amplitudes in  $\mathcal{N} = 8$  SUGRA, from the BCFW form with a sum of  $(n - 2)!$  permutations to a new form as a sum of  $(n - 3)!$  permutations. This is achieved by using the bonus relations, which are relations between tree amplitudes in theories without color ordering. In contrast to the MHV case, a naive use of the bonus relations ruins the structure of the non-MHV ordered tree-level solution, thus we proposed an improved application of the relations, which respects the ordered structure. The key point here is to apply the bonus relations to only one of two lower-point amplitudes in any BCFW diagram, which indeed brings SUGRA amplitudes to a simplified form having a  $(n - 3)!$ -permutation sum with some bonus coefficients. To illustrate the method, we have explicitly calculated simplified amplitudes for the NMHV and  $N^2$ MHV cases. We have also argued that the pattern generalizes to  $N^k$ MHV cases, and presented a simple way for writing down the bonus coefficients of all amplitudes, thus one can recursively obtain the simplified form for general SUGRA tree amplitudes.

Apart from the computational advantages, the simplification is also conceptually interesting. The relations between gravity and gauge theories have been reexamined from various perspectives recently [63, 64]. A common feature, of these “gravity”=“gauge theory”<sup>2</sup> methods, is the freedom of rewriting  $(n - 2)!$  forms of gravity tree amplitudes as  $(n - 3)!$  forms, essentially by using BCJ relations on the gauge theory side. Our result confirms this freedom at an explicit level by directly using it to simplify SUGRA amplitudes, which also suggests that bonus relations may be regarded as explicit gravity relations induced by Yang-Mills BCJ relations. It may be fruitful to understand the exact connections between our method, general forms of KLT

relations, and the square relations. In particular, it would be nice to go beyond SUGRA and see if similar simplifications occur generally, given that both BCFW recursion relations and bonus relations are valid in more general gravity theories.

Bonus relations and simplifications we obtained at tree level can also have implications for loop amplitudes. Through the generalized unitarity-cut method, our new form of tree amplitudes can be used in calculations of loop amplitudes. In addition, the square relations have been conjectured to hold at loop level [65], thus we may expect similar simplifications directly for the SUGRA loop amplitudes.

# Chapter 8

## Conclusions

Before looking forward for the future directions, let us look back and briefly summarize the main ideas we have encountered. In this thesis, we have showed how the power of modern on-shell techniques of computing scattering amplitudes both in  $\mathcal{N} = 4$  SYM and  $\mathcal{N} = 8$  SUGRA. Firstly two dual formalisms, namely twistor string thoery and Grassmannian formulation, of the S-matrix in  $\mathcal{N} = 4$  SYM have been studied in great details, specially we focus on the amazing relation between these two beautiful formalisms, and all tree-level contour in Grassmannian formulation was constructed by using the idea of “adding one particle at a time”. We observed that there is a smooth deformation which interpolates between the connected prescription of twistor string theory and the Grassmannian integrand together with the explicit contour of integration.

Then we turn to study the loop-level amplitudes in  $\mathcal{N} = 4$  SYM using leading singularity methods. We, for the first time, determined all the scalar integral basis

and the corresponding coefficients of three-loop five-point amplitude in  $\mathcal{N} = 4$  SYM. We also use our new obtained result to determine two previously unknown numerical constants in BDS ansatz.

After finishing the study on  $\mathcal{N} = 4$  SYM, we study various aspects of tree-level scattering amplitudes in  $\mathcal{N} = 8$  SUGRA. A new MHV scattering amplitude of  $n$  gravitons at tree level was presented and proved. Some of the interesting features of the formula set it apart as being significantly different from many more familiar ones. We hope the formula will eventually lead to Parke-Taylor-like formula for SUGRA. We also found that the formula has a very simple link representation in twistor space, which may be useful for finding Grassmannian formulation(or twistor string formulation) for  $\mathcal{N} = 8$  SUGRA.

By solving BCFW recursion relations explicitly, an algorithm of computing all tree-level S-matrix in  $\mathcal{N} = 8$  SUGRA was obtained by solving supersymmetric BCFW recursion relations. A very interesting Kawai-Lewellen-Tye (KLT)-like structure between Yang-Mills amplitudes and the gravity amplitudes naturally appears in our tree-level solutions. Meanwhile it has been pointed out that there are reasons to suspect that  $\mathcal{N} = 8$  SUGRA to be ultimately even simpler than SYM. One particular interesting feature is that gravity amplitudes exhibit exceptionally soft behavior under BCFW shift, which leads to an interesting extra relation between gravity amplitudes, which we called bonus relation, which allows us to even simply the obtained all tree-level amplitude.

There various remaining issues that need to be addressed, let us point out some of them here. Firstly, it would be of great interest to find the generalization of the Grassmannian formulation(or the twistor string formulation) for the S-matrix

of  $\mathcal{N} = 8$  SUGRA. Another possibly related exciting direction is the finiteness of  $\mathcal{N} = 8$  SUGRA. All the symmetries of the theory as well as the novel soft behavior of gravity tree-level amplitudes under BCFW shift may finally help us to understand better the perturbative behaviors of SUGRA amplitudes. For  $\mathcal{N} = 4$  SYM, recently a lot efforts have been focused on the loop amplitudes and the so-called remainder functions. Due to the recent exciting developments on the BCFW-type recursion relations for loop integrands as well as many other relevant interesting progresses, we are in a good position to completely understand the  $\mathcal{N} = 4$  SYM in the planar limit and also to have a better understanding of the non-planar case in future. It would not be very surprising if all these subjects are eventually related to each other.

# .1 The Nine-Point $N^2$ MHV Tree Amplitude

Residue	Geometry Problem:	Residue	Geometry Problem:
	$f_7^1 \quad f_7^2 \quad f_8^1 \quad f_8^2 \quad f_9^1 \quad f_9^2$		$f_7^1 \quad f_7^2 \quad f_8^1 \quad f_8^2 \quad f_9^1 \quad f_9^2$
$(2)(3)^2(4)^2(5)_{456}^{91}$	$(4567)(5671)(5678)(1346)(2367)(1347)$	$(2)(4)(5)^2(6)(9)_{67}^{17}$	$(4567)(5671)(5678)(6781)(6789)(9123)$
$(4)(5)^2(6)^2(7)_{678}^{23}$	$(4567)(5671)(5678)(6781)(6789)(7891)$	$(2)(4)(5)[(8)(9)]_{16}^{16}$	$(4567)(5671)(5678)(1238)(9126)(9123)$
$(6)(7)^2(8)^2(9)_{891}^{45}$	$(1247)(1237)(1258)(6781)(9126)(9123)$	$[(2)(3)](4)(6)(7)_{4}^{9}$	$(4567)(3451)(2356)(6781)(6789)(7891)$
$(2)(3)^2(4)(7)_{45}^{9}$	$(4567)(3451)(2356)(1346)(2367)(7891)$	$[(2)(3)](4)(8)(9)_{4}^{9}$	$(4567)(3451)(2356)(1238)(2367)(9123)$
$(2)(3)^2(4)(9)_{45}^{9}$	$(4567)(3451)(2356)(1346)(9126)(9123)$	$[(4)(5)](6)(8)(9)_{6}^{2}$	$(4567)(5671)(5678)(1238)(6789)(9123)$
$(4)(5)^2(6)(9)_{67}^{2}$	$(4567)(5671)(5678)(6781)(6789)(9123)$	$(2)[(5)(6)](7)(9)_{7}^{3}$	$(2345)(5671)(5678)(6781)(6789)(9123)$
$(2)(5)(6)^2(7)_{78}^{3}$	$(2345)(5671)(5678)(6781)(6789)(7891)$	$(2)(3)(5)[(6)(7)]_{8}^{3}$	$(2345)(5671)(5678)(6781)(6789)(7891)$
$(2)(7)(8)^2(9)_{91}^{5}$	$(2345)(1237)(1258)(1238)(9126)(9123)$	$(2)(3)(7)[(8)(9)]_{1}^{5}$	$(2345)(1237)(2356)(1238)(9126)(9123)$
$(4)(7)(8)^2(9)_{91}^{5}$	$(4567)(1237)(1258)(1238)(9126)(9123)$	$(2)(5)(7)[(8)(9)]_{1}^{5}$	$(2345)(1237)(5678)(1238)(9126)(9123)$
$[(2)(3)][(6)(7)]_{48}^{1}$	$(2345)(3451)(2356)(6781)(6789)(7891)$	$(4)(5)(7)[(8)(9)]_{1}^{5}$	$(4567)(1237)(5678)(1238)(9126)(9123)$
$[(2)(3)][(8)(9)]_{14}^{1}$	$(2345)(3451)(2356)(1238)(9126)(9123)$	$[(2)(3)](6)(7)(9)_{4}^{4}$	$(2345)(3451)(2356)(6781)(6789)(9123)$
$[(4)(5)][(8)(9)]_{16}^{1}$	$(4567)(5671)(5678)(1238)(9126)(9123)$	$[(2)(3)](6)(8)(9)_{4}^{4}$	$(2345)(3451)(2356)(1238)(6789)(9123)$
$(2)(3)^2(4)(6)(7)_{458}^{1}$	$(4567)(3451)(2356)(1346)(6789)(7891)$	$(2)(3)(5)(6)(8)(9)_{147}^{1}$	$(2345)(3451)(5678)(6781)(9126)(9123)$
$(2)(3)^2(4)(8)(9)_{451}^{1}$	$(4567)(3451)(2356)(1346)(9126)(9123)$	$(2)(3)(4)(5)(6)(7)_{6}^{39}$	$(4567)(5671)(5678)(6781)(6789)(7891)$
$(2)(3)(5)(6)^2(7)_{478}^{1}$	$(2345)(3451)(5678)(6781)(6789)(7891)$	$(4)(5)(6)(7)(8)(9)_{8}^{25}$	$(4567)(1237)(5678)(1238)(6789)(9123)$
$(2)(3)(7)(8)^2(9)_{491}^{1}$	$(2345)(3451)(1258)(1238)(9126)(9123)$	$(1)(2)(3)(5)(6)(9)_{2}^{8}$	$(2345)(3451)(5678)(1346)(6789)(9123)$
$(4)(5)^2(6)(8)(9)_{671}^{1}$	$(4567)(5671)(5678)(6781)(9126)(9123)$	$(2)(3)(4)(5)(8)(9)_{6}^{9}$	$(4567)(5671)(5678)(1238)(2367)(9123)$
$(4)(5)(7)(8)^2(9)_{691}^{1}$	$(4567)(5671)(5678)(1238)(9126)(9123)$	$(2)(3)(6)(7)(8)(9)_{8}^{5}$	$(2345)(1237)(2356)(1238)(6789)(9123)$
$(1)(2)^2(3)(6)(9)_{24}^{8}$	$(2345)(3451)(2356)(1346)(6789)(9123)$	$(2)(5)(6)(7)(8)(9)_{8}^{5}$	$(2345)(1237)(5678)(1238)(6789)(9123)$
$(9)(1)^2(2)(5)(8)_{12}^{7}$	$(2345)(3451)(5678)(1238)(9126)(9123)$	$(2)(5)(6)(7)(8)(9)_{9}^{3}$	$(2345)(5671)(5678)(6781)(6789)(9123)$
$(1)(2)[(5)(6)][9]_{27}^{1}$	$(2345)(3451)(5678)(6781)(6789)(9123)$	$(1)(2)(5)(6)(8)(9)_{2}^{1}$	$(2345)(3451)(5678)(1238)(6789)(9123)$
$(2)(3)^2(4)(6)(9)_{45}^{1}$	$(4567)(3451)(2356)(1346)(9126)(9123)$	$(2)(3)(5)(6)(8)(9)_{4}^{4}$	$(2345)(3451)(5678)(1238)(6789)(9123)$
$[(2)(3)][(5)(6)][9]_{47}^{1}$	$(2345)(3451)(5678)(6781)(6789)(9123)$	$(2)(4)(5)(6)(8)(9)_{6}^{6}$	$(4567)(5671)(5678)(1238)(6789)(9123)$
$(2)(3)(5)[(5)(6)][9]_{47}^{1}$	$(2345)(3451)(5678)(6781)(6789)(9123)$	$(2)(3)(4)(7)(8)(9)_{59}^{59}$	$(2345)(1237)(2356)(1238)(2367)(7891)$
$(2)(3)(5)[(8)(9)]_{14}^{1}$	$(2345)(3451)(5678)(1238)(9126)(9123)$	$(2)(3)(5)(6)(7)(9)_{3}^{3}$	$(2345)(5671)(5678)(6781)(6789)(7891)$

# Bibliography

- [1] Z. Bern, L. J. Dixon, D. C. Dunbar and D. A. Kosower, “One loop n point gauge theory amplitudes, unitarity and collinear limits,” *Nucl. Phys. B* **425**, 217 (1994) [arXiv:hep-ph/9403226].
- [2] R. Britto, F. Cachazo and B. Feng, “New recursion relations for tree amplitudes of gluons,” arXiv:hep-th/0412308.
- [3] R. Britto, F. Cachazo, B. Feng and E. Witten, “Direct proof of tree-level recursion relation in Yang-Mills theory,” arXiv:hep-th/0501052.
- [4] J. Bedford, A. Brandhuber, B. Spence and G. Travaglini, arXiv:hep-th/0502146.
- [5] F. Cachazo and P. Svrcek, “Tree level recursion relations in general relativity,” arXiv:hep-th/0502160.
- [6] N. Arkani-Hamed, J. L. Bourjaily, F. Cachazo, S. Caron-Huot and J. Trnka, *JHEP* **1101**, 041 (2011) [arXiv:1008.2958 [hep-th]].
- [7] J. M. Drummond and J. M. Henn, arXiv:0808.2475 [hep-th].
- [8] N. Arkani-Hamed, F. Cachazo, C. Cheung and J. Kaplan, “A Duality For The S Matrix,” arXiv:0907.5418.

- [9] D. Nandan, A. Volovich, and C. Wen, “A Grassmannian Étude in NMHV Minors,” arXiv:0912.3705 [hep-th].
- [10] N. Arkani-Hamed, J. Bourjaily, F. Cachazo, and J. Trnka, “Unification of Residues and Grassmannian Dualities,” arXiv:0912.4912 [hep-th].
- [11] C. Anastasiou, Z. Bern, L. J. Dixon and D. A. Kosower, Phys. Rev. Lett. **91**, 251602 (2003) [arXiv:hep-th/0309040].
- [12] Z. Bern, L. J. Dixon and V. A. Smirnov, Phys. Rev. D **72**, 085001 (2005) [arXiv:hep-th/0505205].
- [13] F. Cachazo, M. Spradlin and A. Volovich, Phys. Rev. D **74**, 045020 (2006) [arXiv:hep-th/0602228].
- [14] Z. Bern, M. Czakon, D. A. Kosower, R. Roiban and V. A. Smirnov, Phys. Rev. Lett. **97**, 181601 (2006) [arXiv:hep-th/0604074].
- [15] L. F. Alday and J. Maldacena, JHEP **0711**, 068 (2007) [arXiv:0710.1060].
- [16] R. C. Brower, H. Nastase, H. J. Schnitzer and C.-I. Tan, arXiv:0801.3891.
- [17] J. Bartels, L. N. Lipatov and A. Sabio Vera, arXiv:0802.2065.
- [18] Z. Bern, L. J. Dixon, D. A. Kosower, R. Roiban, M. Spradlin, C. Vergu and A. Volovich, Phys. Rev. D **78**, 045007 (2008) [arXiv:0803.1465 [hep-th]].
- [19] J. M. Drummond, J. Henn, G. P. Korchemsky and E. Sokatchev, arXiv:0712.1223.
- [20] N. Arkani-Hamed, F. Cachazo and J. Kaplan, arXiv:0808.1446 [hep-th].

- [21] R. Roiban, M. Spradlin and A. Volovich, JHEP **0404**, 012 (2004). R. Roiban and A. Volovich, Phys. Rev. Lett. **93**, 131602 (2004). R. Roiban, M. Spradlin and A. Volovich, Phys. Rev. D **70**, 026009 (2004).
- [22] M. Spradlin and A. Volovich, Phys. Rev. D **80**, 085022 (2009) [arXiv:0909.0229 [hep-th]].
- [23] L. Dolan and P. Goddard, arXiv:0909.0499 [hep-th].
- [24] N. Arkani-Hamed, F. Cachazo, C. Cheung and J. Kaplan, “The S-Matrix in Twistor Space,” arXiv:0903.2110.
- [25] N. Arkani-Hamed, F. Cachazo and C. Cheung, arXiv:0909.0483 [hep-th].
- [26] M. Bullimore, L. Mason and D. Skinner, arXiv:0912.0539 [hep-th].
- [27] G. P. Korchemsky and E. Sokatchev, arXiv:0907.4107 [hep-th].
- [28] C. Vergu, Phys. Rev. D **75**, 025028 (2007).
- [29] H.S. White, “Seven Points on a Twisted Cubic Curve,” Proc. Natl. Acad. Sci. **1**, 464 (1915).
- [30] N. Arkani-Hamed, J. Bourjaily, F. Cachazo, and J. Trnka, “Local Spacetime Physics from the Grassmannian,” arXiv:0912.3249 [hep-th].
- [31] L. Dolan and P. Goddard, “General Split Helicity Gluon Tree Amplitudes in Open Twistor String Theory,” arXiv:1002.4852 [hep-th].
- [32] F. Cachazo, arXiv:0803.1988.
- [33] F. Cachazo, M. Spradlin and A. Volovich, JHEP **0607**, 007 (2006) [arXiv:hep-th/0601031].

- [34] F. Cachazo, M. Spradlin and A. Volovich, Phys. Rev. D **75**, 105011 (2007) [arXiv:hep-th/0612309].
- [35] Z. Bern, L. J. Dixon, D. C. Dunbar and D. A. Kosower, Nucl. Phys. B **435**, 59 (1995) [arXiv:hep-ph/9409265].
- [36] Z. Bern and A. G. Morgan, Nucl. Phys. B **467**, 479 (1996) [arXiv:hep-ph/9511336].
- [37] Z. Bern, L. J. Dixon and D. A. Kosower, Ann. Rev. Nucl. Part. Sci. **46**, 109 (1996) [arXiv:hep-ph/9602280].
- [38] Z. Bern, L. J. Dixon, D. C. Dunbar and D. A. Kosower, Phys. Lett. B **394**, 105 (1997) [arXiv:hep-th/9611127].
- [39] Z. Bern, L. J. Dixon and D. A. Kosower, Nucl. Phys. B **513**, 3 (1998) [arXiv:hep-ph/9708239].
- [40] Z. Bern, L. J. Dixon and D. A. Kosower, JHEP **0408**, 012 (2004) [arXiv:hep-ph/0404293].
- [41] R. Britto, F. Cachazo and B. Feng, Nucl. Phys. B **725**, 275 (2005) [arXiv:hep-th/0412103].
- [42] E. I. Buchbinder and F. Cachazo, JHEP **0511**, 036 (2005) [arXiv:hep-th/0506126].
- [43] Z. Bern, J. J. M. Carrasco, H. Johansson and D. A. Kosower, Phys. Rev. D **76**, 125020 (2007) [arXiv:0705.1864].
- [44] F. Cachazo and D. Skinner, arXiv:0801.4574.

- [45] F. Cachazo, M. Spradlin and A. Volovich, arXiv:0805.4832.
- [46] F. Cachazo, M. Spradlin and A. Volovich, Phys. Rev. D **76**, 106004 (2007) [arXiv:0707.1903].
- [47] Z. Bern, M. Czakon, L. J. Dixon, D. A. Kosower and V. A. Smirnov, Phys. Rev. D **75**, 085010 (2007) [arXiv:hep-th/0610248].
- [48] R. Akhoury, Phys. Rev. D **19**, 1250 (1979);  
 J. C. Collins, Phys. Rev. D **22**, 1478 (1980);  
 A. Sen, Phys. Rev. D **24**, 3281 (1981);  
 G. P. Korchemsky, Phys. Lett. B **220**, 629 (1989);  
 L. Magnea and G. Sterman, Phys. Rev. D **42**, 4222 (1990);  
 G. P. Korchemsky and G. Marchesini, Phys. Lett. B **313** (1993) 433;  
 S. Catani, Phys. Lett. B **427**, 161 (1998) [arXiv:hep-ph/9802439];  
 G. Sterman and M. E. Tejeda-Yeomans, Phys. Lett. B **552**, 48 (2003)  
 [arXiv:hep-ph/0210130].
- [49] J. Bartels, L. N. Lipatov and A. Sabio Vera, arXiv:0807.0894.
- [50] H. Kawai, D. C. Lewellen and S. H. H. Tye, Nucl. Phys. B **269**, 1 (1986).
- [51] F. A. Berends, W. T. Giele and H. Kuijf, Phys. Lett. B **211**, 91 (1988).
- [52] Z. Bern, Living Rev. Rel. **5**, 5 (2002) [arXiv:gr-qc/0206071].
- [53] L. Mason, D. Skinner, arXiv:0808.3907.
- [54] H. Elvang and D. Z. Freedman, JHEP **0805**, 096 (2008) [arXiv:0710.1270 [hep-th]].

- [55] Z. Bern, L. J. Dixon and R. Roiban, Phys. Lett. B **644**, 265 (2007) [arXiv:hep-th/0611086].
- [56] L. J. Mason and D. Skinner, JHEP **1001**, 064 (2010) [arXiv:0903.2083 [hep-th]].
- [57] J. M. Drummond, J. Henn, V. A. Smirnov and E. Sokatchev, JHEP **0701**, 064 (2007) [arXiv:hep-th/0607160].
- [58] J. M. Drummond, G. P. Korchemsky and E. Sokatchev, Nucl. Phys. B **795**, 385 (2008) [arXiv:0707.0243 [hep-th]].
- [59] J. M. Drummond, J. Henn, G. P. Korchemsky and E. Sokatchev, arXiv:0807.1095 [hep-th].
- [60] A. Brandhuber, P. Heslop and G. Travaglini, arXiv:0807.4097 [hep-th].
- [61] J. M. Drummond, J. Henn, G. P. Korchemsky and E. Sokatchev, arXiv:0808.0491 [hep-th].
- [62] M. Spradlin, A. Volovich and C. Wen, arXiv:0812.4767 [hep-th].
- [63] Z. Bern, J. J. M. Carrasco and H. Johansson, Phys. Rev. D **78**, 085011 (2008) [arXiv:0805.3993 [hep-ph]].
- [64] N. E. J. Bjerrum-Bohr, P. H. Damgaard, B. Feng and T. Sondergaard, arXiv:1005.4367 [hep-th].
- [65] Z. Bern, J. J. M. Carrasco and H. Johansson, Phys. Rev. Lett. **105**, 061602 (2010) [arXiv:1004.0476 [hep-th]].